NTNU – Trondheim
Norwegian University of
Science and Technology

The Effect of Brine Composition and Rock Type on Oil Recovery by the Use of Combined Low-Salinity Waterflooding and Surfactant Flooding

A Literature Review and Experimental Study

Ida Baltzersen Enge

Petroleum Geoscience and Engineering
Submission date: June 2014
Supervisor: Ole Torsæter, IPT

Norwegian University of Science and Technology
Department of Petroleum Engineering and Applied Geophysics

Abstract

The possibility of achieving incremental oil recovery by the use of low salinity injection water has been demonstrated by numerous laboratory experiments and an increasing amount of field trials. The underlying mechanisms behind this phenomenon are not well understood, but many researchers have suggested that it is related to complex crude oil/brine/rock interactions. In recent years, positive results have been presented regarding the combination of low salinity water and surfactant injection. This Thesis aims to investigate the effect of brine composition and rock type on low salinity surfactant injection.

A series of coreflooding experiments were conducted on two different types of outcrop Berea sandstone cores, with different mineral composition, aged with different compositions of brine containing varying concentrations of NaCl, $CaCl_2$ and $MgCl_2$ and one crude oil. The cores were flooded with low salinity brine in secondary mode, and a low salinity surfactant solution, using the anionic surfactant Sodium Dodecylbenzene Sulfonate, in tertiary mode, both performed at 60 °C. Oil recovery and the shape of production curves were analyzed and compared.

The results show a clear trend that oil recovery is highest when the contrast between in-situ- and flooding divalent cation content is highest. Cores saturated with a brine containing 10% divalents, where 9% of this was $CaCl_2$, and flooded with pure NaCl brine, produced the highest amount of oil during low salinity brine injection for both types of Berea cores. The low salinity oil recovery ranged from 42.3 to 57.7% OOIP. Low salinity surfactant injection recovered incremental oil for all the corefloods, varying from 2.1 to 8.5% OOIP. Another observation was that cores aged with brines containing divalent cations appeared to be more oil-wet, and had a larger benefit from the low ionic strength of the injection brine, regardless of the mineral composition of the rock. The shape of the production curve for some of these cores indicated a change in wettability during the low salinity brine injection.

There is an increasing interest in designing an injection brine composition with the aim of recovering maximum amount of oil. Optimized composition can also lead to maximum recovery of a chemical flood. This research was carried out having this mindset. It was observed that by changing the chemistry of the injection brine, while everything else was fixed in the COBR system, there was an 11% difference in in oil recovery in low salinity waterflooding and an 18% difference in final oil recovery after tertiary low salinity surfactant flooding. This reinforces the importance of the brine composition on oil recovery, and presents a basis for further research.

Sammendrag

Muligheten for å oppnå økt oljeutvinning ved bruk av injeksjonsvann med lavt saltinnhold har blitt demonstrert gjennom en rekke laboratorieforsøk og et økende antall feltstudier. De lærde strides om hvilke underliggende mekanismer som ligger til grunn for dette fenomenet, men det er bred enighet om at det er knyttet til komplekse "crude oil/brine/rock" ineraksjoner. I senere år har det blitt publisert oppløftende resultanter angående en kombinasjon av vann med lavere saltinnhold og surfaktanter. Denne oppgaven tar sikte på å undersøke effekten av vannkomposisjon og bergartstype på lavsalinitetsinjeksjon kombinert med surfaktanter.

En serie kjerneflømminger ble gjenomført på to forskjellige Berea sandsteiner med ulik mineralsammensetning. Disse ble mettet med ulike saltvannsløsninger med varierende innhold av NaCl, $CaCl^{2+}$ og $MgCl^{2+}$, og modnet med samme type råolje. Kjerneprøvene ble deretter fløммet med en sekundær lavsalinitetsløsning, etterfulgt av en tertiær surfaktantløsning med samme lave saltinnhold. Surfaktantet som ble brukt var det anioniske surfaktantet Natrium Dodecylbenzen Sulfonat. Hele eksperimentet ble gjennomført ved 60 °C. Oljeproduksjon og formen på utvinningskurvene ble sammenlignet og analysert.

Resultatene viser en klar trend. Oljeutvinningen er høyest når kontrasten mellom divalent kationeinnhold i metningsvann og injeksjonsvann er høyest. Kjerneprøver mettet med saltvann som inneholdt 10% divalente kationer, hvorav 9% var $CaCl_2$, og fløммet med saltvann som kun inneholdt NaCl, produserte den største mengden olje for begge typer Berea sandstein. Oljeutvinningen fra den rene vanninjeksjonen varierte fra 42.3 til 57.7% av opprinnelig olje. Surfaktantløsningen produserte ytterligere olje for alle kjerneprøvene, og utvinningsgraden varierte fra 2.1 til 8.5% av opprinnelig olje. En ytterligere observasjon var at kjerneprøvene som var modnet med saltvann som inneholdt divalente kationer syntes å være mer oljefuktede, og hadde et større utbytte av den lave ioniske styrken til injeksjonsvannet. Dette var uavhengig av mineralsammensetningen til kjerneprøvene. Produksjonekurvene indikerte en endring i fuktegenskaper mot mer vannfuktet for flere av kjerneprøvene.

Det er en økende interesse for å designe saltvannskomposisjoner med mål om å utvinne mest mulig olje. En optimalisert komposisjon kan også føre til maksimal mengde olje for en kjemisk fløммingsprosess. Disse eksperimentene er utført med dette i tankene. Det ble observert at ved å endre den kjemiske sammensetningen til injeksjonsvannet, mens alt annet var konstant, kunne man oppnå en 11% forskjell i oljeutvinning ved ren vanninjeksjon med lavt saltinnhold. En 18% forskjell i endelig utvinningsgrad ble oppnådd etter tertiær surfaktantinjeksjon med samme lave saltinnhold. Dette bekrefter betydningen av vannkomposisjon i forbindelse med oljeutvinning, og legger et grunnlag for videre forskning.

Acknowledgements

First of all I would like to thank my supervisor Professor Ole Torsæter for getting me interested in Reservoir Engineering back in the second year of my Petroleum studies. Without his enthusiasm and communication skills, I might not have ended up working on this very interesting subject. He is always welcoming when I come to talk with him and makes me want to do a better job. I am also deeply in debt to my mentor Hamid Hosseinzade Khanamiri, without whom this project would never have been possible. He is always willing to share his knowledge and tricks, and push me to work harder. Without his help in the laboratory, and with discussions, this Thesis would have looked very different. He has been a true delight to work with, and has become a good friend. I would also like to thank our lab technician Roger Overå for always being willing to help, and answer questions.

My family has been very important throughout this project, always interested in hearing all the last updates and achievements. There have been many long phone conversations including both joy when things were successful, and disappointments when it felt like everything was working against me. They would listen for hours to me rambling on about complicated theory they didn't even understand. They have supported me throughout these months, because they knew how important this was to me. For this, I am very thankful.

Finally, I would like to thank my friends, who have stood by me during the last couple of years, regardless of my sometimes questionable mood. A special thanks goes to Thomas Sahl for an extremely thorough proofreading of my entire Thesis.

All parts of this thesis have been written independently, and in accordance with rules set down by the Examination Regulations made by the Norwegian University of Science and Technology. I hereby declare that this thesis, apart from properly cited quotations, is my own work and contains no plagiarism.

Ida Baltzersen Enge

TRONDHEIM 04.06.14

Date

Contents

Nomenclature

Δp	Differential pressure
γ_{ow}	Oil-water interfacial tension
γ_{so}	Solid-oil interfacial tension
γ_{sw}	Solid-water interfacial tension
ϕ	Core porosity
AN	Acid Number
ASP	Alkali/Surfactant/Polymer
BN	Base Number
$CaCl_2$	Calcium Chloride
CDC	Capillary Desaturation Curve
CMC	Critical Micelle Concentration
COBR	Crude Oil/Brine/Rock
DLE	Double Layer Expansion
E_A	Areal sweep
E_D	Microscopic displacement
E_I	Horizontal sweep
E_R	Overall recovery efficiency
E_V	Volumetric sweep efficiency
EOR	Enhanced Oil Recovery
HS	High salinity water
IFT	Interfacial tension
IOR	Increased Oil Recovery

k_o Effective oil permeability

k_r Relative permeability

k_w Effective water permeability

LS Low salinity water

LSS Low salinity surfactant solution

M Mobility ratio

$MgCl_2$ Magnesium Chloride

MIE Multicomponent Ionic Exchange

N_c Capillary number

NaCl Sodium Chloride

OOIP Original Oil In Place

pH $-\log[H^+]$

PV Pore Volume

PVi Pore volume injected

RB Reservoir Brine

S_o Oil saturation

S_w Water saturation

S_{oi} Initial oil saturation

S_{or} Residual oil saturation

S_{wirr} Irreducible water saturation

SAGD Steam Assisted Gravity Drainage

SAM Scanning Auger electron Microscopy

SDBS Sodium Dodecylbenzene Sulfonate

SWCT Single Well Chemical Tracer

TDS Total Dissolved Solids

USBM United States Bureau of Mines

WBT Water breakthrough

WI Wettablity Index

XPS X-ray Photoelectron Spectroscopy

XRD X-ray diffraction

List of Figures

List of Tables

Chapter 1

Introduction

1.1 Motivation

Waterflooding has been the main secondary production method in the petroleum industry for a long time. The water displaces the oil towards the production wells while simultaneously maintaining the pressure in the reservoir. It is a well known fact that after a conventional waterflooding process of an oil reservoir, a significant amount of oil is left in the reservoir. This may be due to dominating capillary forces or poor sweep efficiency of the injection fluids. This makes it necessary to implement better solutions in order to recover more of the remaining oil.

Enhanced oil recovery (EOR) by chemical injection has long been experiencing a declining interest. The application has been proved technically feasible, but the high cost per barrel of incremental oil has prevented it from being economically viable. Lately, the oil price has risen to a stable high level, which has sparked renewed interest in chemical EOR. New technologies have made cheaper and more efficient chemicals available.

Low salinity waterflooding, in itself, has been shown to be able to enhance oil recovery compared to conventional high salinity waterfloods. Many suggestions for which mechanism causes this effect have been presented over the last decade, but researchers can't seem to agree on what the dominating factor is. The only thing they seem to agree on is that low salinity waterflooding tends to alter the reservoir wettability towards a more water-wet state. Laboratory experiments and field trials have shown conflicting results. Nevertheless, important factors of the crude oil/brine/rock system seems to be the presence of active clay material, the presence of an initial water saturation, and exposure to crude oil to create mixed-wet conditions (Morrow and Buckley 1999).

The knowledge that injection of surfactants can decrease the interfacial tension between oil and water, and thus increase the oil recovery, has been around for a long time. The effectiveness of this process depends on a variety of factors such as salinity, temperature, and oil composition. It can be difficult to tailor a surfactant flood to the salinity normally present in a reservoir. By combining the use of modern surfactants and low salinity water injection, one can reap the benefits

of both the individual effects of each method. The lower salinity can make the surfactant more effective by minimizing surfactant loss by retention, and keep it within a more desirable phase behavior. Promising research has been done on the combination of low salinity waterflooding and surfactant flooding (Alagic 2010; Alagic and Skauge 2010; Alagic et al. 2011), indicating that this may well be the future of surfactant flooding. This research has mostly focused on the injection of pure NaCl brine, so an interesting step further could be to investigate the effect of other injection brine compositions, and how important the mineral composition of the rock itself is to oil recovery.

1.2 Goal

The main goal of this thesis is to obtain information about how different connate and injection brine compositions affect secondary low salinity waterflooding and tertiary low salinity surfactant flooding of initially water-wet Berea sandstones. The brines will contain different fractions of Na^+, Ca^{2+}, and Mg^{2+} ions with the same ionic strength of around 0.556 mol/liter, and a salinity of approximately 31000-32000 ppm. The brine will be diluted to 1/10 of the original high salinity prior to flooding, which corresponds to approximately 3100-3200 ppm total dissolved solids (TDS). The effect of mineral composition and the different bulk clay content of the rock will also be investigated. Another goal for this thesis is to build on the previous research conducted to promote the implementation of low salinity surfactant flooding in the petroleum industry. Hopefully, this can provide useful data for the future research on the topic

1.3 Approach and organization

This thesis is an experimental study with emphasis on oil recovery by different brine and rock compositions. An extensive literature review of both low salinity waterflooding and surfactant flooding has been performed in order to obtain a sound theoretical base for discussions and conclusions. Some of the theoretical content is transferred from the project thesis, carried out the previous semester, and adjusted to be in accordance with the current problem. The thesis will be organized as follows:

- Chapter 2 is an overview of the basic rock and fluid properties of a reservoir.
- Chapter 3 gives an overview of the EOR techniques used in the petroleum industry today, together with recovery efficiency on a macroscopic and microscopic level. It also gives an overview of the different recovery phases including primary, secondary, and tertiary recovery.
- Chapter 4 introduces the concept of wettability, a reservoir property that is central to this study. It includes the definition, the practical importance in regards to oil recovery, as well as how wettability may be altered.

- Chapter 5 contains a literature review of the low salinity waterflooding technique, including previous research on the topic and the proposed mechanisms behind the low salinity EOR effect.
- Chapter 6 contains a literature review of surfactant flooding, including surfactant properties, phase behavior, retention, and previous research regarding the combination of low salinity waterflooding and surfactants.
- Chapter 7 gives a summary of the experimental study. The general preparations necessary to perform the flooding experiments and the main results are presented in this chapter.
- In chapter 8 the results are discussed, analyzed and compared. Relevant literature and similar research by other authors are reviewed to support the discussion.
- Chapter 9 rounds up the thesis by presenting the conclusions drawn from this work.
- Chapter 10 presents further recommendations and proposals of future focus areas.

Chapter 2

Basic Reservoir Properties

Some basic terms from reservoir engineering are important in order to understand flow in porous media. The following topics in this chapter are highly relevant to every experimental study of reservoir processes.

2.1 Porosity

The porosity of a rock is defined as the void volume of the rock's total volume. This volume is unoccupied by grains and minerals, and can therefore hold and transport fluids. There are mainly two types of porosity; absolute porosity and effective porosity. The absolute porosity is the ratio of total void volume to the bulk volume. The effective porosity is the ratio of the interconnected void volume, that can contribute to fluid transportation, to the bulk volume. The porosity is an important factor as it determines the storage capacity of the rock. The definition of porosity is given by Equation 2.1.

$$\phi = \frac{\text{Pore Volume}}{\text{Bulk Volume}} \tag{2.1}$$

There are several factors which influence effective porosity, and the most important are rock type, grain size range, grain packing and orientation, cementation, weathering, leaching, as well as the type, content, and hydration of clay minerals (Zolotukhin and Ursin 2000). Porosity can also be divided into primary and secondary porosity. Primary porosity is formed during the deposition of sediments and is the original porosity. Secondary porosity forms after the sediments are deposited. It is an alteration of the rock, and includes fracturing, cementation, and dolomization (Schlumberger 2013, porosity).

2.2 Absolute Permeability

Permeability is a property of the porous medium and is a measure of the capacity of the medium to transmit fluids (Torsæter and Abtahi 2003). Permeability is a

directional property, and is usually measured in either darcies [D] or millidarcies [mD]. The absolute permeability is regarded as a constant property of the porous medium when a single fluid is flowing through the medium. However, the relationship changes dramatically when there are more than one fluid flowing in the pores. This is called the effective permeability for each of the fluids (Zolotukhin and Ursin 2000). The absolute permeability is denoted k and is defined through Darcy's law:

$$q = -\frac{kA}{\mu}\frac{\Delta p}{L}, \tag{2.2}$$

where q is the flow rate, k is the absolute permeability, A is the cross sectional area, μ is the viscosity of the the fluid, Δp is the differential pressure, and L is the length. Darcy's law is only valid if the following conditions are satisfied:

- 100% saturated with one fluid
- Incompressible fluid
- Laminar flow (valid for low flow rates)
- No chemical reaction between rock and fluid
- Horizontal fluid flow (i.e. eliminate the gravity forces)

The absolute permeability is calculated by rearranging Equation 2.2:

$$k = -\frac{q\mu}{A}\frac{L}{\Delta p} \tag{2.3}$$

2.3 Saturation

Saturation is defined as the ratio of the volume of a certain fluid present in the pores to the total pore volume of the porous medium.

$$S_i = \frac{V_i}{V_p},\ i = 1, ..., n \tag{2.4}$$

where n denotes the total number of fluid phases present in the porous medium. The sum of all saturations is always 1. Saturation is not constant throughout a reservoir. It can be considered as a function of both the position in the reservoir, and the time during production (Zolotukhin and Ursin 2000).

2.4 Viscosity

The molecules of a flowing fluid are subject to frictional interaction, which effectively acts as a force resisting the flow. Viscosity is the parameter defining this internal resistance of a fluid to shear (Zolotukhin and Ursin 2000). Water and oil are called Newtonian fluids, which shows a straight line when plotting shear

stress (x-axis) versus shear rate (y-axis) in a Cartesian coordinate system. For Newtonian fluids, the equation of deformation is given below.

$$\tau = \mu \frac{dv_x}{dy} \tag{2.5}$$

where τ is the shear stress, μ is the fluid viscosity, v_x is the fluid flow velocity in direction x and y is the vertical direction, normal to the flow vector.

There are also a wide range of fluids used in the oil industry that do not act as Newtonian fluids. Examples of these are slurries, suspensions, gels and colloids (Pumps and Systems 2013). For Newtonian fluids, viscosity does not depend on shear rate. If the shear rate changes, the viscosity remains constant. For non-Newtonian fluids however, the viscosity does depend on share rate. Non-Newtonian fluids are usually either shear thickening (dilatant) or shear thinning (pseudoplastic). Figure 2.1 below shows how the different fluids behave with shear stress and shear rate.

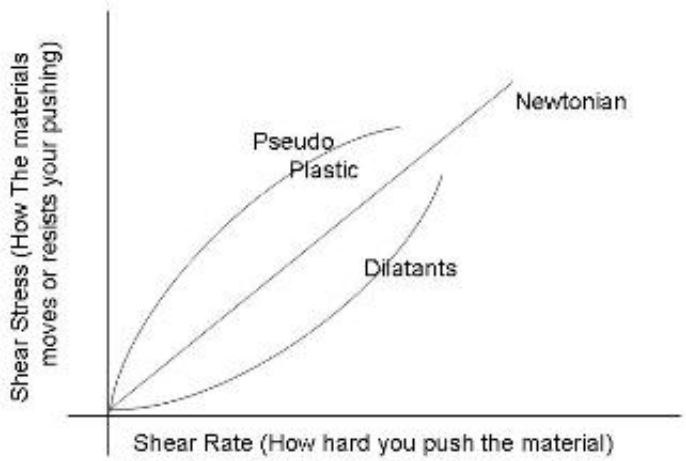

Figure 2.1: Behavior of Newtonian and non-Newtonian fluids (Dispensetips 2013)

2.5 Capillary Pressure

When two immiscible phases (like oil and water) are present in a reservoir, the pressure difference between the phases at the interface is known as the capillary pressure. Capillary pressure is defined as the pressure of the non-wetting phase minus the pressure of the wetting phase, and can for hydrostatic conditions be written as Equation 2.6 below.

$$P_c = P_{nw} - P_w = \rho_{nw} gh - \rho_w gh = \Delta \rho gh \tag{2.6}$$

where ρ is the density of the specific phase, g is the gravitational constant, and h is the depth.

2.6 Surface and Interfacial Tension

Surface and interfacial tension of fluids result from molecular properties occurring at the surface or interface. Surface tension is the tendency of a liquid to expose a minimum free surface (Torsæter and Abtahi 2003). When talking about surface tension, it is the tension at the interface between a liquid and a gas. Interfacial tension (henceforth abbreviated as IFT) is the term used for two immiscible liquids in contact. IFT has a great impact on oil recovery. The higher the IFT between oil and water, the higher the amount of residual oil after primary and secondary production. By lowering the IFT, the forces acting at the oil and water interface are reduced, and the residual oil saturation is thus reduced. A goal in surfactant enhanced oil recovery is to lower IFT to ultra-low values of around 10^{-3} mN/m.

2.7 Relative Permeability

Relative permeability is a term used when there are more than one phase present in a reservoir. The concept is used to relate the absolute permeability of a porous system to the effective permeability of a particular fluid in the system. One fluid will hinder the free flow of the other, which will lead to a lower permeability for each of the fluids. The relationship between effective permeability and absolute permeability is given by Equation 2.7.

$$k_{rj} = \frac{k_{ej}}{k}, \ j = w, o, g. \tag{2.7}$$

When describing fluid flow for multiple phases with the Darcy law, one has to use one equation for each of the fluid phases present, as shown below.

$$q_j = k_{ej} \frac{A}{\mu_j} \frac{\Delta p_j}{\Delta x} \tag{2.8}$$

Where j denotes the fluid phase and k_{ej} is the effective permeability for that particular phase. By manipulating Equation 2.7 above, we get the expression for the effective phase permeability.

$$k_{ej} = k_{rj} k \tag{2.9}$$

This can then be inserted into the flow equation.

Relative permeabilities are strongly related to saturation, and they are usually plotted together in a two-phase relative permeability plot as shown in Figure 2.2 below:

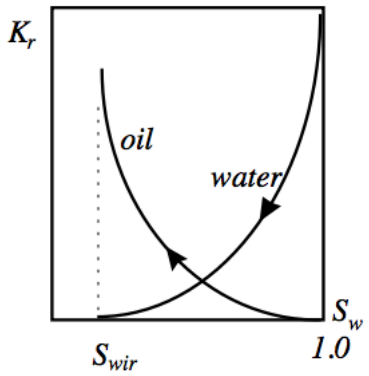

Figure 2.2: Typical two-phase relative permeability curves for oil-water system (Kleppe 2013)

where S_{wir} is the irreducible water saturation. Relative permeability values are strictly between 0 and 1.

Chapter 3

Enhanced Oil Recovery

Enhanced oil recovery is a term used for the injection of fluids in order to recover incremental oil from an oil reservoir. It is often confused with the terms increased oil recovery (IOR) or tertiary recovery. IOR usually means recovering more oil through waterflooding, gas injection or artificial lift techniques. Calling it tertiary recovery is not completely correct either, since EOR techniques can be implemented at any stage in the recovery process. The most common definition of EOR is enhanced recovery by fluids that are not naturally present in the reservoir, such as solvents or chemicals. Oil recovery is traditionally divided into three phases:

- *Primary recovery*: When a reservoir first starts to produce, it is mainly by the natural pressure drive. The bottom-hole pressure in the production wells is usually much lower than the reservoir pressure, and this pressure difference will drive the reservoir fluids towards the wells. This natural drive can be maintained by the expansion of a reservoir gas cap (if the reservoir pressure is below the bubble-point pressure), gravity drainage, or a water drive from an underlying aquifer. It is also possible to install artificial lift, such as an electrical pump or a gas lift installation. However, the reservoir pressure will eventually drop to a level where the hydrocarbons can no longer be produced at an economical level. Primary recovery typically produces around 10% of the initial oil in place, henceforth abbreviated as OOIP (Schlumberger 2013, primary recovery).

- *Secondary recovery*: After primary recovery can no longer produce hydrocarbons at a high enough rate, additional methods have to be implemented in order to maintain reservoir pressure. The most common forms of secondary recovery are waterflooding and/or gas injection. Due to gravity segregation, the gas is injected into a gas cap at the top of the reservoir, and the water is injected in the bottom, in order to sweep oil towards the producing wells. Secondary recovery methods do not have to wait until the primary recovery is no longer effective, but can be implemented at any stage in the production to boost pressure from the beginning. Injection wells are often drilled at the same time as production wells during the development of a field. Secondary recovery methods reaches their limit when considerable amounts of the in-

jected fluids are produced through the production wells and the production is no longer economical. Primary recovery combined with secondary recovery typically produces around 15-40% of OOIP (Schlumberger 2013, secondary recovery).

- *Tertiary recovery*: This is traditionally the third stage of hydrocarbon production, and includes techniques such as miscible gas injection, thermal recovery, and chemical injection. Tertiary recovery is often used as a synonym for EOR. This can be misleading since EOR methods may, as mentioned, be implemented at any stage in a reservoir development (Schlumberger 2013, tertiary recovery). EOR methods seek to improve sweep efficiency, increase oil mobility and reduce IFT between water and oil in a reservoir.

3.1 Recovery Efficiency

In order to understand the different EOR alternatives, it is important to understand the mechanisms that control the recovery of a displacement process. A dimensionless term called recovery efficiency is used to describe this. The overall recovery efficiency of a reservoir is a function of the microscopic displacement efficiency (E_D) and the volumetric sweep efficiency (E_V) (Lake 1989).

$$E_R = E_D E_V \tag{3.1}$$

Recovery efficiency has a value between 0 and 1, where 1 is 100% recovery. Due to the fact that neither displacement efficiency nor sweep efficiency is optimal, the recovery efficiency is usually much lower. In order to increase oil recovery, one, or both of these efficiencies needs to be improved.

3.1.1 Microscopic Displacement Efficiency

The microscopic displacement efficiency relates to displacement or mobilization on a pore scale. There are several trapping mechanisms, and they are known to depend on the pore structure, wettability, capillary forces, relative permeability, and IFT. When injecting, for exapmle, surfactants or nanoparticles into a reservoir, one seeks to improve the microscopic displacement efficiency. Equation 3.2 defines this parameter (Lake 1989).

$$E_D = \frac{\text{Amount of oil displaced}}{\text{Amount of oil contacted by displacing agent}} \tag{3.2}$$

3.1.2 Volumetric Sweep Efficiency

The volumetric sweep efficiency is a measure of the effectiveness of an enhanced oil recovery process. It depends on the volume of the reservoir contacted by the injected fluid. There are many parameters which affect the volumetric sweep efficiency (Schlumberger 2013, volumetric sweep efficiency):

- Selected injection pattern and off-pattern wells
- Fractures in the reservoir
- Position of gas/oil and water/oil contacts
- Reservoir thickness
- Permeability, areal, and vertical heterogeneity
- Mobility ratio
- Density difference between the displacing and the displaced fluid
- Flow rate

The volumetric sweep efficiency is defined as (Lake 1989):

$$E_V = \frac{\text{Volumes of oil contacted by displacing agent}}{\text{Volumes of oil originally in place}} \tag{3.3}$$

The total volumetric sweep efficiency is a function of the areal sweep (E_A) and vertical sweep (E_I), where

$$E_A = \frac{\text{Area contacted by displacing agent}}{\text{Total area}} \tag{3.4}$$

$$E_I = \frac{\text{Cross-sectional area contacted by displacing agent}}{\text{Total cross-sectional area}} \tag{3.5}$$

Both areal and vertical sweep efficiencies are strongly dependent on the fluid mobility. The mobility ratio, M, is defined as the ratio of mobility of the displacing fluid to that of the displaced fluid, usually oil displaced by water, as shown in Equation 3.6.

$$M = \frac{\mu_o}{k_o}\frac{k_w}{\mu_w} \tag{3.6}$$

Here, a mobility ratio less than one is considered favourable. This allows the oil to travel through the reservoir at the same rate as the injected water, preventing the water from "fingering" through the oil and bypassing it through water channels. Since fluid mobility is a function of viscosity, an increase in water viscosity will lower the mobility ratio resulting in a more effective displacement. This can be achieved by adding polymer to the water in order to increase the viscosity and decrease viscous instability. An example of how this might look is shown in Figure 3.1

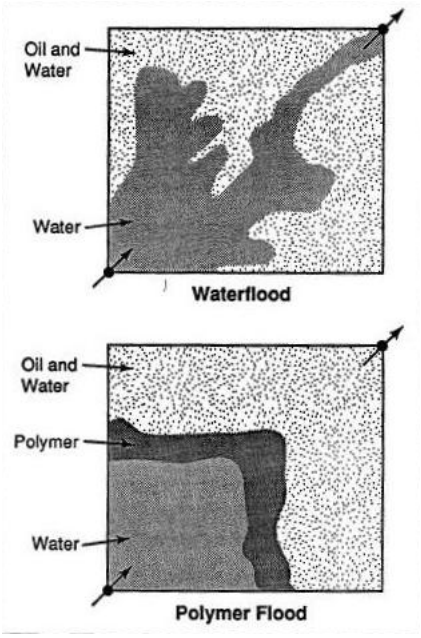

Figure 3.1: Schematic of macroscopic displacement efficiency improvement with polymer-augmented waterflood (ReservoirBlog 2014)

3.2 EOR Categories

Almost all types of enhanced oil recovery methods can be placed in one ore more of three main categories.

Thermal

Thermal recovery means introducing heat to a reservoir in order to lower the viscosity of heavy oil, allowing it to flow more easily to the production wells. This is the most used technique for enhanced oil recovery and accounts for more than 50% of applied EOR in the U.S. (RigZone 2013). The heat is usually provided by steam injection. The heat from the steam breaks up long hydrocarbon chains and lowers the resistance to flow. A widely used technique for recovery of heavy oil is Steam Assisted Gravity Drainage (SAGD). Steam is injected through a horizontal injector and is allowed to soak the reservoir. The steam will rise up in the reservoir and mobilize the otherwise highly viscous and immobile oil. The oil will flow downwards to a horizontal producer due to gravity forces. In-situ combustion is another thermal method, that involves injection of air that eventually will combust, and light the oil in the vicinity of the well on fire. The heat will generate a mobile oil front which moves through the reservoir and mobilizes the heavy oil, so that it can be produced through the production well. Approximately 6-10% of the oil will be consumed as fuel throughout the process.

Chemical

Chemical EOR means that a chemical solution is injected into the reservoir in-order to mobilize the remaining trapped oil. The chemicals injected promotes a decrease in mobility ratio and/or a decrease in the IFT between oil and water in the reservoir. The major chemical flooding processes are polymer flooding, surfactant flooding, alkaline flooding, micellar flooding, and ASP (alkali/surfactant/polymer) flooding. Other methods tested includes emulsion, foam, and the use of microbes, but the impact of these processes have not yet been proved significant (Thomas 2007). Lately, the injection of low salinity water has also been classified as a chemical EOR method. The chemical methods are used primarily to improve the microscopic sweep efficiency of the reservoir.

Miscible/Solvent

Miscible flooding means that the injected fluid is miscible with the reservoir oil either at first contact or after multiple contacts. A narrow transition zone (mixing zone) develops between the displacing fluid and the oil, inducing a piston-like displacement. The mixing zone and the solvent profile spread as the flood advances (Thomas 2007). The main forms of miscible flooding are:

- *Miscible slug process:* A solvent such as propane or pentane is injected as a slug, and then driven by gas or water. This is a single contact miscible process.
- *Enriched gas drive:* Continuous injection of natural gas, flue gas, or nitrogen enriched with C_2-C_4 fractions. These fractions condense into the oil and develop a transition zone. This is a multiple contact miscible process.
- *Vaporizing gas drive:* Continuous injection of natural gas, flue gas, or nitrogen under high pressure (10-15 MPa), where C_2-C_6 fractions in the oil is vaporized into the injected gas. This is a multiple contact miscible process.
- *High pressure gas (CO_2 or N_2) injection:* CO_2 extracts heavier fractions (C_5-C_{30}) from the reservoir oil and develops miscibility after multiple contacts.

Chapter 4

Wettability

4.1 General Aspects

Wettability is defined as the tendency of a fluid to adhere to, or spread onto, a rock surface. Forces of wetting influence hydrocarbon reservoir behavior in many ways, including saturation, multiphase flow and certain log interpretation parameters (Abdallah et al. 2007). When two fluids are present near a surface at the same time, the preferentially wetting fluid will displace the other fluid at the surface, and in the most extreme case, spread over it entirely. When it comes to hydrocarbon reservoirs, one often talks about reservoirs as being either water-wet or oil-wet. Wettability is, however, not like a binary switch where it is the one or the other, but rather a continuum of wetting degrees. Water-wet or oil-wet are just the two extremes of that continuum. If the wetting conditions are neither strongly oil-wet nor strongly water-wet, the balance of forces in the system will result in a contact angle, θ, between the fluids and the solid surface as shown in Figure 4.1 below. On the left, an oil drop on a strongly water-wet surface will form a bead and the contact angle is approximately zero. An intermediate-wet surface, depicted in the center, also forms a bead, but the contact angle comes from the force balance between the interfacial tension terms, which are γ_{so} and γ_{sw} for the surface/oil and surface/water terms, respectively, and γ_{ow} for the oil/water term. On the right, the same oil drop will spread on a strongly oil-wet surface and the contact angle becomes close to 180 ° (Abdallah et al. 2007).

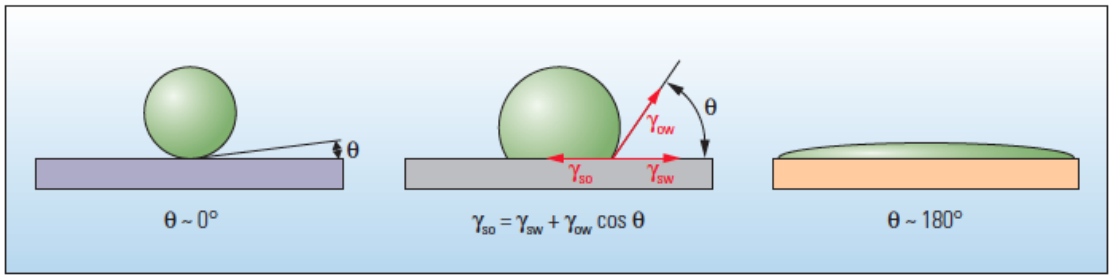

Figure 4.1: Contact angle for an oil drop on a water-wet surface (Abdallah et al. 2007)

It is not uncommon to confuse the terms intermediate wettability and mixed wettability, and to think that they are the same. An intermediate-wet rock does not have a strong preference for one or the other, while mixed wettability means that the rock has a variety of preferences, which may also include intermediate wetting. In a mixed-wet rock, the preference for either oil or water (or gas) can vary from pore to pore depending on saturation history. Understanding the complexity of the wettability term and how it plays a role in oil recovery, is important in order to maximize recovery. Figure 4.2 shows how the different wetting states distributes the fluids in the pore system.

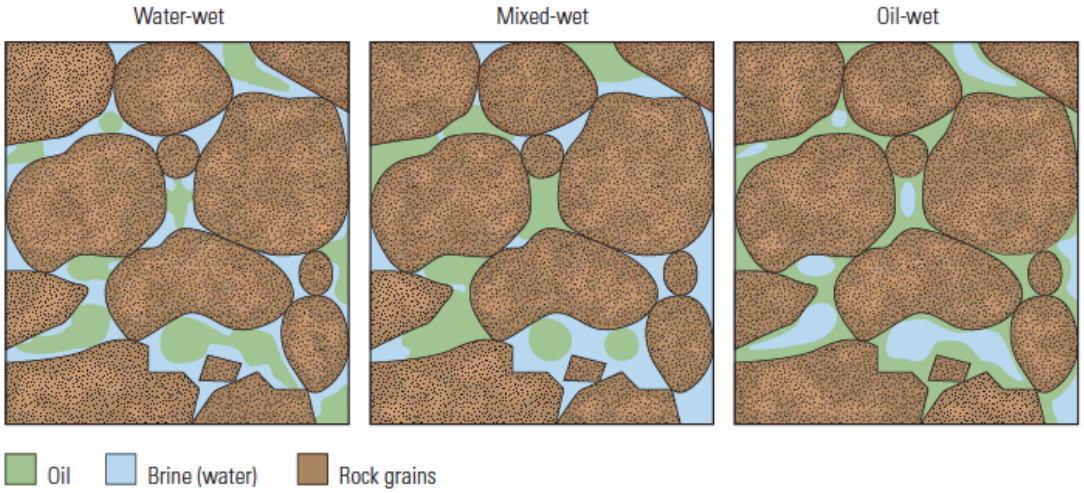

Figure 4.2: Wetting in porous media (Abdallah et al. 2007)

4.2 Practical Importance

The wettability state of a reservoir can have a great impact on both oil recovery and field economics, especially in sandstone reservoirs under waterflooding. The wettability dictates how the fluids are distributed throughout the pore system. In a water-wet reservoir, the pore walls are coated by water, and capillary forces between the oil and water prevents the oil from entering the smaller pores. The oil is therefore usually contained in larger pores. Initially, both oil and water phases are continuous, but after the start of production, the oil may eventually snap off and become trapped inside the pores. This can lead to a high residual oil saturation. However, when implementing waterflooding to maintain reservoir pressure, water breakthrough occurs late and most of the oil is produced before the breakthrough, which has its economical advantages. Factors associated with oil-wet reservoirs are early water breakthrough accompanied by high water cuts and a long tail production, which is not desirable. Even though the residual oil saturation is usually lower in oil wet reservoirs due to the the oil film on the surface creating a continuous oil phase, more money is made by producing the oil at an earlier time.

4.3 Wettability alteration

Historically, porous media of reservoirs have been considered being originally water-wet (Alagic 2010). The most common minerals present in reservoirs - quartz, carbonate and dolomite - are typically water-wet prior to oil migration. When oil migrates into an originally water-wet reservoir, the saturation history changes. Surface wetting is influenced by saturation history, system temperature and pressure, which leads to an equilibrium condition between the three substances: solid, brine and oil. Oil composition is central in changing a water-wet surface towards more oil-wet. Polar crude oil components, especially in the heavy asphaltene and resin fractions, can adsorb on mineral surfaces and alter their wetting properties (Buckley et al. 1998). Buckley et al. (1998) studied the mechanisms of wetting alteration by crude oils through experimental observations of contact angles between pure fluids on flat surfaces after exposure to crude oil. The main categories of crude oil/brine/rock (COBR) interactions identified in that study were:

- polar interactions that predominate in the absence of a water film between oil and solid
- surface precipitation, mainly dependent on crude oil solvent properties with respect to asphaltenes
- acid/base interactions that control surface charge at oil/water and solid/water interfaces
- ion binding or specific interactions between charged sites and higher valency ions

The first mechanism is not very likely to happen in a reservoir, since water is always initially present. Surface precipitation depends on the oil's ability to dissolve its asphaltenes, where poor solubility leads to increasing wetting alteration ability towards less water-wet. The acid/base interactions are based on the presence of a thin water film on water-wet surfaces. When this film is stable, strongly water-wet conditions can be maintained. The part of the water film that is closest to the surface film is often referred to as the electrical double layer. Excess charges on the solid surface are countered by electrolyte ions of opposite charge (Abdallah et al. 2007). The first layer closest to the surface is called the Stern layer. Here, the ions are firmly attached to the surface and no ions are exchanged. The second layer, or the Diffuse layer, is exchanging ions with the bulk water. A graphical representation of the electrical double layer is shown in Figure 4.3.

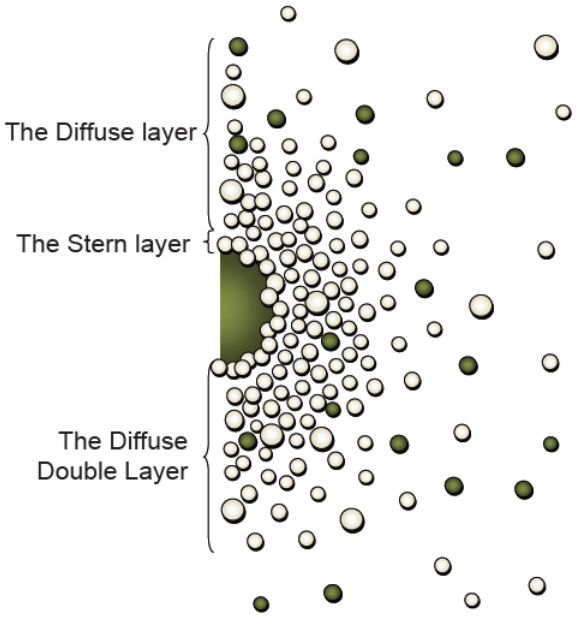

Figure 4.3: Schematic of the electrical double layer (Jansson 2007)

For a given oil or solid surface, surface charge depends on the extent of acid/base dissociation reactions which in turn depends on the pH at the surface (Buckley et al. 1998). A variety of forces, including van der Waals, electrostatic, and structural or solvation interactions, are acting on the solid/brine and oil/brine interfaces. The net force is often expressed as a force per unit area, termed the disjoining pressure (Abdallah et al. 2007). A positive disjoining pressure will keep the interfaces apart, while a negative disjoining pressure will attract the interfaces. When the charges at the two interfaces are the same, repulsive forces will stabilize the water film and crude oil components are not able to adsorb at the solid surface. The presence of dissolved divalent cations, such as Ca^{2+} and Mg^{2+}, may also contribute to destabilization of the water film through ion binding as shown in Figure 4.4:

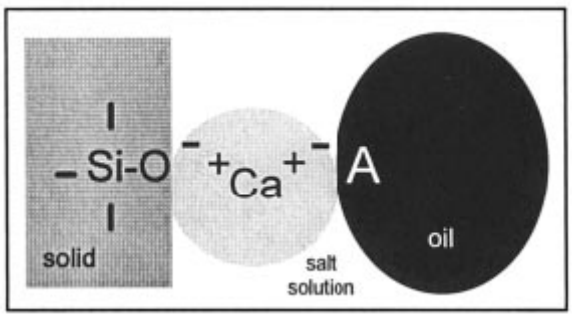

Figure 4.4: Ion-binding interaction between crude oil components and solid surface (Buckley et al. 1998)

4.4 Measuring Wettability

Measuring wettability is done in the lab. Due to the complex pore geometry of the reservoir rock, it is difficult to measure the wettability directly. The most common way of measuring wettability is the contact angle method, where a drop of liquid is placed on a smooth, flat surface, surrounded by another immiscible liquid. If the surface has an extreme preference for water, a water drop surrounded by oil will spread completely on the solid surface. When the opposite is the case, the drop will form a bead where the contact between the drop and the surface is at a minimum. Intermediate wettability results in a balance of forces giving a contact angle between the drop and the surface. A coarse division suggests that contact angles less than 60 - 75 ° are classified as water-wet, whereas contact angles larger than 105 - 130 ° are termed as oil wet. The range of contact angles in between these two extremes is referred to as intermediate or neutral wet (Alagic 2010).

The contact angle method is not very accurate due to the fact that it does not account for the rugosity of the pore system. It may give an indication of the wettability of certain minerals, but a reservoir rock usually comprises several different minerals with different wetting preferences. The single smooth surface used in contact angle measurement is not representative for a bulk rock system.

Another method of measuring wettability, which gives a more accurate result for the rock system, is the Amott-Harvey imbibition method. A core sample, saturated with oil to irreducible water saturation, S_{wirr}, is placed in a cell containing water. The water will imbibe the core sample, and the rate and amount of oil expelled from the core is measured. An experiment like this should last for at least 10 days, but it is usually run much longer (Abdallah et al. 2007). After a given time for imbibition, the sample is placed in a centrifuge or flow cell to force more water through the core, in order to obtain the residual oil saturation, S_{or}. The additional oil recovery by forced imbibition is recorded. The process is repeated with an oil-filled imbibition tube, and then an oil-flooding apparatus (Abdallah et al. 2007). By recording all volumes produced, it is possible to calculate a wettability index, WI (Torsæter and Abtahi 2003):

$$WI = \frac{V_{o1}}{V_{o1} + V_{o2}} - \frac{V_{w1}}{V_{w1} - V_{w2}} \tag{4.1}$$

where V_{o1} is the volume of oil produced during spontaneous water imbibition, V_{o2} is the volume of oil produced during forced water imbibition, V_{w1} is the volume of water produced by oil "imbibition", and V_{w2} is the volume of water produced by oil flooding. Given this equation, the wettability index will be a number ranging from -1 for completely oil-wetting, to 0 for neutral-wetting and, 1 for completely water-wetting. The wettability index can of course be any number along this continuum for different degrees of wetting.

The third standard method for measuring wettability is the US Bureau of Mines (USBM) method. While the Amott-Harvey index is based on the relative change in saturation, the USBM index gives a measure of the energy required to

make the forced displacement. A centrifuge is used to spin the core at stepwise increasing speeds, first with a core at S_{wirr} surrounded by water. After reaching S_{or}, the surrounding fluid is replaced by oil for another set of measurements. The areas between each of the capillary pressure curves and the zero capillary pressure line are calculated, and the logarithm of the ratio of the water-increasing to oil-increasing areas gives the USBM wettability index (Abdallah et al. 2007). The index can in teory range from -∞ to +∞, but most measurement results are in the range of -1 to +1 for strongly oil-wet and water-wet respectively. Figure 4.5 depicts a typical pressure curve for a water wet system where the areas for the USBM index are shown.

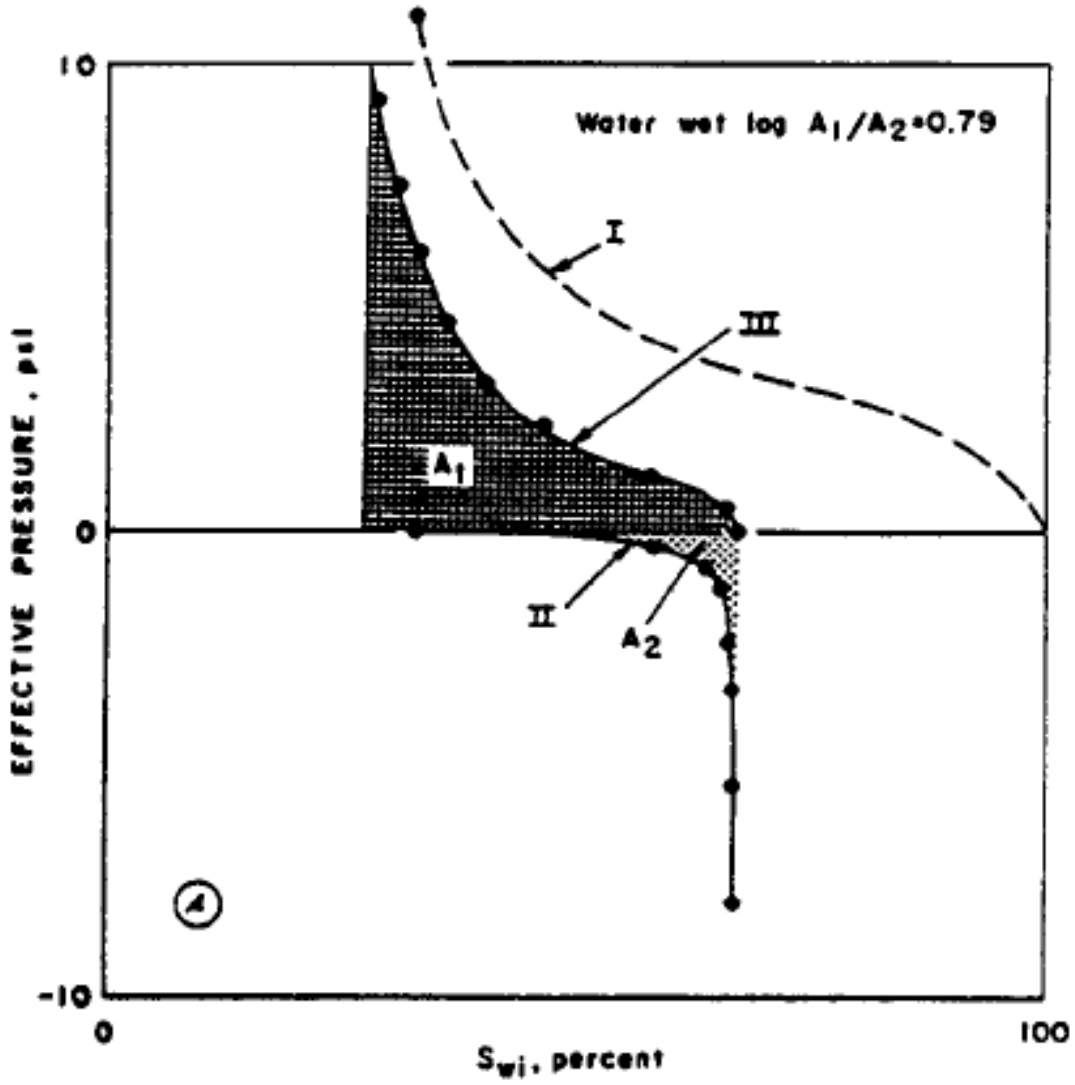

Figure 4.5: Typical pressure curve with under-curve areas for a water-wet system (Torsæter and Abtahi 2003)

When only flooding experiments are performed, mainly due to time constraints, it is also possible to get an indication of the wettability without direct measure-

ments, by studying and comparing the production profiles. The later the breakthrough, the more water-wet the core is, and very little oil is produced after breakthrough. An early breakthrough followed by significant oil recovery is an indication of a more oil-wet core. This also takes into account the entire system of minerals in the core, and gives an indication of the bulk wettability compared to contact angle measurements.

Chapter 5

Low Salinity Waterflooding

Waterflooding has been the most widely used method for enhancing oil production, and is mainly used for pressure maintenance and sweeping of oil through the reservoir. Little thought has been given to the chemistry of the water. The water has normally been provided from the closest and cheapest source, being mainly injection of seawater and re-injection of produced formation water. Injecting fresh water into a reservoir is known to induce swelling of clay particles, resulting in severe reservoir damage and permeability reduction, and has been adviced against. Recent research has shown that the ionic strength and multivalent cation content of the water can have an effect on the oil recovery. In the pH ranges typically encountered in sandstone reservoirs, both the crude oil/brine and the rock/brine interfaces are negatively charged. One would therefore expect repulsion between the interfaces. It is believed that divalent ions are key to the adsorption of oil onto pore surfaces, and may contribute to the S_{or} obtained during a normal high salinity waterflood (Lee et al. 2010). Ca^{2+} and Mg^{2+} can act as cation bridges between the negatively charged oil and rock, binding the oil to the rock surface (see Figure 4.4). Lowering the salinity of the injected water implies a lower concentration of multivalent cations to bind the oil and an expansion of the water layer surrounding the rock. This provides a greater opportunity for the oil to be swept by the imposed flow, thus improving the microscopic sweep efficiency. Research suggests that low salinity waterflooding can be a cheap and effective new method of EOR. Increase in oil recovery by low salinity waterflooding is highly specific to the COBR combinations and much remains to be learned about the recovery mechanisms under various circumstances (Zhang and Morrow 2006).

5.1 Low Salinity Waterflooding History

It is often believed, that lowering brine salinity in order to improve oil recovery is a relatively new theory, but the first experiment testing this hypothesis was published as early as 1967. Bernard (1967) observed increased oil recovery when lowering the sodium chloride content of the injection brine to 0.1%. The research interest fell after this, but over the last couple of decades, extensive research has been carried out on the subject, rejuvenated by Morrow and coworkers (Jadhunandan and Morrow 1995; Tang and Morrow 1997; Morrow et al. 1998; Tang and

Morrow 1999a; Tang and Morrow 1999b). Oil companies such as BP (Lager et al. 2006; Lager et al. 2008; Sorbie and Collins 2010; Lee et al. 2010), Shell (Ligthelm et al. 2009; Suijkerbuijk et al. 2012; Suijkerbuijk et al. 2013; Sorop et al. 2013), Total (Cissokho et al. 2009; Boussour et al. 2009), and Statoil (Ashraf et al. 2010; Skrettingland et al. 2011; Hadia et al. 2012; Hadia et al. 2013) have all shown a great interest in low salinity waterflooding as an EOR method through several research projects.

In the first publication of results from a single-well test, Webb et al. (2004) reported a 25-50% reduction in residual oil saturation when waterflooding with low salinity brine during a log-inject-log field test in a clastic reservoir. Four Single Well Chemical Tracer (SWCT) tests performed in the Ivishak, Kuparuk and Kekiktuk sandstoned of the Alaska North Slope indicated that the benefits of low salinity EOR ranged from 6 to 12% OOIP (McGuire et al. 2005). In 2007, Robertson (2007) published a paper summarizing important historical field evidence of the effect of low salinity waterflooding. This was mostly fields with an unintentional low salinity injection, where the injection water was just retrieved from the cheapest source. Still, the waterfloods provided some evidence of the effect of low salinity injection. The result of this analysis, which included three Minnelusa formation fields, tended to corroborate laboratory results of improved oil recovery potential from low salinity waterfloods, and data showed that oil recovery tended to increase as the salinity ratio of waterfloods decreased. The first comprehensive inter-well field trial was described by Seccombe et al. (2010) to demonstrate that reduced-salinity waterflooding worked as well at inter-well distances as it did in corefloods and single well tests. Pilot oil recovery after 1.6 pore volumes of low salinity water injection was 10% of the total pore volume swept, which was on track towards the 13% predicted recovery from the scaled coreflood recovery profile. In the Omar field in Syria, Vledder et al. (2010) observed dual steps in watercut development during secondary flood application supporting the assumption of a wettability change from oil-wet to water-wet in field scale. The wettability change was associated with an incremental oil recovery of 10-15%. An average of 23.7% of remaining oil left after effluent waterflood was recovered by low salinity waterflood in the Greater Burgan field in Kuwait. These observations were made in two SWCT tests in two reservoirs of the field, and no damage in the injectivity of the wells for the relatively low clay rich zone were observed when reducing the salinity to 5000 ppm (Abdulla et al. 2013).

Not all experimental and field trials have yielded an exclusively successful result. Zhang and Morrow (2006) reported no increased oil recovery in secondary mode for a crude oil/Berea sandstone system, but a significant increase in tertiary mode for the same combination. For another combination of a different crude oil/Berea sandstone, there was a substantial increase in oil recovery in secondary mode, but little additional oil was produced in tertiary mode. Rivet et al. (2010) observed an increase in oil recovery in mixed-wet systems in secondary mode, but none at all in tertiary low salinity injection. Nasralla et al. (2011) also observed a significant improvement in oil recovery by low salinity injection in secondary mode, but none in tertiary mode. In a study by Gamage and Thyne (2011), us-

ing Berea sandstone yielded an increase in recovery by low salinity injection in both secondary and tertiary mode. However, higher oil recoveries were observed when low salinity waterflooding was implemented as a secondary recovery method. Low salinity waterflooding in a reservoir outcrop core also had high oil recovery in secondary mode, but little to no response was observed for tertiary low salinity injection. The attempt by Skrettingland et al. (2011) to identify the potential for low salinity EOR at the Snorre field on the Norwegian continental shelf through coreflooding experiments and a single-well field pilot, resulted in only marginal improvements although all the right conditions seemed to be present for low salinity success. It was believed that the wetting conditions in the Snorre field was naturally close to optimal so that seawater injection was already efficient.

5.2 Proposed Mechanisms of Enhanced Oil Recovery by Low Salinity Waterflooding

In most laboratory experiments, low salinity injection will lead to an increase in oil recovery. There is even some promising data from the field indicating this positive effect. Several mechanisms have been proposed over the years, based on observations from experiments. Still, researchers have not yet been able to agree on the main mechanism behind this increase in recovery. Some of the necessary prerequisites for the observation of the low salinity effect are known, such as presence of formation water, presence of multivalent cations in the formation water, polar components in the oil, and the presence of active clay material in/on the rock (Morrow and Buckley 1999), but these conditions are not sufficient in order to explain the observed experimental results. For some of the cases in the literature, the necessary prerequisites were met, but no low salinity effect was observed (Skrettingland et al. 2011). In order for the hypothesized mechanisms to be *the* exclusive mechanism, they need to be able to explain all the observed low salinity behavior, and the events they predict should be observed consistently during the course of each low salinity flooding experiment (Suijkerbuijk et al. 2012).

The following section will introduce, and try to explain the most prominent proposed mechanisms and why other researchers may disagree with the hypotheses.

5.2.1 Fines Migration

Tang and Morrow (1999a) proposed that the migration of fine particles, mainly kaolinite, might play a key role in the sensitivity of oil recovery to salinity. Several coreflood experiments were performed on both outcrop cores and a reservoir core. The reservoir core was saturated with crude oil and flooded with reservoir brine (RB) to obtain the base case of flooding with connate and injected brine of the same composition. When switching to 0.1 RB, oil recovery increased, and production of fines was observed. The core was subjected to several flood cycles, and the amount of fines produced decreased with each cycle.

A Berea sandstone core was subjected to firing and acidizing in order to stabilize the fines, and neutralize metal oxides formed after firing. Oil recovery by

waterflooding increased markedly with decrease in salinity for Berea, but showed only slight difference for fired and acidized Berea. The results suggested that potentially mobile fines play an important role in the mechanism by which salinity affects waterflood recovery. Bentheimer and Clashach outcrop cores, which contain less clay than Berea and reservoir cores also showed less oil recovery by reduction in salinity. These results signified the importance of clay in oil recovery by low salinity waterflooding. Imbibition experiments done on dry Berea cores fully saturated with oil showed no effect of invading water salinity, which also indicated that the presence of initial water saturation was important for oil recovery by low salinity water. No significant increase in oil production by diluted brine was observed when cores were saturated with refined oil, which indicated that adsorption of polar components from crude oil was necessary.

Tang and Morrow (1999a) concluded that a range of observation, related to oil recovery and wettability, could be explained by assuming that heavy polar components of crude oil adsorbed onto particles and pore walls to obtain mixed-wet fines. Changes in oil recovery with salinity could be partly ascribed to the effect of brine chemistry on the forces needed to strip these particles from the pore walls during the course of waterflooding. The mobilization of the fines would expose the underlying surface, thus increasing the water-wetness of the system, and the previously retained oil droplets attached to these clays would be mobilized, allowing an increase in oil recovery.

Another theory related to fines migration was that when these fines detached and migrated, they would plug pore throats and reduce permeability. This would result in the water having to take different paths through the reservoir, and sweep otherwise unswept zones, to produce more oil. Lemon et al. (2011) investigated the concept that this permeability decline might be used for mobility control during waterflooding. They concluded through modelling that injection of low salinity brine could be used for mobility control to increase sweep efficiency for a given volume of water injected and for reduced early water-cut in layer-cake reservoirs. However, the induced formation damage required an increase in injection pressure.

Even though Tang and Morrow showed that it was possible to have fines migration during low salinity waterflooding, numerous corefloods performed by, for example BP, has shown increased oil recovery without the migration of any fines or significant permeability reduction (Lager et al. 2006). Based on this, it could not be claimed that fines migration was a predominant or necessary mechanism for increased oil recovery by low salinity waterflooding.

5.2.2 pH Variation

Another mechanism for enhanced oil recovery by low salinity injection was proposed by McGuire et al. (2005), suggesting that generation of surfactants from the residual oil at elevated pH levels was the major mechanism behind the increased oil response. The changes in reservoir fluids, fluid/rock interactions, and changes in wettability seemed to be similar to those that occur during alkaline and surfactant flooding. Coreflood experiments done on Berea sandstone cores with a North Sea crude oil was used to illustrate this point. As low salinity water is injected into

the core, hydroxyl (OH^-) ions are generated through reactions with the minerals native to the reservoir, and increase pH of the effluent from around 7 to 8 up to a pH of 9 or more (McGuire et al. 2005). The low salinity injection was therefore believed to decrease interfacial tension between oil and water by the generation of in-situ surfactants due to saponification of the polar or acid material in the crude oil. Like alkaline flooding, the elevated pH increases the water-wetness of the reservoir. However, other researchers in the field have argued that low salinity flooding has also been successful in corefloods with crude oils having an extremely low acid number where alkaline-like waterflooding cannot be effective (Lager et al. 2006; Boussour et al. 2009). Additionally, the oil/brine interfacial tension of the effluent is generally too high for increased oil recovery to have been caused by saponification of oil components (Emadi and Sohrabi 2013).

Another theory related to the variation of pH was proposed by Austad et al. (2010). Clay minerals in the rock, acting as cation exchangers, played a central role in this mechanism. As the low salinity water invades the pore space, causing a disturbance of the brine-rock interactions equilibrium, a localized increase in pH at the clay surface is caused by the desorption of active cations, especially Ca^{2+}, which is substituted by H^+ from the water. A fast reaction between OH^- and the adsorbed acidic and protonated basic material will cause desorption of organic material from the clay, which in turn increases the water-wetness of the rock and thus increases oil recovery. The substitution of Ca^{2+} by H^+ is illustrated by Equation 5.1 below.

$$\text{Clay}Ca^{2+} + H_2O = \text{Clay}H^+ + Ca^{2+} + OH^- \tag{5.1}$$

The local increase in in pH close to the clay surface causes reactions between adsorbed basic and acidic material as shown by the ordinary acid-base proton transfer reactions in Equations 5.2 and 5.3.

$$\text{Clay}NHR_3^+ + OH^- = \text{Clay} + R_3N + H_2O \tag{5.2}$$

$$\text{Clay}RCOOH + OH^- = \text{Clay} + RCOO^- + H_2O \tag{5.3}$$

The main problem with the mechanism of elevated pH is the natural occurrence of CO_2 in most petroleum reservoirs, which acts as a proton buffer, rendering an increase in pH up adequate levels for surfactant generation unlikely, if not impossible. Proton buffering due to the desorption of proton from oxides will also act as a proton buffer, making it even more difficult (Lager et al. 2006). The local pH increase suggested by Austad et al. (2010) is also questioned. Suijkerbuijk et al. (2012) performed a series of spontaneous imbibition experiments that directly contradicted this. As the pH did not consistently rise during each experiment, pH effects might just as well be interpreted as a result of the low salinity effect rather than its cause. In some of the experiments, there was even a substantial decrease in pH while significant incremental oil was produced. They discussed that the hypothesis of Austad et al. (2010) also implied that polar oil components and divalent

cations are competing to bind to rock surfaces instead of aiding each other. This was not in line with their observations in which increasing divalent cation content of formation brine resulted in more oil wetness. It was also pointed out that Na^+ interference in the pH measurements during low salinity experiments could give improper values of pH. In most measurements, the pH is actually not measured, but rather electrode potentials, and pH is inferred from this. In addition to protons, Na^+ ions can penetrate the glass electrode and create a potential difference between the outer and inner surfaces of the electrode and replace protons, which in turn suppresses the true pH value (Suijkerbuijk et al. 2012). The proposal of elevated pH as the main mechanism behind enhanced oil recovery by low salinity waterflooding has therefore not been accepted in the general literature.

5.2.3 Multicomponent Ionic Exchange

In 2006, Lager et al. (2006), launched another mechanism called Multicomponent Ionic Exchange (MIE). This theory involved the competition between all the ions in the pore water for the mineral matrix exchange sites. Tests performed by BP and the Heriot Watt University observed a decrease in cation concentration in the effluent compared to the invading and connate brine. This indicated that divalent cations (mainly Mg^{2+} and Ca^{2+}) were adsorbed by the rock matrix.

On an oil-wet surface, organo-metallic complexes will be formed by bonding of multivalent cations to polar compounds in the oil. This is known to promote oil-wetness in petroleum reservoirs. At the same time, some organic polar compounds will be adsorbed directly onto the mineral surface, displacing the most liable cations at the clay surface, which in turn enhances the oil wetness of the clay surface (Lager et al. 2006). Injection of low salinity brine is believed to result in MIE, where polar organic compounds and organo-metallic complexes are removed from the surface and replaced by uncomplexed cations. This should, in theory, result in a more water-wet surface and thus increased oil recovery.

The theory was tested by Lager et al. (2006) by removing all the multivalent cations present at the mineral surface by flushing with only NaCl brine. After oil saturation and aging, the core was flooded with a high salinity NaCl brine followed by a low salinity NaCl brine, and finally a low salinity brine containing Ca^{2+} and Mg^{2+}. If MIE was to be the dominating mechanism, the primary high salinity flood should yield a higher oil recovery due to the absence of oil adsorption. Subsequently, the secondary low salinity injection should not recover any additional oil because all the mobile oil would have been displaced by the primary flood and no organo-metallic complexes are present to be desorbed. Finally, the tertiary low salinity injection containing some divalents should not produce any oil, as only non-complexable monovalent cations would be desorbed from the mineral surface by the divalent cations in the injection brine. All these predictions were fulfilled by the experiments, and it was therefore concluded that MIE was the predominant mechanism behind increased oil recovery by low salinity brine injection.

Although this seemed to be a logical conclusion, Suijkerbuijk et al. (2013) was not convinced that this could be the main mechanism. They argued that as a

direct consequence of ion exchange in the reservoir, a "self-freshening zone" is created separating the virgin reservoir from the injected water composition by several pore volumes. This was then confirmed by calculations using PHREEQC[1], which showed that injection of low salinity brine into a higher saline formation would lead to three separate water zones as presented in Figure 5.1: The original high salinity formation water; the low salinity brine, stripped from multivalent cations (self-freshening zone); and the low salinity brine as injected. This figure shows schematically the evolution of the solution normality of the brine and the fraction of divalent cations on the calys as the low salinity slug moves through the reservoir. This process creates a "salinity front" and a "retardation front" (Suijkerbuijk et al. 2013).

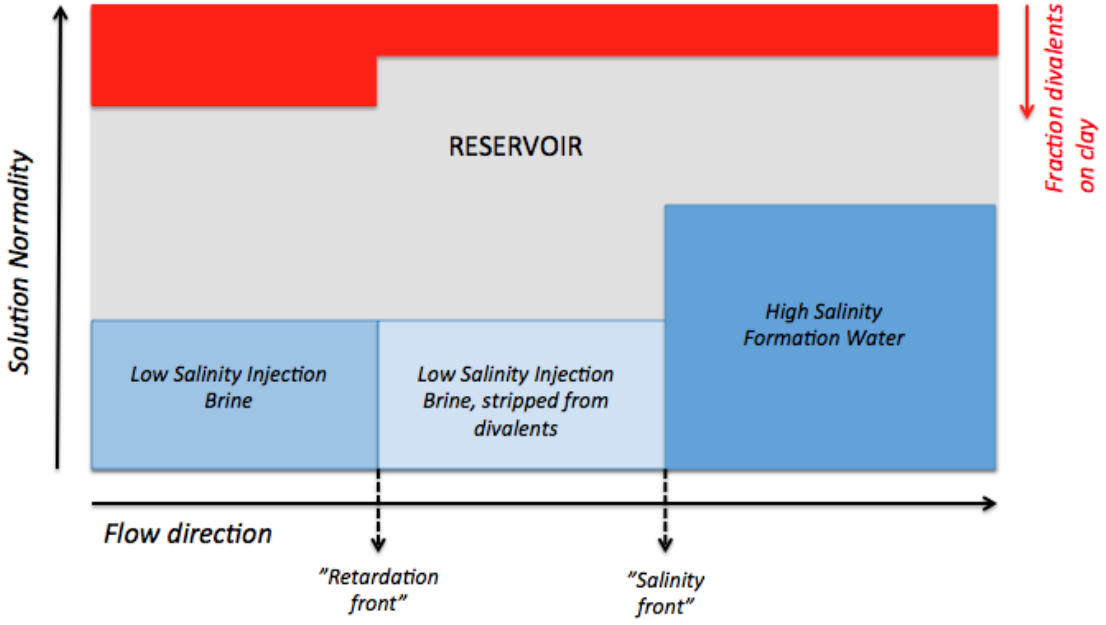

Figure 5.1: Schematic of water zones, adapted from Suijkerbuijk et al. (2013)

In a low salinity environment, divalent metal ions bind more strongly to the clays than in a high saline environment. This leads to the stripping of the divalent ions in the injected low salinity brine, which again leads to a retardation of the divalents with respect to the low salinity brine they were injected in, moving with the salinity front (Suijkerbuijk et al. 2013). This would mean that MIE could only take place at the retardation front. In an inter-well field trial, performed in the Alaskan Endicott field, reported by Seccombe et al. (2010) the timing of the drop in water cut coincided with the breakthrough of low-salinity water at the producer, which implied that the incremental oil was produced at, or just after, the breakthrough. The same was reported by Vledder et al. (2010) from the Omar Field in Syria. Consequently, the increase in oil recovery at the Salinity front could not be due MIE, as the cation exchange happened several pore volumes behind

[1]Geochemical modelling software available from the US Geological Survey

at the retardation front and would render the method economically unattractive. Something else had to be responsible for the oil recovery at the salinity front, which, by Ligthelm et al. (2009), was proposed to be the Double-Layer Expansion mechanism, further elaborated in the following section.

5.2.4 Double-Layer Expansion

As mentioned in the previous chapter, the electrical double layer is considered to be the part of the water film coating the surface of a water-wet material that is closest to the surface (Abdallah et al. 2007). The innermost layer is the Stern layer, containing strongly bound ions of either positive or negative charge. The outer layer, or diffuse layer, contains ions in random motion suspended in the adjacent fluid. The distance over which the ion distribution/concentration differs from the bulk value is referred to as the double layer thickness (Lee et al. 2010). This thickness has been found to be dependent on the electrolyte concentration and ion valency of the fluid, which increases with decreasing ionic strength and ion valency. This is illustrated in Figure 5.2.

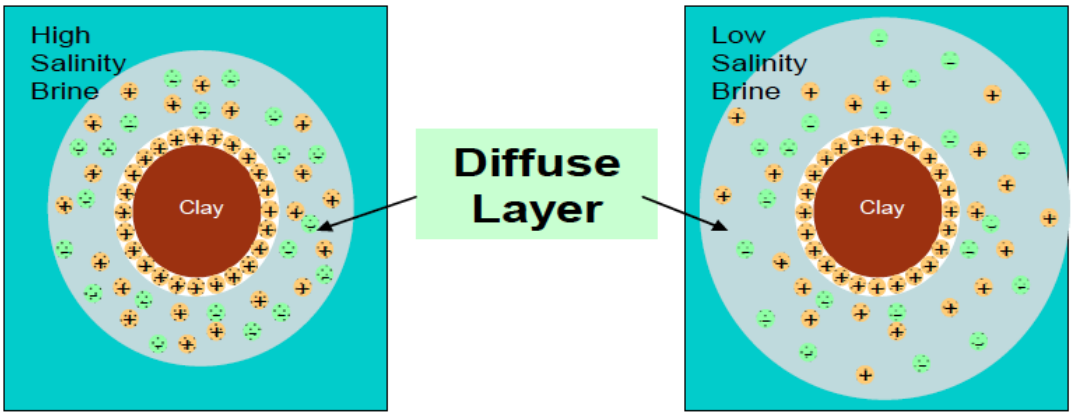

Figure 5.2: Impact of salinity on electrical double layers (Lee et al. 2010)

Ligthelm et al. (2009) performed flooding experiments on Middle Eastern Sandstone cores. Based on theoretical arguments, it was believed that the expansion of the electrical double layers that caused the increased oil recovery. To test this hypothesis, a coreflood experiment was conducted in five stages. Stage 1 involved the injection of over 50 pore volumes of high salinity formation water containing both Na^+, Ca^{2+}, and Mg^{2+}. During this stage, a certain fraction of the clay particles was expected to become occupied by the multivalent cations. The next stage was to inject around 30 pore volumes of pure NaCl brine with the same ionic strength as the first high salinity brine. Some incremental oil recovery was observed while the multivalent cations were flushed out of the rock, but only an insignificant amount. This showed that merely flushing out the multivalent cations, without double-layer expansion by significant reduction in ionic strength, was not sufficient to significantly change the wettability to a more water-wet state and

obtain a significant increase in oil recovery. The third stage involved the injection of a $1/100^{th}$ dilution of the pure NaCl brine. As both the clays and the solution now only contained Na^+, no cation exchange or stripping effects were expected to occur, and thus, there should be no incremental oil recovery, based on MIE theory. Nevertheless, a significant amount of oil was produced during this stage, indicating further removal of hydrocarbons from the clays and change to a more water-wet state. Two additional stages involving low salinity brine with varying amount of Ca^{2+} did not yield any incremental oil recovery due to the suppression of double layer expansion. Ligthelm et al. (2009) therefore concluded that even though cation exchange processes may be partly responsible for the wettability change, the major contribution to such wettability modification would have to come from sufficient reduction in the ionic strength of the brine and therefore increased repulsive electrostatic forces due to double layer expansion.

As of today, the is no definite agreement on which mechanism is dominant in improving oil recovery, but the double-layer expansion and the multicomponent ionic exchange are the two most accepted hypotheses for wettability alteration towards more water-wet (Emadi and Sohrabi 2013). However, a very recent study shows that there are additional mechanisms that could possibly contribute to the low salinity EOR effect, as presented in the next section.

5.2.5 Water Micro-Dispersions

The early assumption that the presence of significant clay fraction is required for improved oil recovery by low salinity waterflooding has resulted in very little attention towards one of the most direct technique of wettability investigations, namely flow visualization test using glass micromodels. However, recent work has shown that there can be advantages of low salinity waterflooding even in clean, or carbonate systems without, or with very low clay content. Yousef et al. (2012) showed that injection of diluted seawater was able to change the surface charge of carbonate rock, and eventually alter rock wettability, resulting in up to 10% additional oil recovery. Pu et al. (2008) reported up to 9.5% additional recovery by injection of low salinity coalbed methane water in sandstone cores with very low clay content.

Based on this, Emadi and Sohrabi (2013) wanted to challenge the old assumption and investigate low salinity waterflooding from a novel perspective by the use of glass micromodels. The main observation from the experiment was the formation of dark material at the oil/water interface during injection of low salinity brine, which was later identified as water micro-dispersions as shown in Figure 5.3 below. These water micro-dispersions were not observed during injection of high salinity brine. In water-wet pores, the water micro-dispersions were formed and segregated, and settled at the bottom of isolated oil ganglia. This did not result in any redistribution of fluids or additional oil recovery. In slightly oil-wet pores, however, this was observed and attributed to the release of surface active components from the oil/water interface. In aqueous phase, surfactant monomers aggregate with their hydrophilic heads pointing outwards towards the solution

and their hydrophobic tails pointing inwards (see Chapter 6 for more information about surfactants). However, if the bulk phase is non-aqueous, inverse micelles (water micro-dispersions) may form with polar heads pointing inwards into a water core (Emadi and Sohrabi 2013). Two new mechanisms by which the release of surface active components from oil/water interface and formation of water micro-dispersions could contribute to increased oil recovery were presented based on the micromodel observations; (1) wettability alteration due to a change in the balance between binding and repulsive forces between oil/water and rock/water interfaces and, (2) swelling of high salinity connate water droplets due to micro-dispersion coalescence at the oil/high salinity water interface.

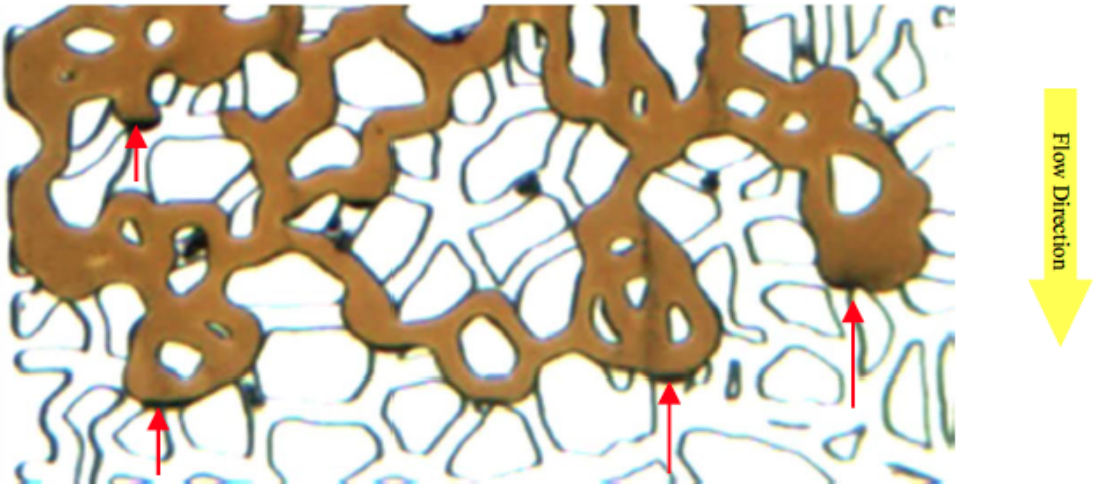

Figure 5.3: A highly magnified section of the micromodel which clearly shows formation and precipitation of dark particles (water micro-dispersions) in the oil phase during low salinity waterflooding (Emadi and Sohrabi 2013)

This hypothesis broadens the application of low salinity water injection and shows that a significant clay fraction may not be necessary for increased oil recovery. It can open up a whole new portfolio of potential low salinity EOR projects worldwide.

Chapter 6

Surfactant Flooding

6.1 Surfactant Flooding History

The concept of injecting surfactants in order to reduce the interfacial tension between oil and water is not new. Uren and Fahmy (1927) showed, through laboratory experiments, that the injection of various solutions of water-soluble flooding agents could indeed lower the interfacial tension between the oil and flood-water, which lead to an increase in oil recovery efficiency. It was also assumed that these flooding agents could change the wettability of the mineral surface. In the same year, a patent was issued to Atkinson (1927) which proposed the use of aqueous solutions of soap or other materials to decrease the surface tension between oil and water to increase oil recovery.

In the 1960's, two different approaches stimulated significant advances in surfactant EOR; surfactants made by direct sulfonation of aromatic groups in refinery streams or crude oils, or by organic synthesis of alkyl/aryl sulfonates which allowed for the surfactant to be tailored to the reservoir of interest. The other approach involved injection of a surfactant formulation made of a petroleum sulfonate and alcohol in an aqueous electrolyte solution (Hirasaki et al. 2011). Taber (1969) formulated that the oil removed from a reservoir was a unique function of the ratio $\Delta P/L\sigma$, where ΔP is the pressure drop across the distance L, and σ is the IFT between the oil and water. It was found that no residual oil can be removed from a porous rock until a critical value of $\Delta P/L\sigma$ is exceeded. Either increasing the differential pressure or decreasing the IFT would result in incremental oil recovery. Foster (1973) concluded, from field studies, that a tertiary oil bank could form in a reservoir using low-tension surfactants. He also concluded that mobility control immediately behind the bank was essential to insure that a significant fraction of the mobilized oil would be driven to producing wells. Melrose and Brandner (1974) indicated that ultra-low values for the water-oil interfacial tension were required in order to achieve improved recovery. At typical reservoir velocities, IFT between crude oil and brine had to be reduced from 20 to 30 mN/m to 0.001 to 0.01 mN/m in order to achieve very low values of residual oil saturation (Hirasaki et al. 2011). It was also discovered that systematic variations of IFT were achieved when changing variables such as salinity, oil composition, and temperature (Foster 1973; Hill et al. 1973; Cayias et al. 1977). An important contribution was the work of Healy

et al. (1976), who identified the three basic types of multiphase systems, labeling phase transitions that occurred when changes were made in salinity, temperature, oil composition, surfactant structure, cosolvent, and dissolved solids in the aqueous phase. They established a relationship between IFT and microemulsion phase behavior, and IFTs were found to correlate with the solubilization parameter for the various microemulsion phases, a result that could substantially reduce the number of IFTs that had to be determined experimentally for a given application.

From the mid-1980s until present day, the oil price experienced a massive drop, and the interest in surfactant EOR decreased due to high cost per barrel of incremental oil. The recent increase in oil price, together with new technologies to produce cheaper and more efficient chamicals, has renewed this interest. Combining surfactants with alkali and polymer (ASP flooding) has shown a positive synergy effect where less surfactant is needed (Sheng 2013), and the combination of low salinity waterflooding and surfactants has given encouraging results (Alagic 2010). This indicates that there is a future for the application of surfactants for enhanced oil recovery.

6.2 Capillary Number and Desaturation Curve

Studies have shown that there is a correlation between residual oil saturation and the dimensionless ratio between the viscous and the capillary forces, today known as the capillary number, derived from the original ratio presented by Taber (1969). The ratio is given by Equation 6.1:

$$N_c = \frac{u\mu}{\sigma} \tag{6.1}$$

where u is the Darcy velocity, μ is the viscosity of the displacing fluid, and σ is the IFT between the oil and surfactant solution (Skjæveland and Kleppe 1992). The larger the capillary number, the lower the residual oil saturation. Theoretically, there are three ways of increasing capillary number based on the equation above; increasing displacement velocity, increasing the viscosity of the displacing fluid, or lower the interfacial tension. However, it may not be practical to increase velocity or viscosity by such a magnitude, because doing so would require, or result in a very high pressure difference between the injector and the producer. Such a high pressure difference could fracture the formation (Sheng 2011). This shows that the only practical way of increasing the capillary number is to decrease the IFT, which can be achieved by injecting surfactants.

The capillary desaturation curve is a plot of residual saturation versus capillary number as shown in Figure 6.1. This plot also shows the difference in capillary desaturation for wetting phase and non-wetting phase displacement. Desaturation will start at a lower value of N_c for the non-wetting phase than for the wetting-phase displacement, illustrated in Figure 6.1(a). The value of N_c when desaturation starts is called the critical N_c. Pore-size distribution will also affect the desaturation curves as shown in Figure 6.1(b). As pore-size distribution becomes more narrow, the oil saturation starts to drop at a higher N_c, but zero residual oil saturation is obtained at a lower N_c (Skjæveland and Kleppe 1992).

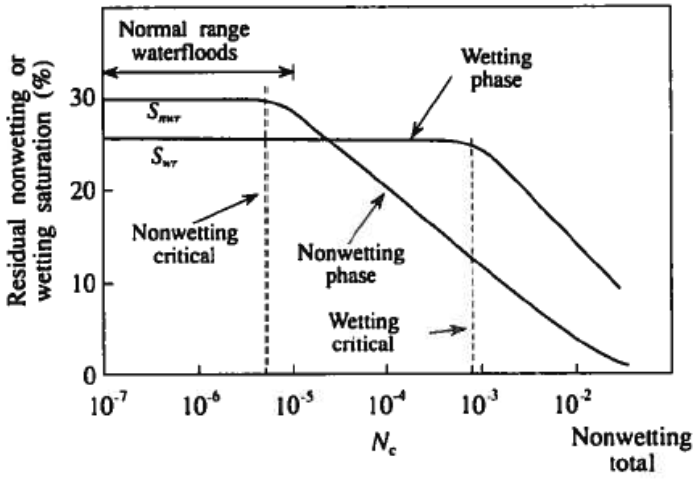

(a) Effect of wettability on residual oil CDC

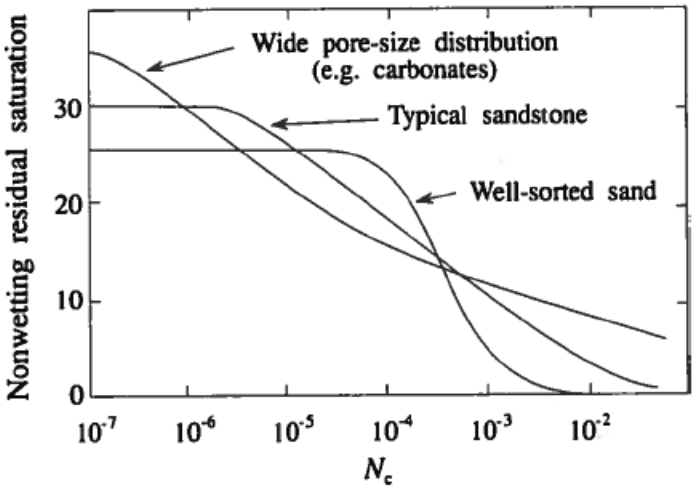

(b) Effect of pore-size distribution on CDC

Figure 6.1: Characteristic capillary desaturation curves (Skjæveland and Kleppe 1992)

6.3 Surfactant Properties

The word "Surfactant" is an abbreviation of the term "surface active agent". A typical surfactant molecule (also known as an amphiphilic molecule) is dualistic in nature and consists of a polar hydrophilic "head", and a non-polar hydrophobic/lipophilic "tail" (Sheng 2011). This property allows the molecule to be soluble in both water and organic solvents. They are known to spontaneously aggregate into a variety of microstructures in order to minimize unfavorable solvophobic interactions, known as micelles. The hydrophobic part of the surfactant may be either branched or linear (Alagic 2010). There are four classifications of surfactants based on the ionic nature of the head group:

- *Anionic*: The surface-active portion has a negative charge and is therefore relatively resistant to adsorption onto sandstone rock surfaces, which also have a negative charge. They are effective at reducing IFT, stable, and inexpensive. These properties combined makes this type the most widely used surfactant in chemical flooding operations (Zolotukhin and Ursin 2000).

- *Cationic*: The surface-active portion has a positive charge and will therefore heavily adsorb to sandstone rock and clays. High adsorption will lead to high surfactant losses, and will not be economical. They can, however, be used in carbonate reservoirs to change the wettability from oil-wet to water-wet (Mwangi 2010).

- *Nonionics*: The surface-active portion of this type of surfactant has no charge. They have, until now, been mostly used as co-surfactants, but increasingly as a primary surfactant. The nonionics are also more tolerant of high salinities than anionics (Mwangi 2010).

- *Amphoteric/Zwitterionic*: This type of surfactant contain two surface-active groups, and can be either nonionic-anionic, nonionic-cationic, or anionic-cationic. Amphoteric surfactants have a high tolerance for temperature and salinity, but they are very expensive (Sheng 2011).

6.3.1 Self-assembly of Amphiphiles

When surfactants are added to an aqueous solution, they first occur as single molecules, so called monomers. As the surfactant concentration increases, the lipophilic moieties of the surfactant begin to associate among themselves to form aggregates or micelles, containing several monomers each (Lake 1989). The plot of surfactant monomer concentration versus total surfactant concentration is shown in Figure 6.2:

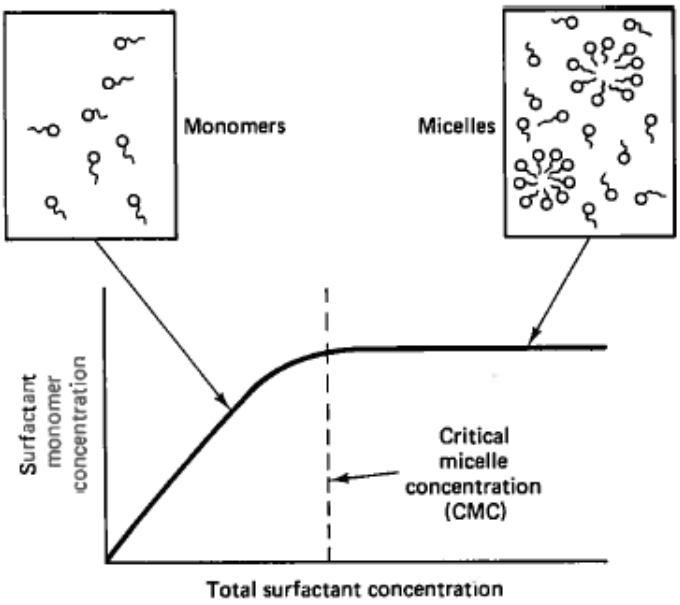

Figure 6.2: Critical micelle concentration (Lake 1989)

The monomer concentration increases linearly with total surfactant concentration until it levels out at the critical micelle concentration (CMC). The value of CMC is typically very low, about 10^{-5} to 10^{-3} kg-moles/m^3 (Lake 1989). After reaching the CMC, an increase in surfactant concentration will only result in an increase in micelle concentration. The hydrocarbon chains sequester themselves inside the aggregate, orienting the polar head groups toward the aqueous phase. Self-aggregation of the surfactant molecules into the sperical micelles is accompanied by a sharp decrease in IFT (Alagic 2010). Organic molecules can be solubilized in the non polar interior of such micelles (Skjæveland and Kleppe 1992). Further addition of surfactant after the CMC is reached will simply increase the number of micelles, but when the concentration reaches a certain level the micellar solution will reach a saturation point. At this point, intermicellar repulsions will induce micellar growth rather than create more micelles, to allow better packing of the micelles. New aggregate structures can form based on the balance between the non-polar and polar parts of the surfactant molecules. A variety of shapes are shown in Figure 6.3 below. Inverted micelles, where the polar heads are oriented towards the center of the micelle and the non-polar hydrocarbon tails are facing outwards, can occur if the bulk phase is non-aqueous. These inverted micelles can carry a droplet of water in their interior. If the ionic strength of the water is lowered, polar components may leave the oil/water interface towards the bulk of the oil phase. This results in formation of a large number of inverted micelles (Emadi and Sohrabi 2013).

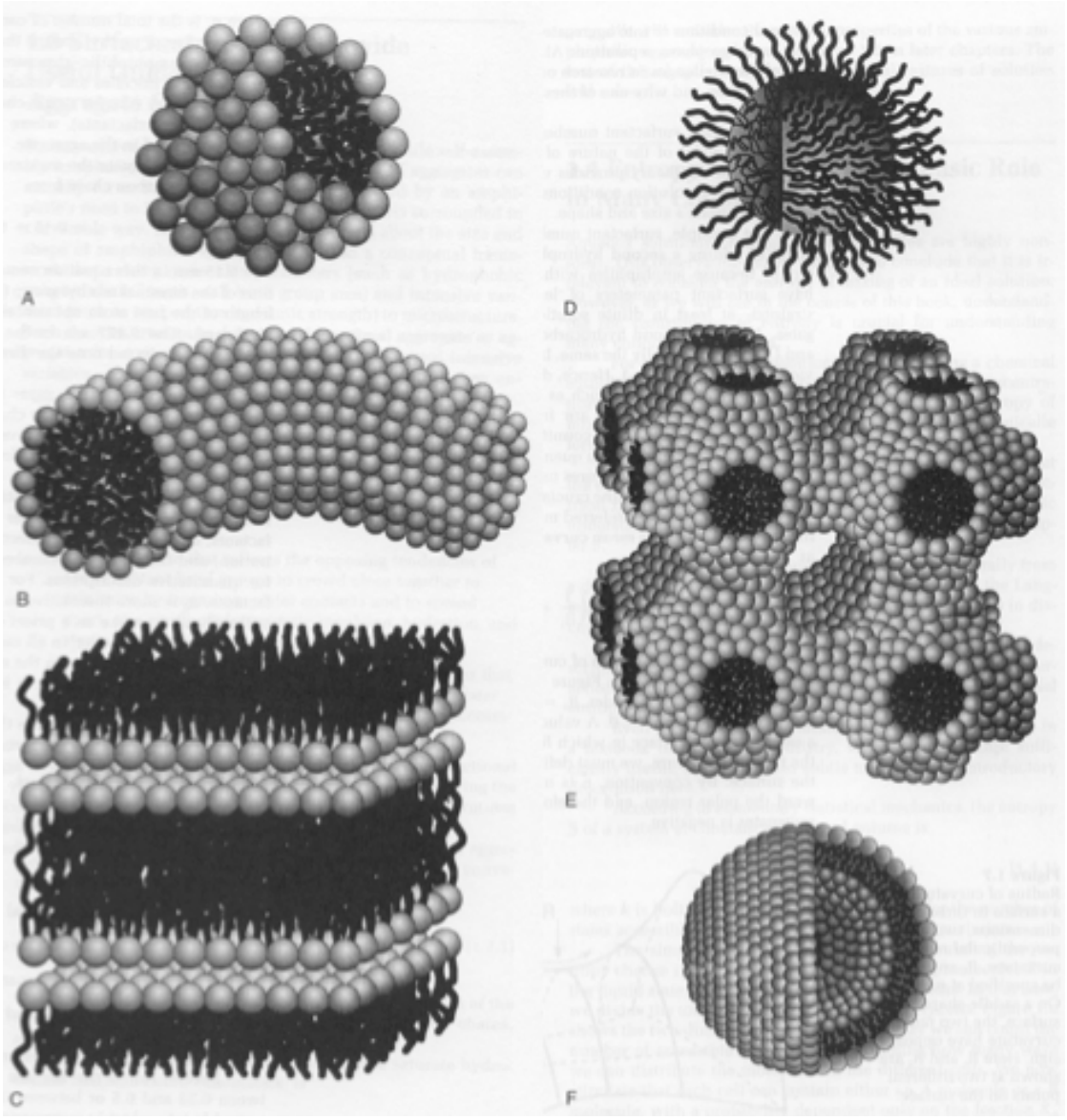

Figure 6.3: Amphiphilic aggregate structures: (A) Spherical micelles, (B) cylindrical micelles, (C) planar bilayers, (D) inverted micelles, (E) bicontinuous structures, and (F) vesicles. (Evans and Wennerström 1999)

6.3.2 Phase Behavior

Three different types of phase systems can form, depending of the salt concentration in the brine. In general, increasing the salinity of the brine decreases the solubility of the anionic surfactant in that brine. Microemulsions, in contrast to ordinary emulsions, are thermodynamically stable and form during simple mixing of water, oil, and surfactant, and do not require the high shear conditions generally needed in the formation of standard emulsions (Sheng 2011).

Type II(-) System

When salinity is low, the surfactant will exhibit a good solubility in the water phase and poor solubility in the oil phase. The system separates into an excess oil phase and a water-external microemulsion phase, where the oil phase rests on top of the microemulsion phase due to the density difference. This is also called lower-phase microemulsion. The different phase types can be represented in a ternary diagram as shown in Figure 6.4:

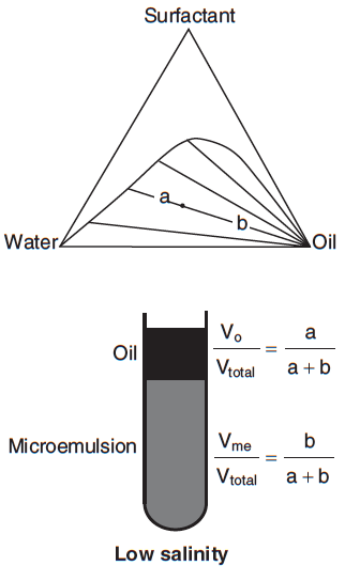

Figure 6.4: Lower-phase microemulsion (Sheng 2011)

The phase environment is called *type II(-)* system because (Zolotukhin and Ursin 2000)

- only two phases can form near the oil-brine boundary
- the tie lines in the two-phase region have *negative* slopes

It is also not uncommon to encounter the name "Windsor type I" in the literature. This type of phase behavior is not favorable for achieving ultra-low IFTs in surfactant EOR.

Type II(+) System

At high salt concentrations, electrostatic forces of the brine drastically reduce the surfactant solubility in the aqueous phase. The system separates into an excess brine phase and an oil-external microemulsion phase, where the microemulsion phase rests on the top of the oil-external phase. Because of this, it is also often called an upper-phase microemulsion. The ternary diagram for this phase type is shown in Figure 6.5 below

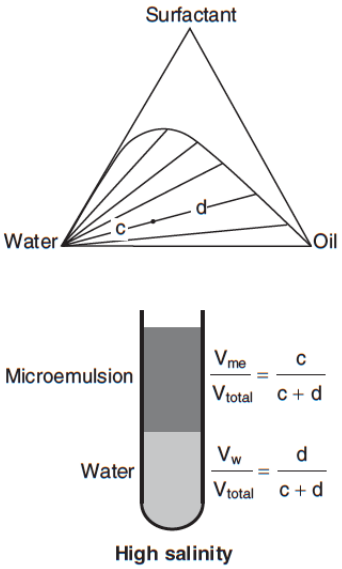

Figure 6.5: Upper-phase microemulsion (Sheng 2011)

The phase environment is called *type II(+)* system because (Zolotukhin and Ursin 2000)

- only two phases can form near the oil-brine boundary
- the tie lines in the two-phase region have *positive* slopes

It is also normal to encounter the name "Windsor type II" in the literature. The formation of a water-in-oil emulsion in the oil phase may lead to surfactant retention in the oil phase, which can retard the whole displacement process. This is not a favorable phase behavior for enhanced oil recovery.

Type III System

At intermediate salt concentrations a third surfactant-rich phase can form. The system separates into three phases: excess oil, microemulsion, and excess water. In this case, the microemulsion phase resides between the oil and water phase and is called middle-phase microemulsion (Sheng 2011). The ternary diagram is shown in Figure 6.6:

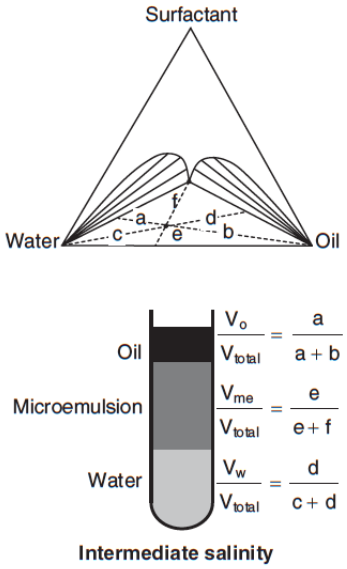

Figure 6.6: Middle-phase microemulsion (Sheng 2011)

The presence of three separate phases gives it the name "Windsor type III". This type has two IFTs: between the oil and microemulsion (σ_{mo}) and between the microemulsion and brine (σ_{mw}) (Zolotukhin and Ursin 2000). The formation of a microemulsion in a separate phase containing surfactant, water, and dissolved hydrocarbons between the oil and the aqueous phase is ideal for achieving ultra-low IFT values, and is highly favorable for enhanced oil recovery (Schlumberger 2013, Windsor phase behavior).

Optimal Salinity

The value of salinity at which $\sigma_{mo} = \sigma_{mw}$ is called the optimum salinity for IFT (Sheng 2011). In other words, when the IFT between microemulsion and oil is equal to the IFT between microemulsion and brine. It can also be said to be when the solubilization ratios for oil and brine are equal. This condition depends on several factors, such as oil composition, salinity, pressure, temperature, and the properties and concentration of the surfactant (Roshanfekr and Johns 2011). Figure 6.7 shows an example plot of IFTs versus the brine salinity and indicates the area of optimum salinity, and thus optimum phase behavior with a middle-phase microemulsion. One can estimate the value of equilibrium IFT at the optimal salinity from the value of solubilization parameters at the optimal salinity (Hirasaki et al. 2011). The optimal salinity can exist in an extremely narrow range, and can therefore be difficult to achieve in a flooding situation, even when the system is tailored to Windsor type III phase behavior. At the front of the surfactant slug, where the slug meets the high salinity connate water, the system will move into a Windsor type II system. At the back of the slug, where the surfactant is diluted by the injection water, Windsor type I can form. Water mixing in the reservoir during the injection process can also give unknown and local changes in the salinity which

affects the phase behavior. This is especially difficult when injecting low salinity surfactant, where there will be a large salinity contrast between the connate water and the injection water. The final salinity of such a system is practically impossible to predict.

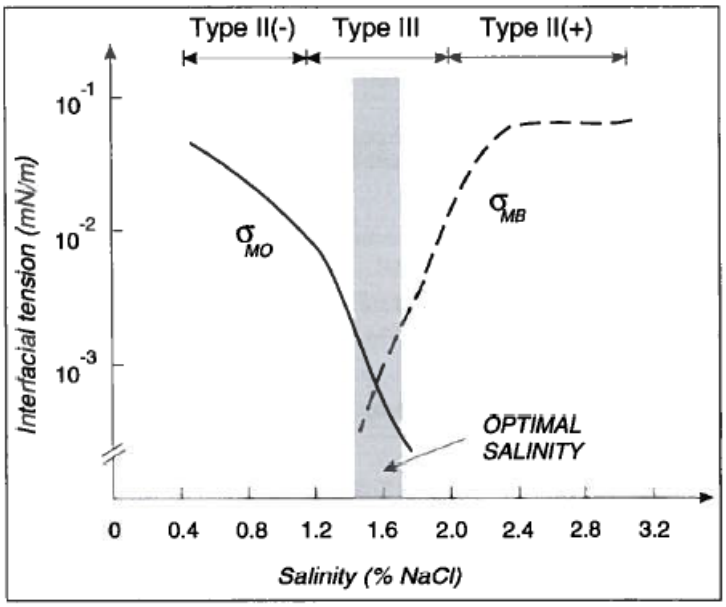

Figure 6.7: Interfacial tensions versus brine salinity (Zolotukhin and Ursin 2000)

6.4 Surfactant Retention

One of the major challenges with the use of surfactants in chemical EOR is their tendency to adsorb on the reservoir rock surface, which is a transfer of surfactant molecules from bulk solution phase to the surface interface. This leads to a serious loss of chemicals which is very often the factor that can make or break a surfactant EOR project. The surfactant concentration in the chemical slug will decrease dramatically, which in turn decreases the slug's ability to reduce IFT. The cost of chemicals is often more than half of the total cost of a chemical EOR project (Sheng 2011). In general, the adsorption of surfactants involves single ions rather than micelles, and adsorption shows a two-step character (Zhu and Gu 1991). First, the polar head group of the surfactant is adsorbed through electrostatic interaction with the rock surface. In the second step, the surfactant is adsorbed through hydrophobic interaction (if the adsorption is from aqueous solution) between the adsorbed surfactants. The total loss of surfactant is expressed by the concept of retention. The retention of surfactant is in turn dependent on several mechanisms including adsorption, phase trapping, precipitation, thermal degradation, and dispersion of surfactants (Alagic 2010). There are several factors that are important to control in order to minimize the surfactant losses, and the most important are listed below:

- *Surfactant concentration*: Surfactant adsorption is a function of concentration. At low surfactant concentrations and up to the CMC, when the surfac-

tant is mainly solubilized monomers, the surfactant adsorption will increase with increased concentration. This is determined by the affinity for the surface. At concentrations above the CMC, adsorption is practically constant and may be determined both by the affinity for the surface and the surfactant tendency to form micelles (Alagic 2010). Adsorption is considered to be irreversible with surfactant concentration (Sheng 2011).

- *Molecular weight*: The higher the molecular weight, the higher the adsorption level. Anionic surfactants with high molecular weight are considered more effective at reducing IFT, but surfactants with low molecular weight are more resistant to adsorption (Cuong et al. 2011). One has to weigh the benefit of larger reduction of IFT against the resistance to adsorption in order to find the optimal molecular weight.

- *pH*: For pure silica, which is the main mineral in sandstone reservoirs, the isoelectric point (zero charge) lies around pH 2, and the surface charge will be negative above this pH. A negatively charged surface will repel the polar head of anionic surfactants. For oxides in simple electrolyte solution the charge is typically positive at low pH, and the negatively charged anionic surfactant will be adsorbed due to opposite charge. When the pH increases, the charge will decrease and eventually become negative (Paria and Khilar 2004). The most common way of increasing pH is the addition of alkalies such as NaOH and Na_2CO_3 (Sheng 2011).

- *Salinity*: Surfactant adsorption increases with increasing salinity. An increase in salt concentration drives the surfactant to the interface and decreases the repulsion in the adsorbed layer. When adding divalent ions to the mix (Ca^{2+} and Mg^{2+}), the adsorption will increase even more (Cuong et al. 2011). A high divalent ion environment can lead to an excessive formation of calcium and magnesium salts that either precipitates or partitions into the oil. At the front of the surfactant slug, where the surfactant meets the high salinity connate water, Windsor type II will form and the surfactant moves from the original aqueous phase to a stationary/mobile oleic phase. This can lead to phase trapping and increases the retention dramatically (Alagic 2010). Adsorption is reversible with salinity, so if the salt concentration was to decrease, so would the adsorption (Sheng 2011).

6.5 Combination of Low Salinity Waterflooding and Surfactants

The bulk of the research done on low salinity surfactant injection has been carries out by a group of researchers from the Center of Integrated Petroleum Research (CIPR) in Bergen. There are several benefits of combining surfactant flooding with a low saline environment. At low salinity, the surfactant stays in the aqueous phase where it forms a micoremulsion by solubilizing the oil in water. At high salinities the surfactant will go into the oil phase, which may cause retention of

the oil and less effective recovery. When injection water displaces connate water, it will not be in a piston-like manner, but with some degree of mixing. Due to this, it will be practically impossible to design a flood that displays a middle-phase microemulsion at optimal salinity. A lower phase microemulsion is therefore preferred. Low salinities, which naturally has lower concentrations of divalent cations, will also contribute to increase the solubilization of the surfactant and decrease of both adsorption and retention.

Coreflood experiments performed by Alagic and Skauge (2010) using Berea sandstone cores saturated with synthetic seawater and aged with crude oil showed >90% recovery by low salinity surfactant flooding in tertiary mode. The experiments also showed a significantly higher ultimate recovery when the tertiary low salinity surfactant slug was preceded by a low salinity secondary waterflood instead of a high saline one. The presence of multivalent ions such as Mg^{2+} and Ca^{2+}, originating from the high salinity secondary injection, can make the actual surfactant less effective in reducing the interfacial tension. When comparing the two secondary waterfloods, the low salinity waterflood has a later breakthrough than the high salinity one, and an earlier production plateau. This behavior indicates a different wettability state caused by the difference in brine composition, where the low salinity environment is more water-wet.

Since Berea sanstone cores are, by nature, water-wet, aging of the cores with crude oil is an important factor to re-establish reservoir-like wettability conditions towards less water-wet. This was also confirmed by Alagic et al. (2011), where aged cores showed a higher recovery by low salinity and low salinity surfactant flooding than unaged cores.

Riisøen (2012) studied the effect of combined low salinity and surfactant injection in aged Bentheimer sandstones, with permeabilities in the Darcy range, at different temperatures. The potential for enhanced oil recovery by low salinity water injection after flooding with synthetic seawater was marginal, with incremental recoveries of less than 2% OOIP. The poor results were believed to be related to insufficient wettability alteration during aging, and/or the very low amount of clay present in Bentheimer. The low salinity surfactant injection however, increased oil recovery substantially, with recoveries ranging from 8 to 26% OOIP. It was believed that the oil had been redistributed within the core due to changes in COBR interactions during low salinity injection, and by reducing the capillary forces by injection of surfactants, this redistribution gave rise to an increase in the oil recovery beyond that of surfactant flooding alone.

Chapter 7

Laboratory Experiments

The main objective of the laboratory experiment was to compare the effect of the injection brine composition on oil recovery. The experiment would also look at the effect of initial wettability after aging, and the impact of rock composition. Five Berea sandstone cores were saturated with different brine compositions in order to induce a variation in wettability. Injection brine and connate brine were the same for this set of cores. Four cores from the same block as the previous were saturated with the same brine, but flooded with various other brines. The last four cores were from a different block, and thus would have different properties than the first 9 cores. This round was initially designed to be a repetition of the first round, but this was later changed based on results from from the two first rounds. This gave a variation of initial conditions and flooding sequences. All the necessary preparations were done to have full knowledge about porosity, permeability, and saturation prior to the flooding experiment. All cores were aged at 80 °C for three weeks after being saturated with oil.

7.1 Equipment and Procedure

The following section lists and describes the steps necessary in order to perform the coreflood experiments.

7.1.1 Initial Preparations

The core samples were drilled from block 6 and block 14 using tap water as coolant. To make sure all cores were completely clean, they were put in a Soxhlet cleaning apparatus for 24 hours, to be rinsed with methanol. After cleaning, they were left in a heating cabinet for drying. The samples were regularly weighed in order to make sure they were completely dry before continuing the preparations. When the cores were dry, they were weighed and measured before subjected to porosity measurements, and permeability measurements. This was done using a helium porosimetry apparatus, and an air permeability apparatus. The cores were eventually saturated with different brines, and weighed again in order to obtain the pore volume of the cores, using the mass balance method.

Cores

Berea sandstone cores were used for this experiment, taken from two very different blocks. Ten cores were taken from block 6 and four cores were taken from block 14. The core properties are listed in Table 7.1.

Table 7.1: Berea sandstone core properties

Core	**Block no.**	**Length, cm**	**Diameter, cm**	**Bulk volume, cm^3**	**Pore volume, cm^3**	ϕ_{Sat}, %	ϕ_{He}, %	k_{air}, **mD**
1-1	6	9.936	3.804	112.92	17.47	15.47	16.31	309
1-2	6	9.939	3.749	112.36	17.90	15.93	16.34	391
1-3	6	9.942	3.785	111.87	17.73	15.85	15.52	383
1-4	6	9.948	3.801	112.88	17.69	15.67	15.40	286
1-5	6	9.934	3.797	112.49	17.24	15.33	17.77	282
2-1	6	9.950	3.790	112.25	18.05	16.08	17.60	286
2-2	6	9.930	3.800	112.62	17.88	15.88	15.64	307
2-3	6	9.924	3.785	111.66	17.52	15.69	16.71	390
2-4	6	9.930	3.805	112.91	17.04	15.09	18.08	408
3-1	14	9.893	3.819	113.32	17.64	15.57	16.14	34
3-2	14	9.855	3.825	113.24	16.54	16.61	15.88	21
3-3	14	9.828	3.820	113.34	16.14	14.24	16.14	28
3-4	14	9.822	3.822	113.44	16.15	14.24	16.58	35

Berea sandstone cores have been widely recognized by the petroleum industry as the best stone for testing the efficiency of chemical surfactants. Berea sandstone is a sedimentary rock composed mostly of quarts and silica. The rock is classified as homogeneous with relatively high porosity and permeability, making it a good reservoir rock (Berea Sandstone^{TM} Cores 2013). An X-ray diffraction (XRD) was taken for two samples from both blocks in order to identify the minerals present. The results are listed in Tables 7.2 and 7.3:

Table 7.2: XRD results from Block no.6

Mineral	**Chemical formula**	**Type**	**no. 1 wt%**	**no. 2 wt%**
Quartz	SiO_2	-	91.75	92.5
Albite	$NaAlSi_3O_8$	Plagioclase Feldspar	0.78	0.94
Diopside	$MgCaSi_2O_6$	Monocline Pyroxene	0.9	1.34
Microcline Int. 1	$KAlSi_3O_8$	Potassium-rich Alkali Feldspar	6.56	5.22

Table 7.3: XRD results from Block no.14

Mineral	**Chemical formula**	**Type**	**no. 1 wt%**	**no. 2 wt%**
Quartz	SiO_2	-	76.48	76.22
Albite	$NaAlSi_3O_8$	Plagioclase Feldspar	6.62	6.25
Muscovite	$KAl_2(AlSi_3O_{10})(F,OH)_2$	Phyllosilicate group	2.83	1.94
Kaolinite	$Al_2Si_2O_5(OH)_4$	Clay	4.14	3.62
Microcline Int. 1	$KAlSi_3O_8$	Potassium-rich Alkali Feldspar	0.47	0.98
Microcline Int. 2	$KAlSi_3O_8$	Potassium-rich Alkali Feldspar	9.45	10.99

As shown by the XRD, the cores from block 6 do not contain any active clay material which may cancel out the effect of low salinity flooding. Block 14 contains both mica and kaolinite, clays which are known for being important for low salinity flooding. Figure 7.1 below shows micro-CT scans of samples taken from the two blocks. Block 6 is relatively homogeneous with evenly distributed pores, while block 14 is more inhomogeneous with large mineral grains and very small pores. The permeability of block 6 is approximately 10 times higher than that of block 14.

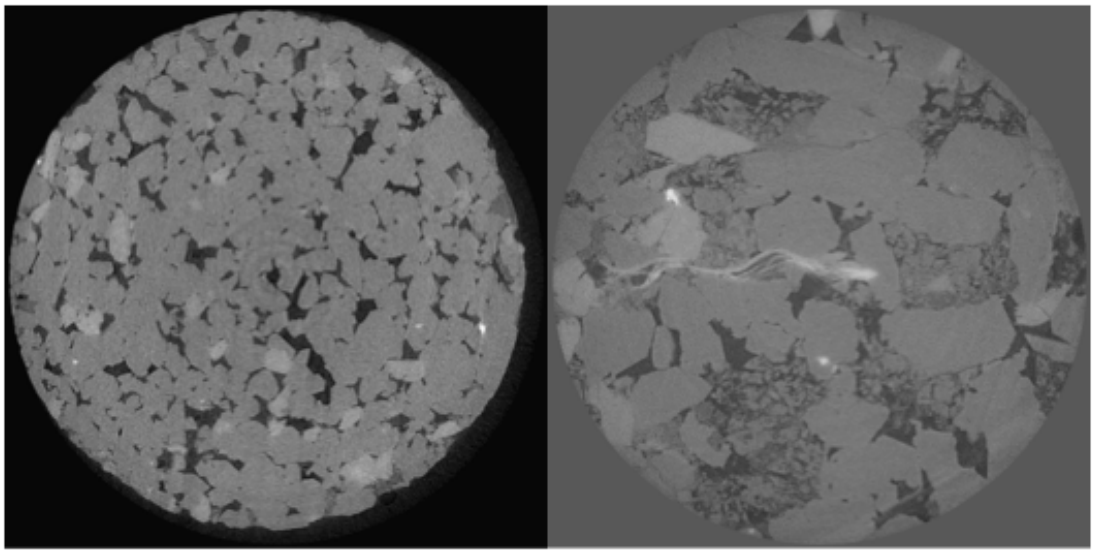

Figure 7.1: Micro-CT images of samples from the two blocks

Brine Compositions

All brines were made using distilled water and adding reagent grade chemicals in order to obtain the desired composition. The different brine compositions are listed in Table 7.4 below. The brines were filtered using a 0.45 μm filter in order to remove any particles and contamination.

Table 7.4: Brine compositions

Brine name	**Portion of ionic strengths**	**NaCl, g/L**	**$CaCl_2$: $2H_2O$, g/L**	**$MgCl_2$: $2H_2O$, g/L**	**TDS, mg/L**	**Ionic strength, mol/L**
B1	100 NaCl	32.500	-	-	32500	0.5561
B2	95 NaCl, 5 $CaCl_2$	30.875	1.362	-	31903	0.5560
B3	95 NaCl, 5 $MgCl_2$	30.875	-	1.885	31758	0.5561
B4	90 NaCl, 5 $CaCl_2$, 5 $MgCl_2$	29.250	1.362	1.885	31161	0.5560
B5	90 NaCl, 9 $CaCl_2$, 1 $MgCl_2$	29.250	2.210	0.305	31061	0.5560

Oil

The oil used for these experiments was a crude oil, henceforth known as Oil A, originating from the North Sea. Chemical composition and physical properties are listed in Tables 7.5 and 7.6 below. The oil was heated, in order to prevent wax clogging the filter, before being filtered through a 5 μm filter in order to remove contamination and other large particles before use.

Table 7.5: Composition of Crude Oil A in weight-%

Saturates	61.19
Aromatics	32.42
Resins	4.93
Asphaltenes	1.46

Table 7.6: Physical properties of Crude Oil A

TAN [mg KOH/g]	1.08
TBN [mg KOH/g]	1.16±0.35
Density, 15 °C [g/cm^3]	0.8582
Density, 60 °C [g/cm^3]	0.8252
API gravity [°API]	33.5
Viscosity, 15 °C [mPas]	19.90
Viscosity, 60 °C [mPas]	4.07

Surfactant

The surfactant used in the experiments was Sodium Dodecylbenzene Sulfonate (SDBS). It is a synthetic surfactant and a member of the *linear* alkylbenzenesulfonates, meaning that the dodecyl group ($C_{12}H_{25}$) is unbranched. The chemical formula is $C_{18}H_{29}NaO_3S$. SDBS is a cheap and widely used surfactant in both detergents and EOR. The sulfonates are effective and do not require a co-surfactant like alcohol to perform optimally. It was delivered in white powder form for easy use. CMC was measured by Tichelkamp et al. (2014) and found to be 1.69 mmol/L for SDBS.

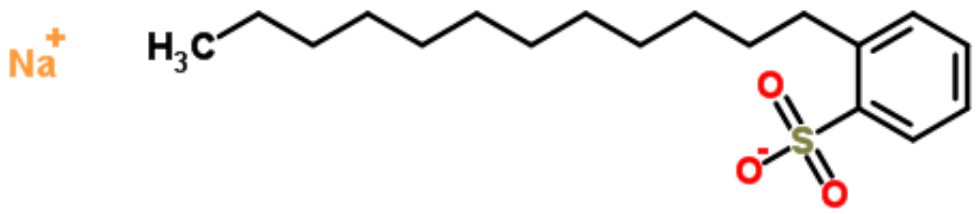

Figure 7.2: SDBS surfactant molecule (Royal Society of Chemistry 2014)

Several bottle tests were prepared to determine the concentration of surfactant to be used in the experiment. The concentration needed to be as high as possible in order to maximize the surfactant effect, but not too high to prevent surfactant precipitation. All brines were diluted to $1/10^{th}$ of the original high salinity and mixed with surfactant. Coreflooding was to be performed at 60 °C, so the solution had to be free of precipitation at this temperature. One flooding experiment with both flooding sequences would take approximately 2 days, so it was important that there would be no precipitation over that time. Four different concentrations of surfactant were tested; 300, 500, 1000, and 3000 ppm SDBS. The bottles were put in a heating cabinet after mixing and checked every 24 hours for three days. If no precipitation was observed, the solution would be valid for this experiment. The deciding brines turned out to be B2 and B5, which showed precipitation in both 1000 and 3000 ppm at 60 °C. Brines B1, B3 and B4 showed no precipitation for any of the concentrations at the elevated temperature. The results are summarized in Table 7.7 below. A concentration of 500 ppm was chosen for all the brines, since it was desired to use the same surfactant concentration for all flooding experiments. Precipitation occurred for concentrations lower than 500 ppm when taking the surfactant solutions out of the heating cabinet, and it was therefore decided to place the reservoirs inside the heating cabinet during flooding.

An interesting observation was that while the total concentration of divalents did not necessarily dictate precipitation, the type of divalent certainly did. Both B2 and B3 contained the same amount of total divalent cations, but B2 had only Ca^{2+}, and B3 only Mg^{2+}. Surfactant precipitated in B2 but not in B3, so it seems that calcium is the dominating factor in regard to divalents and surfactant precipitation. When looking at B4 and B5, which also contains the same amount of total divalents, one could observe that there was no precipitation in B4 in any of the surfactant concentrations. The ratio of calcium and magnesium was equal in B4, but the calcium content in B5 was 9 times higher than that of magnesium. Also, B4 had twice the amount of divalents as B2, and the same amount of Ca^{2+}, but there was no precipitation. It may seem that the amount of magnesium in B4 was counteracting the effect of calcium, preventing precipitation. While this was not investigated further in this experiment, it may be very interesting to test this further to determine how this actually works, and the mechanism behind it when it comes to tailoring surfactants for an EOR flood.

Table 7.7: Bottle tests

Brine	**SDBS, mg/L**	**1 day,** 60 °C	**2 days,** 60 °C	**3 days,** 60 °C
B1	300	no precipitation	no precipitation	no precipitation
	500	no precipitation	no precipitation	no precipitation
	1000	no precipitation	no precipitation	no precipitation
	3000	no precipitation	no precipitation	no precipitation
B2	300	no precipitation	no precipitation	no precipitation
	500	no precipitation	no precipitation	no precipitation
	1000	precipitation	precipitation	precipitation
	3000	precipitation	precipitation	precipitation
B3	300	no precipitation	no precipitation	no precipitation
	500	no precipitation	no precipitation	no precipitation
	1000	no precipitation	no precipitation	no precipitation
	3000	no precipitation	no precipitation	no precipitation
B4	300	no precipitation	no precipitation	no precipitation
	500	no precipitation	no precipitation	no precipitation
	1000	no precipitation	no precipitation	no precipitation
	3000	no precipitation	no precipitation	no precipitation
B5	300	no precipitation	no precipitation	no precipitation
	500	no precipitation	no precipitation	no precipitation
	1000	precipitation	precipitation	precipitation
	3000	precipitation	precipitation	precipitation

Saturating With Oil

The cores were saturated with oil in three rounds using the porous plate setup schematically presented in Figure 7.3. The setup consisted of five vertical core holders in series. The cores were inserted into the core holders, and a reservoir at the inlet on the top of the core holders was filled with oil after applying sleeve pressure. In the bottom of the core holders, underneath the cores, was a porous plate saturated with the same brine as the core. An outlet tube at the bottom of the core holder was connected to a measuring burette, one for each core holder. Air pressure was applied at the inlet, forcing the oil to displace water. The amount of water produced was measured in the burette, corresponding to the amount of oil injected. The pressure was increased in increments until, eventually, no more water was produced. There was also a limit to how much pressure could be applied before the oil would start to leak through the porous plate. Because of time restrictions,

the resulting capillary pressure curve was not exact, since the pressure had to be increased at a certain frequency, and capillary equilibrium was not achieved for each pressure increment.

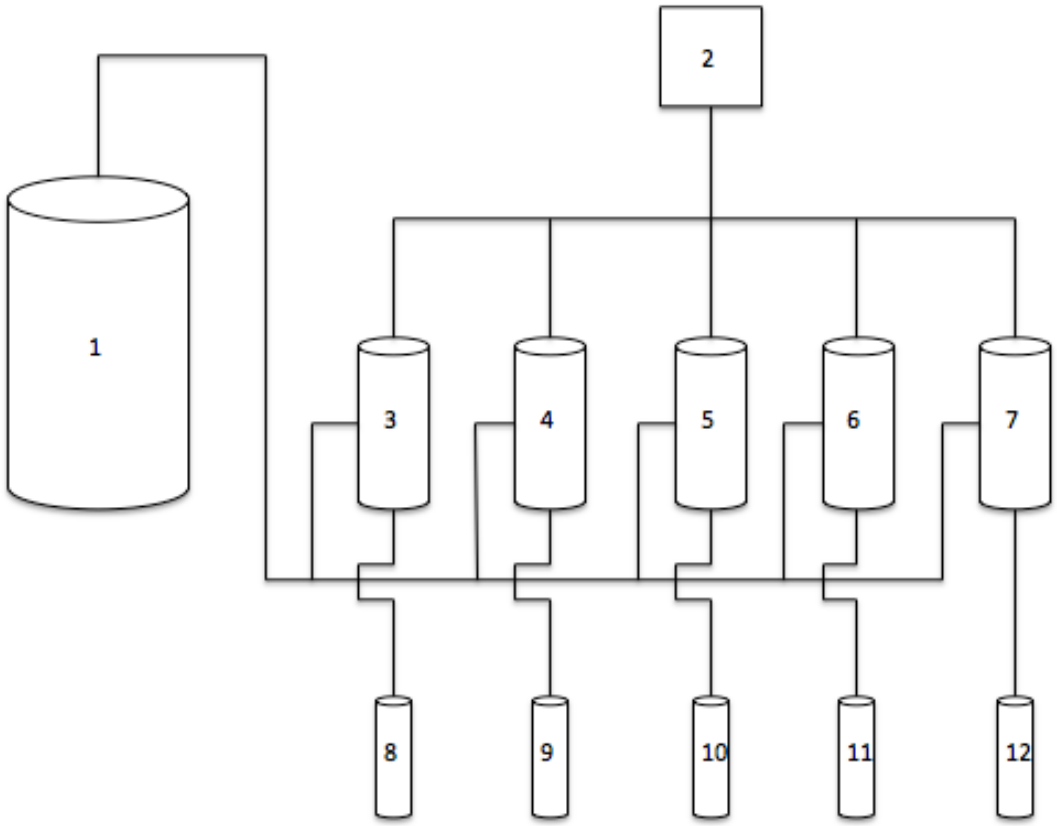

Figure 7.3: Schematic of porous plate apparatus

This setup allowed for a stable displacement of water by oil, using capillary forces. It was time consuming, taking approximately 2-3 weeks per round, but very exact, and eliminated the necessity for large amounts of oil needed for saturation by flooding apparatus. The amount of water produced corresponded to the amount of water replaced by oil. This method could also give the capillary pressure curve, if one has the time to increase the pressure in very small increments, and wait for capillary equilibrium between each step. The apparent capillary pressure curves are shown in Figures 7.4, 7.5 and 7.6.

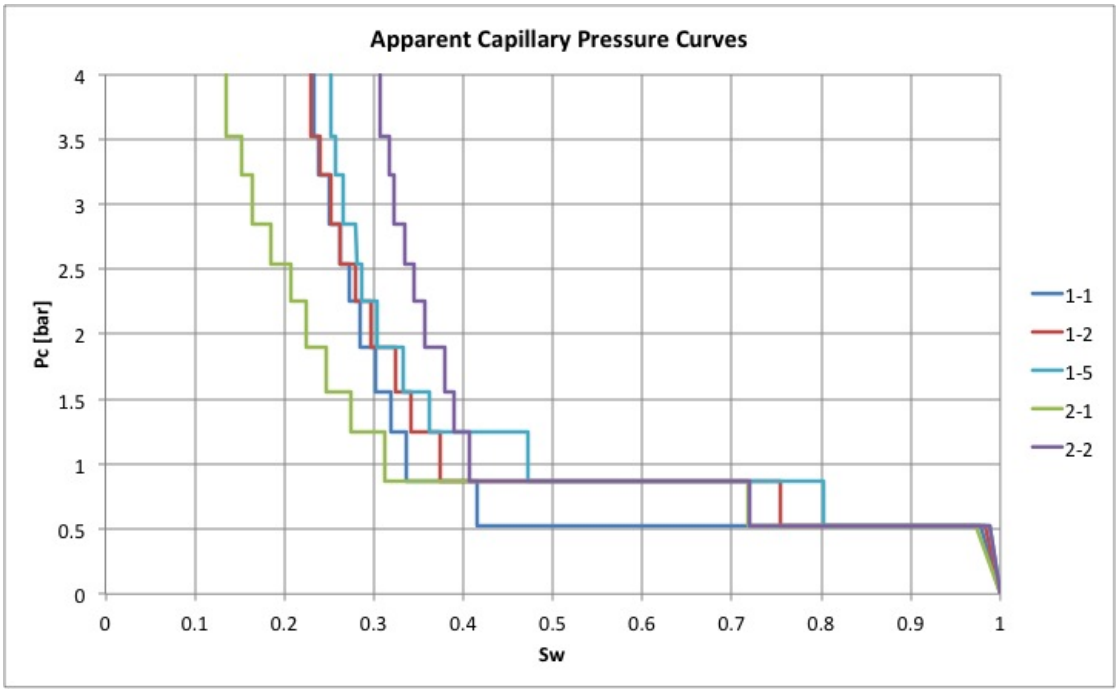

Figure 7.4: Apparent capillary pressure curves for drainage round 1

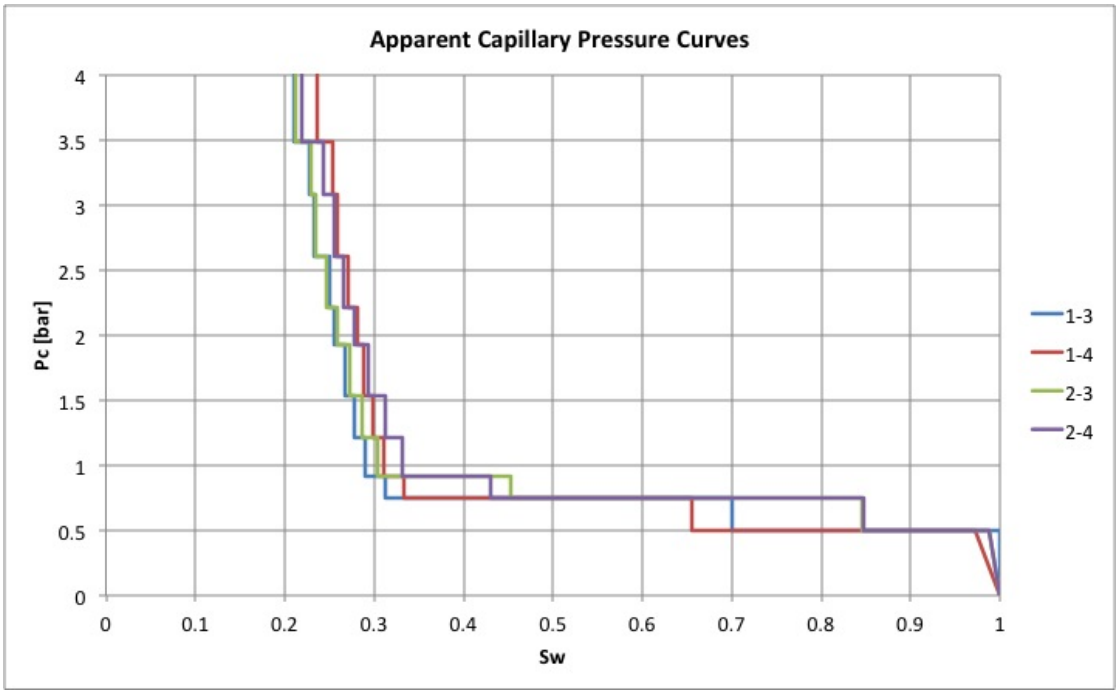

Figure 7.5: Apparent capillary pressure curves for drainage round 2

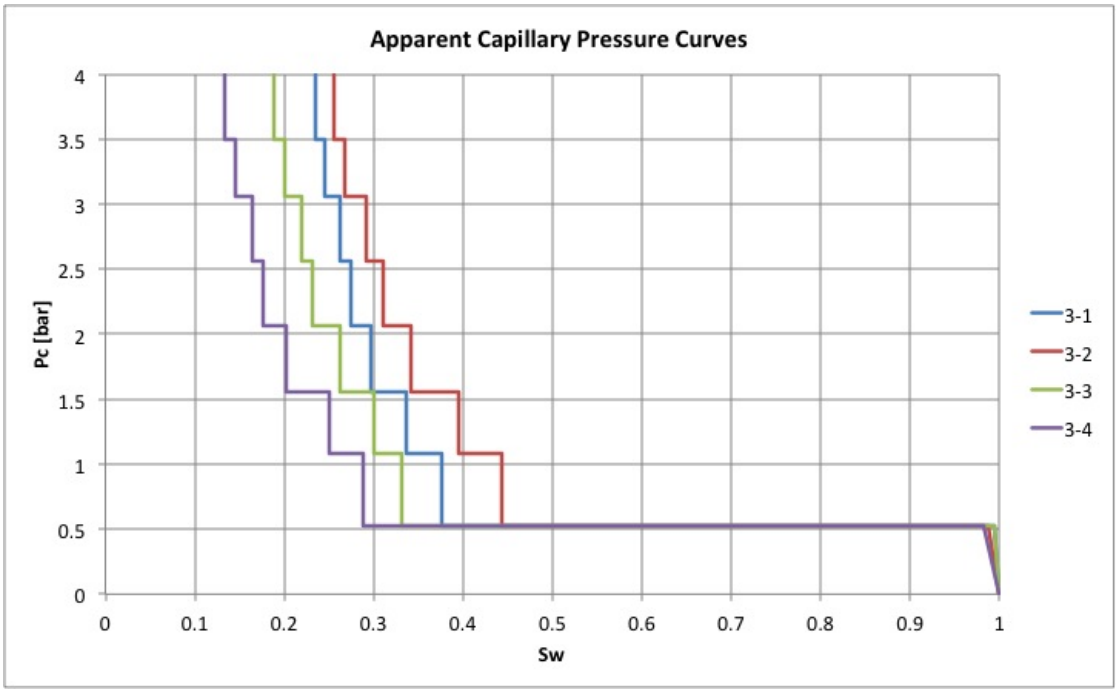

Figure 7.6: Apparent capillary pressure curves for drainage round 3

The results from core holder number 2 from the first drainage round, which contained core 2-1, was suspicious due to high air production and very low residual oil saturation compared to the other cores. It was suspected that a rupture in the rubber sleeve was letting the nitrogen from the sleeve pressure enter the core and displace the water. This core was therefore subjected to additional oilflooding in the flooding apparatus, and oil saturation was found by mass balance method. Core 2-2 was also subjected to additional oilflooding just to compare the mass balance saturation with the volumetric saturation. The difference was found to be negligible for this core, and it was therefore concluded that core holders 1, 3, 4, and 5 were working properly. Core holder number 2 was discarded and not used for the rest of the saturation process. The final fluid saturations are listed in Table 7.8.

Table 7.8: Final fluid saturations

Core	1-1	1-2	1-3	1-4	1-5	2-1	2-2	2-3	2-4	3-1	3-2	3-3	3-4
$\mathbf{S}_{oi}$	0.77	0.77	0.79	0.76	0.75	0.72	0.72	0.79	0.78	0.76	0.74	0.81	0.87
$\mathbf{S}_{wirr}$	0.23	0.23	0.21	0.24	0.25	0.28	0.28	0.21	0.22	0.24	0.26	0.19	0.13

7.1.2 Core Flooding

Thirteen corefloods were performed on thirteen different cores. The floodings were performed using a coreflood apparatus placed in a heating cabinet at 60 °C and with a back-pressure of 3.5 bar. The coreflood setup is shown in Figure 7.7.

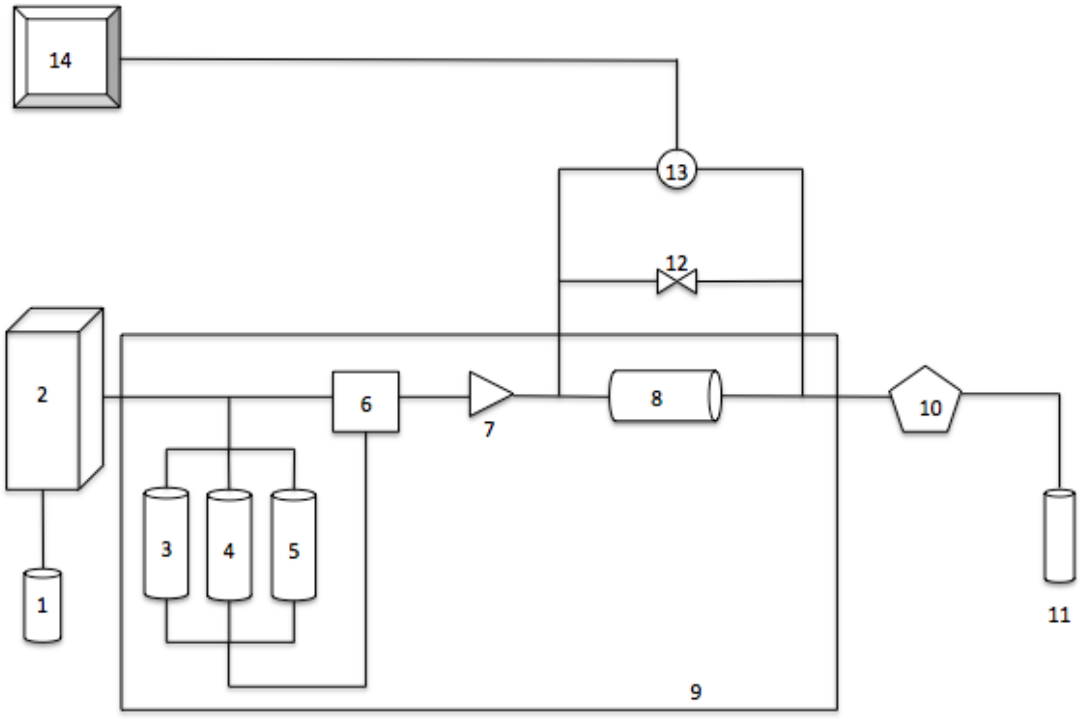

1. Pump reservoir, 2. Positive displacement pump, 3. Reservoir 1, 4. Reservoir 2, 5. Reservoir 3, 6. Manifold, 7. Check-valve, 8. Core holder, 9. Heating cabinet, 10. Back-pressure valve, 11. Effluent collector, 12. Equalizer valve, 13. Differential pressure transmitter, 14. Computer

Figure 7.7: Schematic of core flooding apparatus

Exxol D-60 was used as a pumping medium with injection lines connected to the top of the reservoirs. Lines from the bottom of the reservoirs were connected to a manifold allowing for easy switching between injection fluids. A common line went through a check-valve ahead of the core holder in order to prevent any back-flow if the pressure were to suddenly drop. The reservoirs and core holder were placed inside the heating cabinet. There was a back-pressure valve situated between the core holder and outlet. This is necessary when flooding at high temperatures in order to prevent evaporation of light components from the oil. The pressure drop across the core was measured and recorded by the computer. A camera was monitoring the effluent collector and recording the production over time. The flooding experiment consisted of thirteen corefloods, divided into three reounds, all with the same injection rate of 0.2 ml/min. The entire flooding matrix is given in Table 7.9. All cores were flooded with approximately 10 PV low salinity brine in secondary mode and approximately 10 PV low salinity surfactant in tertiary mode. All cores were initially flooded with Oil A in order to obtain the effective oil permeability (k_o) at irreducible water saturation. The permeability was calculated after pressure stabilization using Darcy's law. The pressure plots can be found in Appendix B. The effective water permeability (k_w) at the end of each flooding sequence was also calculated from the stabilized pressure drop.

In the coreflood setup that was built, inlet lines, outlet lines, and back-pressure regulator added up to a dead volume that would be produced in addition to the fluids from the cores. This volume was measured twice for reassurance, and then subtracted from the oil produced during the experiments. It was therefore important to initially flood with oil before every experiment, so that the entire dead volume would be filled with oil. It would also be easy to identify when all the dead volume had been produced. The setup also required quite a long line from the core holder outlet, through the back-pressure regulator, and to the final outlet in the collector, which meant that the water breakthrough would not be seen before it reached the outlet. Breakthrough and volumes were therefore measured from the final outlet in order to maintain consistency throughout the experiments.

Table 7.9: Core flooding test matrix

Core	**In-situ brine, HS**	**Injection 1, LS**	**Injection 2, LSS**
1-1	B1	(1/10)B1	Surfactant in (1/10)B1
1-2	B2	(1/10)B2	Surfactant in (1/10)B2
1-3	B3	(1/10)B3	Surfactant in (1/10)B3
1-4	B4	(1/10)B4	Surfactant in (1/10)B4
1-5	B5	(1/10)B5	Surfactant in (1/10)B5
2-1	B5	(1/10)B1	Surfactant in (1/10)B1
2-2	B5	(1/10)B2	Surfactant in (1/10)B2
2-3	B5	(1/10)B3	Surfactant in (1/10)B3
2-4	B5	(1/10)B4	Surfactant in (1/10)B4
3-1	B1	(1/10)B1	Surfactant in (1/10)B1
3-2	B2	(1/10)B2	Surfactant in (1/10)B2
3-3	B3	(1/10)B1	Surfactant in (1/10)B1
3-4	B5	(1/10)B1	Surfactant in (1/10)B1

7.2 Results

A summary of the observations from all the corefloods is presented below. Due to the large amount of data, the plots showing recovery and differential pressure across the core, versus injected pore volume, can be found in Appendix A. To review the composition of each brine, refer to Table 7.4

7.2.1 Round 1

1-1

This core was both saturated and flooded with pure NaCl brine (B1). Breakthrough occurred after 0.412 PV injected, and the breakthrough recovery was 46.7% OOIP. Some oil was produced after breakthrough, which gave a final LS recovery of 50.4% after approximately 10 PV injected. Some pressure fluctuations were observed between 4 and 8 PV injected, but this was not associated with oil recovery. LSS recovery was relatively low, only 2.9%. Some small pressure spikes could be observed during the oil recovery. No more oil was produced after approximately 14 PV injected. The final recovery after the end of flooding was 53.3%. See Figure A.1.

1-2

This core was both saturated and flooded with B2. Breakthrough occurred after 0.335 PV injected, and the breakthrough recovery was 41.4% OOIP. A substantial amount of oil was produced after breakthrough, increasing almost linearly before making a big jump after approximately 3.6 PV injected. This large oil production was associated with a large spike in differential pressure across the core. Several other pressure spikes were observed, but did not result in additional oil recovery. The final LS recovery was 52.1%. LSS flooding gave an additional 5% recovery, which brought the total recovery to 57.1% of OOIP. Pressure fluctuations occurred at the time of oil production. Most of the surfactant produced oil was recovered during the first 2 PV of injection. See Figure A.2.

1-3

This core was both saturated and flooded with B3. Breakthrough occurred after 0.378 PV injected, and the breakthrough recovery was 45.7% OOIP. Some oil was recovered after breakthrough, but no more after 0.42 PV injected, which gave an LS recovery of 50%. LSS flooding produced an additional 2.1% of the oil. All the oil from LSS was produced during one period between 11-12 PV injected, following pressure fluctuations. The final recovery after end of flooding was 52.1%. See Figure A.3.

1-4

This core was both saturated and flooded with B4. Breakthrough occurred after 0.334 PV injected, and the breakthrough recovery was 44.4% OOIP. Very little oil was recovered after breakthrough, only 2.3%, and no additional oil was recovered after 0.45 PV injected. A massive pressure spike occured at around 5 PV injected, but this was not associated with any additional oil recovery. The total LS recovery was 46.7%. LSS recovered an additional 5.9%, which brought the final recovery after flooding to 52.6%. See Figure A.4. The LSS recovery occurred during large pressure fluctuations in the system.

1-5

This core was both saturated and flooded with B5. Breakthrough occurred after 0.331 PV injected, and the breakthorugh recovery was 43.8% OOIP. Some oil was recovered after breakthrough, 3.9%, which brought the LS recovery to a total of 47.7%. The pressure showed a smooth decrease from around 3 PV injected until switching to LSS. After switching to surfactant, the oil was produced more or less continuously over the next 3 PV to a total of 5.4% LSS recovery. This oil production was associated with large fluctuations in pressure. No additional oil was recovered after 13 PV of injection. The final recovery was 53.1%. See Figure A.5.

A summary of the key information regarding the core floodings in round 1 is listed in Table 7.10 below.

Table 7.10: Flooding results Round 1

Core	**1-1**	**1-2**	**1-3**	**1-4**	**1-5**
$\mathbf{S}_{wirr}$	0.23	0.23	0.21	0.24	0.25
$\mathbf{k}_o(\mathbf{S}_{wirr})$ **[mD]**	233	383	465	303	273
WBT (PVi)	0.412	0.335	0.378	0.334	0.331
Recovery @ WBT	0.467	0.414	0.457	0.444	0.438
LS recovery	0.504	0.521	0.5	0.467	0.477
$\mathbf{k}_w$ **end of LS [mD]**	68	249	72	80	86
LSS recovery	0.029	0.05	0.021	0.059	0.054
$\mathbf{k}_w$ **end of LSS [mD]**	145	512	256	343	250
Final recovery	0.533	0.571	0.521	0.526	0.531
Total PVi	20.58	19.71	19.53	19.34	20.54

7.2.2 Round 2

2-1

This core was saturated with B5, and flooded with pure NaCl brine (B1). Breakthrough occurred after 0.388 PV injected, and the breakthrough recovery was 50% OOIP. A substantial amount of oil was produced after the breakthrough, approximately 7.7%. A lot of this was attributed to a second phase of production, after 6.3 PV injected, where it started to produce again after 100% water-cut for about 4 PV. During the LS flooding sequence, the pump tripped and the system experienced a pressure drop. Right after switching to LSS, the pressure spiked, and a lot of oil was produced over a very short period of time. Apart from this, the pressure was relatively stable without any major spikes. The total LSS recovery was 8.5%, which brought the final recovery to 66.2%. See Figure A.6.

2-2

This core was saturated with B5, and flooded with B2. Breakthrough occurred after 0.324 PV injected. The breakthrough recovery was 45% OOIP. Some oil was produced after the breakthrough, but nothing after 0.56 PV injected, which gave a total LS recovery of 48.8%. No oil was produced until 16 PV injected after switching to LSS. Oil was recovered slowly over the next 2 PV. This flooding sequence was allowed to continue for a bit longer than 10 PV due to a sudden pressure fluctuation and oil production right before it was supposed to be shut down. In total, 2.4% oil was produced during the LSS flood. The final recovery was 51.2%. See Figure A.7.

2-3

This core was saturated with B5, and, flooded with B3. Breakthrough occurred after 0.388 PV injected, and the breakthrough recovery was 44.9% OOIP. Very little oil was recovered after the breakthrough, only 2.9%, and the final LS recovery was 47.8%. No additional oil was produced after 0.52 PV injected. Oil recovery from LSS flooding was very low, only 2.2%, and all of it was produced during the first 2.3 PV of LSS injection. The oil production was associated with a small fluctuation in the pressure. The final recovery was 50% OOIP. See Figure A.8.

2-4

This core was saturated with B5, and flooded with B4. Breakthrough occurred after 0.335 PV injected, and the breakthrough recovery was 43.6% OOIP. Some oil was produced after breakthrough, and the final LS recovery was 46.6%. No additional oil was recovered after 0.38 PV injected. LSS recovery was low, and only produced 2.3%, most of it around 12 PV injected. The final recovery was the lowest of all, only 48.8%. See Figure A.9.

A summary of the key information regarding core floodings in round 2 is listed in Table 7.11 below.

Table 7.11: Flooding results Round 2

Core	**2-1**	**2-2**	**2-3**	**2-4**
$\mathbf{S}_{wirr}$	0.28	0.28	0.21	0.22
$\mathbf{k}_o(\mathbf{S}_{wirr})$ **[mD]**	294	255	385	397
WBT (PVi)	0.388	0.324	0.388	0.335
Recovery @ WBT	0.5	0.45	0.449	0.436
LS recovery	0.577	0.488	0.478	0.466
$\mathbf{k}_w$ **end of LS [mD]**	44	59	77	115
LSS recovery	0.085	0.024	0.022	0.023
$\mathbf{k}_w$ **end of LSS [mD]**	183	311	205	368
Final recovery	0.662	0.512	0.5	0.489
Total PVi	19.29	21.16	19.77	20.54

7.2.3 Round 3

3-1

This core was saturated and flooded with the same pure NaCl brine (B1). Breakthrough occurred after 0.402 PV injected and the breakthrough recovery was 42.2% OOIP. A small amount of oil was recovered after the breakthrough, but no more after 1 PV injected, and the final LS recovery was 44.4%. LSS flooding recovered an additional 5.2%, which brought the final recovery to 49.6%. Pressure fluctuations could be seen during the oil production from LSS flooding. Some data points from the pressure recording were not available. See Figure A.10.

3-2

This core was saturated and flooded with B2. Breakthrough occurred after 0.392 PV, and the breakthrough recovery was 38.2% OOIP. An additional 4.1% oil was recovered after breakthrough, which resulted in a final LS recovery of 42.3%. After switching to LSS flooding, the pressure decreased smoothly for approximately 3 PV before starting to fluctuate. At this point, oil started to produce. LSS recovery was a substantial 7.3%, and the final recovery was 49.6%. Some data points from the pressure recording were not available. See Figure A.11

3-3

This core was saturated with B3, and flooded with B1. Breakthrough occurred after 0.378 PV injected, and the breakthrough recovery was 39.7% OOIP. An additional 4.6% oil was recovered after breakthrough, mostly between 4-6 PV injected

and at around 9 PV injected. This oil recovery was associated with pressure fluctuations across the core. The final LS recovery was 44.3%. A significant amount of oil was recovered by the LSS flooding, which gave an additional 6.1% oil recovery. The final recovery was 50.4%. See Figure A.12

3-4

This core was saturated with B5 and flooded with B1. Breakthrough occurred after 0.439 PV injected, and the breakthrough recovery was 41.4% OOIP. After the breakthrough, 3.6% more oil was recovered, which gave a final LS recovery of 45%. At around 7 PV injected, the pressure started fluctuating and oil started to produce after approximately 6 PV of no oil. The additional oil was produced during 1 PV of injection. After switching to LSS flooding, no oil was produced for the first 1 PV of LSS injection. At about 13 PV injected, the pressure started fluctuating, and the oil started to produce. Most of the oil recovered by LSS was produced between 11 and 15 PV injected. At around 19 PV injected, the pressure started fluctuating again after a stable period, and a small amount of additional oil was recovered. LSS recovered 7.1% in total, and the finale recovery for this core was 52.1%. See figure A.13

A summary of key information regarding core floodings in round 3 is listed in Table 7.12 below.

Table 7.12: Flooding results Round 3

Core	**3-1**	**3-2**	**3-3**	**3-4**
$\mathbf{S}_{wirr}$	0.24	0.26	0.19	0.13
$\mathbf{k}_o(\mathbf{S}_{wirr})$ **[mD]**	41	25	29	28
WBT (PVi)	0.402	0.393	0.378	0.439
Recovery @ WBT	0.422	0.382	0.397	0.414
LS recovery	0.444	0.423	0.443	0.45
$\mathbf{k}_w$ **end of LS [mD]**	7.5	5	6.9	8.6
LSS recovery	0.052	0.073	0.061	0.071
$\mathbf{k}_w$ **end of LSS [mD]**	15.4	12.8	12.4	18.8
Final recovery	0.496	0.496	0.504	0.521
Total PVi	20.28	21.35	21.92	21.96

Figure 7.8 shows the LS and LSS recovery for all the corefloods. Most of the cores produced around 50% of OOIP in total, except from 1-2 and 2-1, which produced 57.1% and 66.2% respectively. LS recovery ranged from 42.3-57.7%, and LSS recovery ranged from 2.2-8.5%.

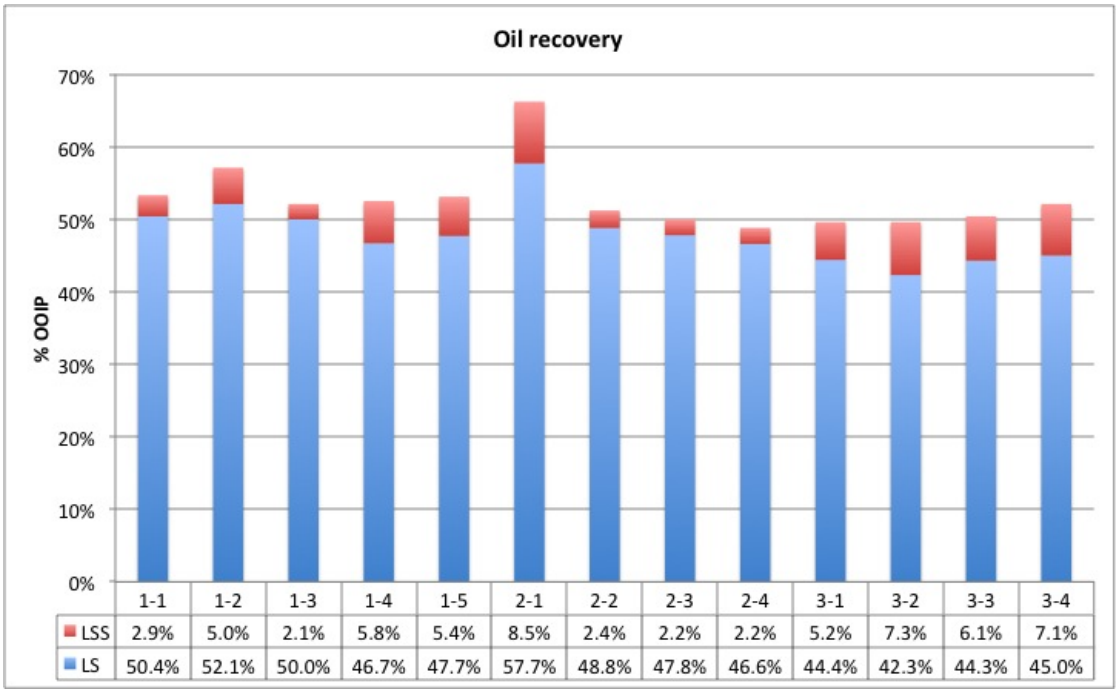

	1-1	1-2	1-3	1-4	1-5	2-1	2-2	2-3	2-4	3-1	3-2	3-3	3-4
LSS	2.9%	5.0%	2.1%	5.8%	5.4%	8.5%	2.4%	2.2%	2.2%	5.2%	7.3%	6.1%	7.1%
LS	50.4%	52.1%	50.0%	46.7%	47.7%	57.7%	48.8%	47.8%	46.6%	44.4%	42.3%	44.3%	45.0%

Figure 7.8: Recovery for all corefloods

Chapter 8

Discussion

8.1 Flooding with B1

The recovery curves for all the cores flooded with B1 are plotted in Figure 8.1 below. Since the recoveries were practically identical up to 40% OOIP, this part was not included in the figure. This makes the figure easier to interpret, while maintaining focus on the key information.

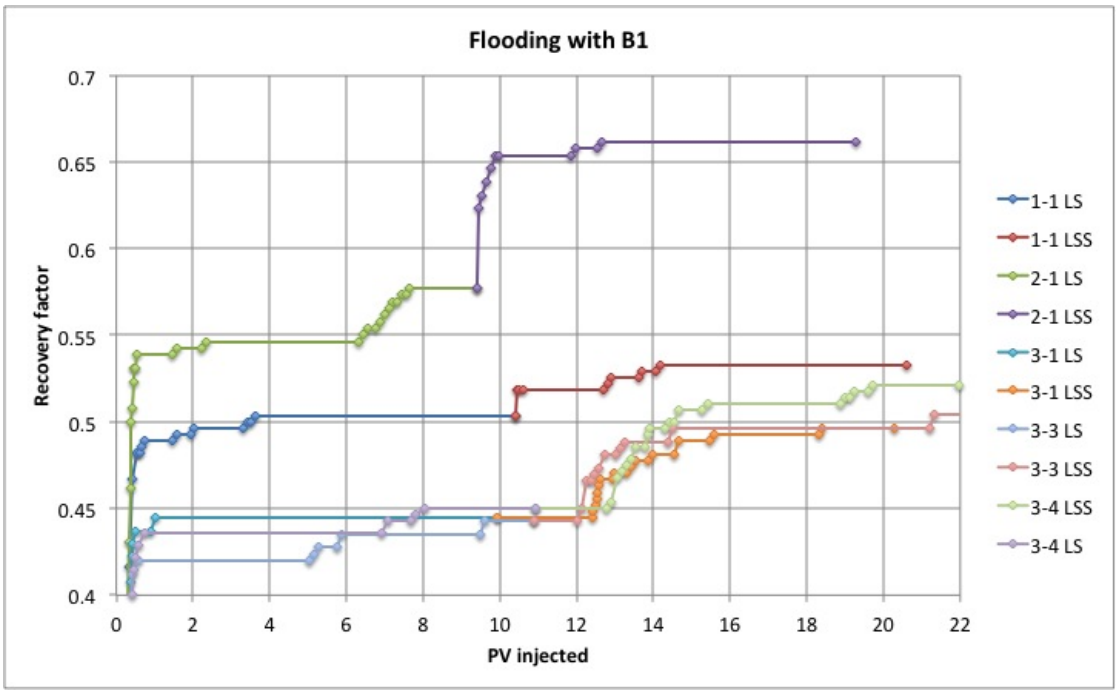

Figure 8.1: Recoveries for cores flooded with B1

The most obvious difference between the cores flooded with B1 is that the cores from round 1 and 2 perform better than all the cores from round 3, especially for LS flooding. The cores are from two different blocks and have different properties. The cores from round 3 have a much lower permeability, and also appears to be more heterogeneous than the cores from round 1 and 2. The cores from round 3

also contain a significant amount of bulk clay. According to the presented theory, clay is very important to LS flooding, and thus cores containing clay should perform better than cores without clay (Morrow and Buckley 1999). It seems, though, that the lower permeability and heterogeneity, which leads to higher capillarity, is more crucial when comparing the performances of the rocks. Due to this, it is difficult to compare the effect of clay directly, as the core properties are so different. Nevertheless, it seems as if the bulk clay content is not very crucial.

The late water-breakthrough for cores 1-1 and 3-1 is consistent with the theory of more water-wet rock after aging with pure NaCl brine. These cores did produce a significant amount of oil, but it might have been just as high if flooded with high salinity brine, and the oil recovery is the effect of viscous forces rather than composition of injection brine. Based on the presented literature, the presence of divalent cations in the connate brine will promote a change towards more oil-wet conditions after aging with crude oil. It is also stated that this is necessary for low salinity waterflooding to be effective (Abdallah et al. 2007). Core 2-1 shows an earlier breakthrough, and higher recovery after breakthrough, which is consistent with a more oil-wet system. The cores saturated with B5 have the highest divalent content. The total low salinity production is also higher in 2-1, which is also consistent with the theory that low salinity works best in a more oil-wet system, where the lower ionic strength promotes a change in wettability towards more water-wet. An indication of this wettability change is seen for 2-1 just after 6 PV injected. The recovery factor has been constant for some time, and then oil recovery resumes. This is similar to the observations of dual steps in water-cut by Vledder et al. (2010). This can also be seen, to some extent, in cores 3-3 and 3-4, where the in-situ brine also contains divalents. This is not seen in the cores saturated with B1, as they have not been aged with divalents and are still water-wet after aging. Core 3-4 has the latest breakthrough of all the cores, which was surprising as one would think it was just as oil-wet as core 2-1. Still, this could be caused by the mineral grain structure and tightness of the core, and may not represent the actual wettability. The core had the highest LS recovery of all the cores from round 3, and the reason for this is the same as for 2-1: High divalent content in the connate brine, and pure NaCl flooding brine.

2-1 also performed best during the surfactant flooding, however, the large pressure spike (as seen in Figure A.6) brings forth scepticicm. A malfunction in the apparatus, probably a faulty reservoir, caused the pressure to spike at the end of LS flooding, and a lot of oil was produced immediately after switching to LSS. Some of this oil may actually have come from the low salinity flooding, even though that is not likely since the recovery factor had not increased for some time during LS. The most likely cause is the large pressure increase to the system, therefore the flooding sequence should be repeated in order to obtain a more accurate result. Nevertheless, 2-1 was far superior to all the other floods during LS injection, indicating that the presence of divalent cations in the connate water is very important in order to obtain full effect of low salinity flooding. This is also the case for 3-4, which had the highest LS recovery of the round 3 cores, and the highest total

recovery in round 3. To summarize, rock with higher divalent content in in-situ brine led to higher recovery when flooded with pure NaCl brine. B1 brine, in this case, has stripped more divalents from the rock surface, converting the wettability towards more water-wet. Therefore, the higher the contrast in divalent content in in-situ brine and injection brine, the more oil is detached from the rock.

8.2 Flooding with B2

Figure 8.2 shows the recovery curves for all the cores flooded with B2 brine.

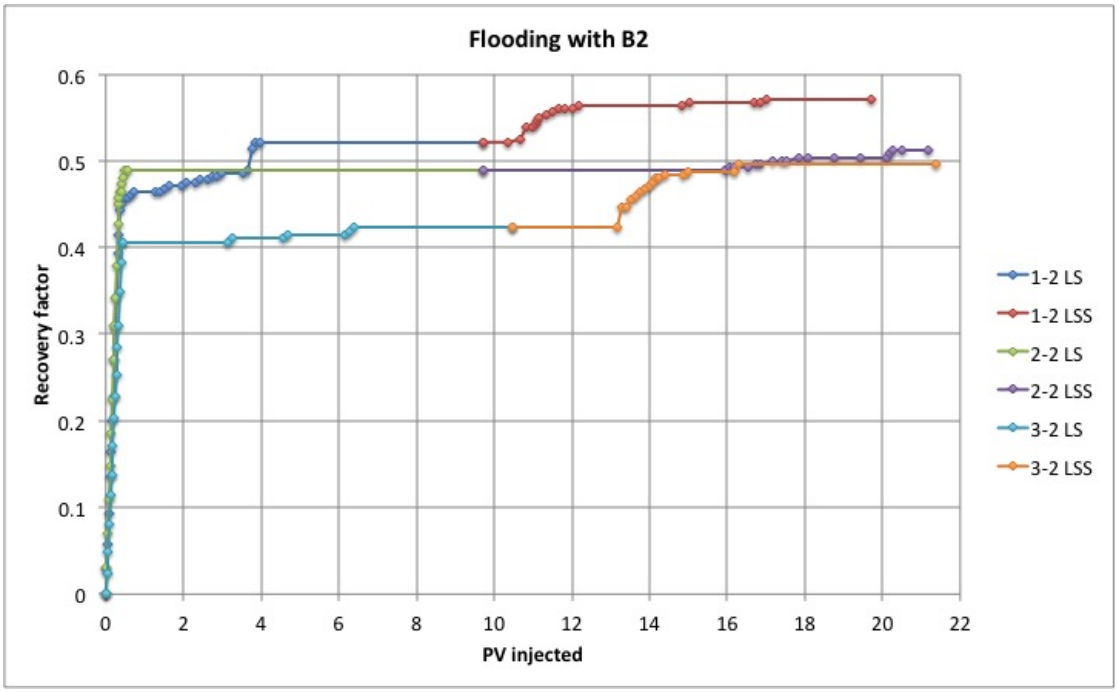

Figure 8.2: Recoveries for cores flooded with B2

Cores 1-2 and 3-2 are both saturated and flooded with B2 brine. They both exhibit indication of wettability alteration during LS flooding. This is most evident for 1-2, where the recovery increases sharply at approximately 3.6 PV injected. This demonstrates the disconnection of Ca^{2+} bridges that allow the polar oil components to be separated from the rock surface. Before this increase in oil recovery, the recovery factor for 1-2 was wqual to that of 2-2. This is not as clear for 3-2, but there is nevertheless an increase in recovery during LS flooding between 3.1 and 6.3 PV injected.

Core 2-2 produces oil for the first 0.5 PV injected, but seizes to produce oil after that, during LS flooding. This shows that low ionic strength does not guarantee a higher recovery if the injected brine has divalent content. Core 2-2 is considered to be the most oil-wet of the three, and according to the literature, higher initial oil-wetness can result in a higher oil recovery by LS flooding. It was observed that

this is true only when the injected brine has a lower divalent content. Injection of B2 in a B5 saturated core could not alter wettability enough, meaning that the presence of divalents in the injection brine suppresses the effect of the lower ionic strength. In 1-2 and 3-2, since the rock was not as strongly oil-wet as 2-2, the injected B2 could recover more oil.

Both 1-2 and 3-2 have a high LSS recovery of 5 and 7.3% respectively. Core 2-2 recovers only 2.4% additional oil during LSS flooding, which does not occur until after 16 PV injected. Core 1-2 starts producing relatively early in the LSS flood, and most of the oil is recovered during the first 2 PV injected. Core 3-2 does not recover any oil until after 2.7 PV LSS injected, however, it recovers the highest amount of LSS oil after that. Despite the lower permeability and large heterogeneity of core 3-2, it recovers almost the same total oil as 2-2. This might be an indication of the positive effect of clay content in core 3-2, or it can be attributed to the capillarity. Surfactant reduces the IFT, which will have a greater impact when there are stronger negative capillary pressures trapping the oil, as is the case for 3-2.

8.3 Flooding with B3

The behavior of the two B3 floods are very similar, but 1-3 recovers 2.2% more oil for the LS flood. The LSS recovery is practically the same, causing the final recovery for 2-3 to be 2.1% less than for 1-3. When the divalent content is high, and the flooding brine also contains divalents, the reduced ionic strength is not sufficient to alter the wettability to such an extent extent that leads to increased recovery. 1-3 is believed to be less oil-wet, and more oil is recovered even though the divalent content in the flooding brine is the same as for 2-3. There is no indication of a wettability alteration in either of the cores. Figure 8.3 shows the two recovery curves.

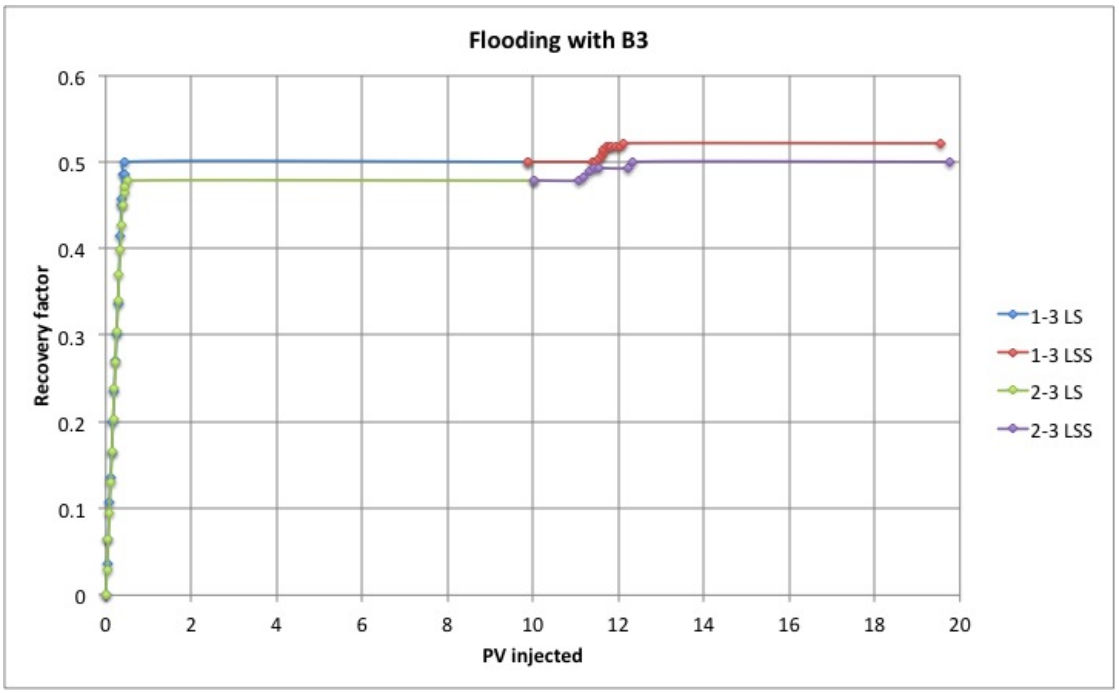

Figure 8.3: Recoveries for cores flooded with B3

8.4 Flooding with B4

For the B4 flooding, the LS recoveries are practically identical, but the LSS recoveries are differe greatly. The LSS recovery for 1-4 is 5.8%, while the LSS recovery for 2-4 is only 2.2%. The in-situ and injection brine in 1-4 contain equal amounts Mg^{2+} and Ca^{2+} in addition to NaCl, while the in-situ brine in 2-4 contains nine times more Ca^{2+} than Mg^{2+}. As seen from the bottle tests, calcium has a much stronger negative reaction with the surfactant, resulting in high precipitation even at low concentrations of SDBS. The magnesium does not have this effect, and it is believed that the lack of calcium in the in-situ brine in 1-4 allows for a better performance of the surfactant. Even though some of the initial calcium might have been flushed out of the system by the initial LS flood, there might be adequate

residual calcium impairing the effect of the LSS flood in 2-4. The increase in oil recovery when the amount of Ca^{2+} in injection LSS is reduced also verifies that there is less surfactant retarded inside the pores by adsorption to the rock surface when the amount of Ca^{2+} is lower in the aqueous phase. Therefore, there is more surfactant available in the aqueous phase to reduce IFT of oil/water. The recovery curves for the cores flooded with B4 is shown in Figure 8.4.

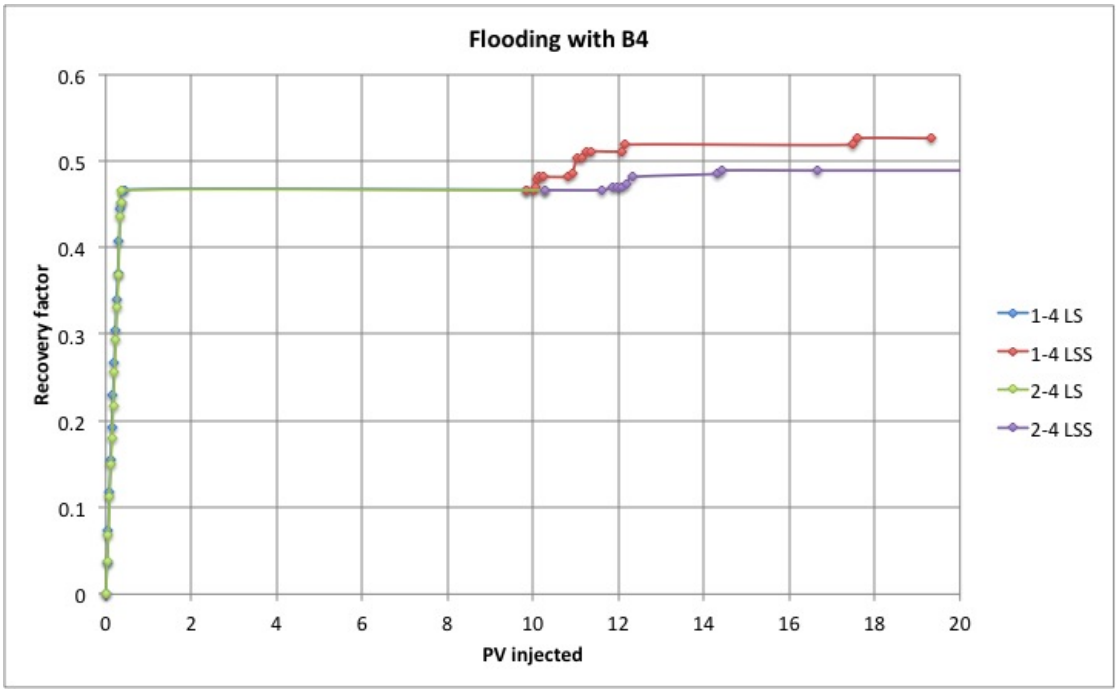

Figure 8.4: Recoveries for cores flooded with B4

8.5 Comparison of performance of cores from the same round

8.5.1 Round 1

Figure 8.5 shows a summary of the LS and LSS recovery for all the cores in round 1.

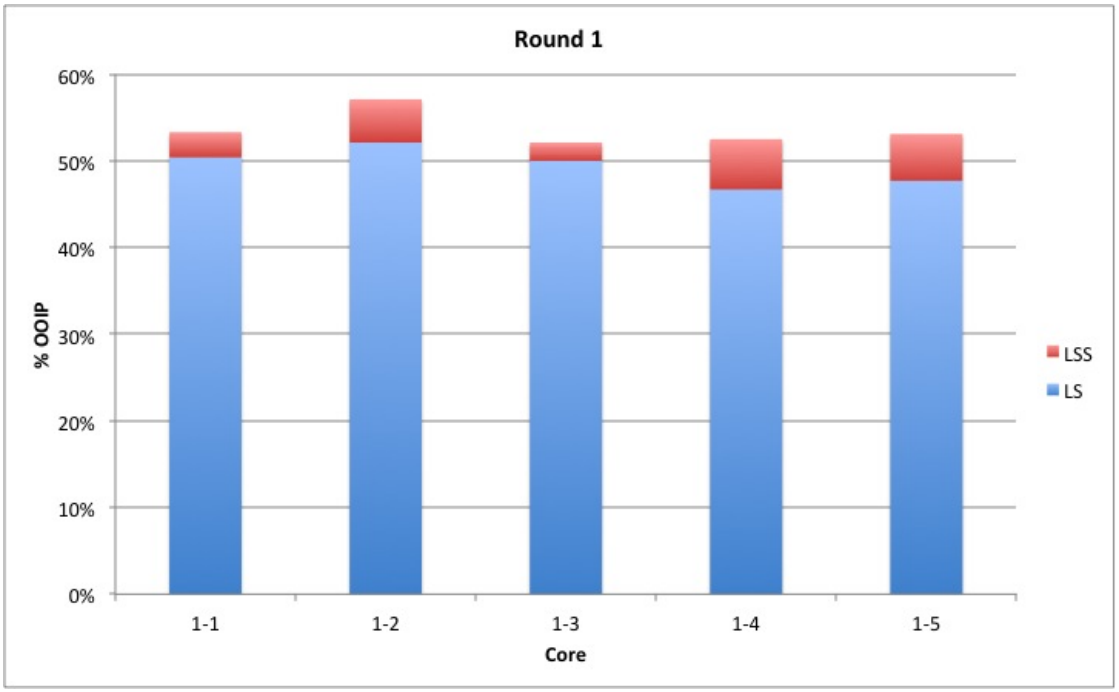

Figure 8.5: Recovery for Round 1 cores

LS flood

In this round, the injection brine composition was the same as in-situ brine, but with $1/10^{th}$ ionic strength. Core 1-1 is believed to be water-wet, and the recovery was therefore relatively high. Cores 1-2 and 1-3 both have 5% divalents in the brine, and are considered to be more oil-wet than 1-1. The core containing calcium, however, recovers 2.1% more oil than the one containing magnesium. There is no clear explanation to this, but it might be that the rock surface has a higher affinity to calcium than magnesium, and thus calcium has a better ability to change the wettability of the core towards more oil-wet during aging than magnesium. Cores 1-4 and 1-5 both had 10% divalents, but for core 1-5, 9% of this was $CaCl_2$. The same fact that calcium better promotes oil-wetness can be applied to explain the higher recovery for core 1-5. This core was more oil-wet, and compared to 1-4, the lower ionic strength of the flooding brine had a better ability to strip polar oil components from the rock surface. According to the XRD results, these cores contains no clay, and low salinity flooding should therefore have little effect. Nevertheless, the results indicate that the lower ionic strength of the flooding water

has an effect on recovery despite the apparent lack of clay. The reason for this can be that the XRD is not accurate enough, and that the cores do contain some clay. A further discussion comments on this later in the chapter.

LSS flood

The most evident observation for the LSS recovery is that the cores containing calcium recovered a larger amount of oil than the cores with no calcium. This directly contradicts the assumption that calcium has a negative effect on the surfactant, as seen from the bottle tests. The observation that was made, indicated that at 60 °C, Mg^{2+} was acting almost like Na^{+} in wettability alteration during aging and during injection. This explains why cores with calcium are more oil-wet, and the lower ionic strength of the flooding brine is changing the wettability towards more water-wet. This, in combination with the effect of surfactant, yields the higher recovery.

8.5.2 Round 2

LS flood

All of these cores are saturated with B5, which contains 10% divalents, so the degree of oil-wetness should theoretically be equal. The most apparent trend for round 2 is that the LS recovery decreases with decreasing contrast between in-situ brine and flooding brine (increasing injection cation content). The highest recovery is obtained when the flooding brine is able to flush out the divalents bridging the polar oil components to the rock surface. This is best obtained when the flooding brine is pure NaCl brine. The wettability changes to a more water-wet state. Core 2-1 is superior in this round and recovers almost 9% more oil than the second best. The difference between 2-2 and 2-3 is only 1%. Both of these cores are flooded with brine containing 5% divalents. Core 2-4 is flooded with B4, which contains 10% divalents, and recovers the lowest amount of oil. The contrast in divalent cation content is low, and thus recovery is low. No wettability change is observed in any of the last three cores (see Appendix A).

LSS flood

Core 1-2 is also superior during the LSS flooding. The initial LS flood has stripped much of the divalents initially present in the core from the connate brine, which allows the surfactant to perform optimally. The surfactant solution has the same low ionic strength, and the positive effect of low salinity brine and surfactant is combined, producing a large amount of incremental oil. The LSS recovery for the other three cores is very low, just over 2%. It is evident that changing Ca^{2+}/Na^{+} ratio to design an optimized EOR process is not easy, if not impossible (see section 8.6). Having a little Ca^{2+} in the system to optimize surfactant phase behavior is less effective than simply having no Ca^{2+} (2-1), where it is guaranteed that the SDBS adsorption to the rock surface is minimum. This implies that there is more surfactant available in aqueous solution to lower IFT. Furthermore, no Ca^{2+} in

solution leads to more desorption of oil from the surface of the rock. The presence of calcium in the flooding brine reduces the effect of the surfactant, making it unable to strip enough cations to release oil.

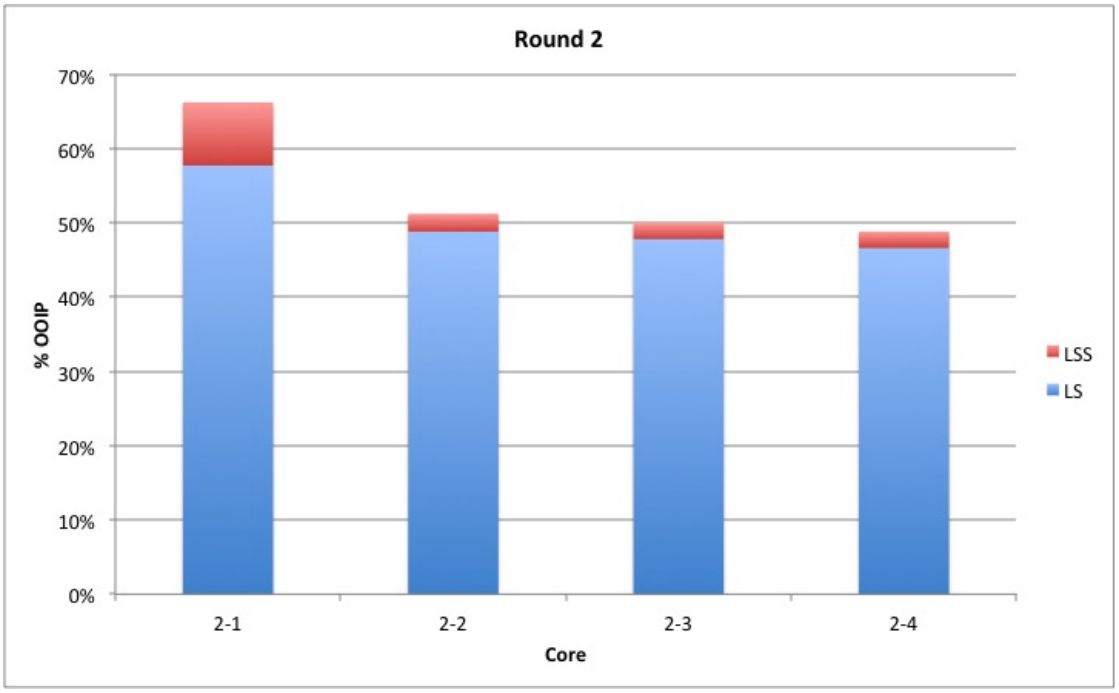

Figure 8.6: Recovery for Round 2 cores

8.5.3 Round 3

LS flood

The same trend seen in round 2 is also evident in round 3. Core 3-4 had the highest divalent contrast between in-situ brine and flooding brine, and therefore gave the highest LS recovery. The core was the most oil-wet, and an apparent change in wettability was observed during the LS flood. Core 3-3 was also saturated with divalents, and flooded with pure NaCl brine. However, the contrast was not as substantial, and it did not recover as much oil. Core 3-2 was both saturated and flooded with B2 brine. While there was evidence of a slight wettability alteration, the final LS recovery was the lowest of the round. Core 3-1 is believed to be water-wet, so while there is no wettability alteration, according to literature, a water-wet rock generally recovers more oil than an oil-wet rock.

LSS flood

The LSS recovery was generally high for all the cores in round 3, over 5% for all of them. This is attributed to the high capillarity, and the higher impact of IFT reduction in tight cores compared to high permeability cores. Core 3-1, being water-wet, had the lowest recovery. The effect of the LSS flooding is probably mostly due to the surfactant's ability to lower the interfacial tension between oil

and water. The other cores were all more oil-wet to some extent, and the LSS recovery was higher for all of them. The combination of wettability alteration and lower IFT results in high LSS recovery.

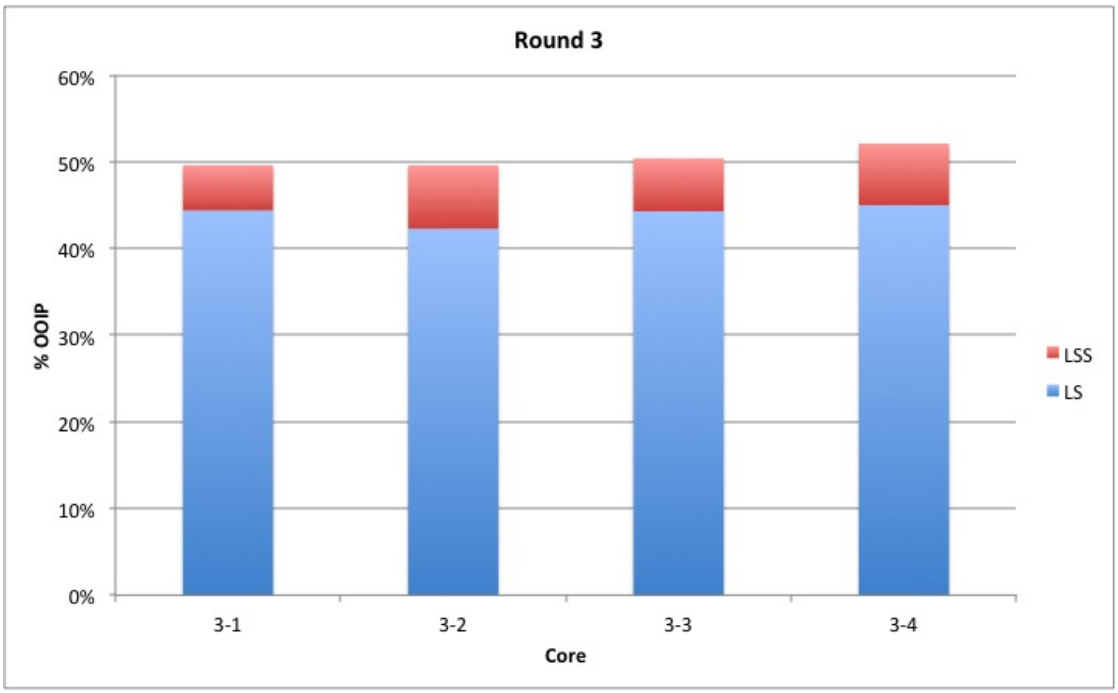

Figure 8.7: Recovery for Round 3 cores

8.6 Effect of calcium in surfactant flooding

Ca^{2+} has two major impacts on surfactant flooding: adsorption of surfactant to the rock surface, and stabilization of surfactant micelles. The former will have a negative impact on oil surfactant recovery, while the latter is positive . Comparison of 1-2 and 1-4 with 2-2, 2-3, and 2-4, shows the negative impact of the presence of more Ca^{2+} where in 2-2, 2-3, and 2-4, the SDBS molecules are retarded in the porous media. Discussing the positive impact of Ca^{2+} refers to the impact on micellization. The higher valency of Ca^{2+} allows the formation of larger, and more stable, micelles in aqueous solution. However, there is a limit for Ca^{2+} content, above which the calcium tends to precipitate surfactant molecules out of solution. The optimal value of Ca^{2+}/Na^{+} in order to obtain lower IFT can be found experimentally, and usually looks similar to Figure 8.8. Unfortunately, it is not possible to control this ratio and sustain it during flooding. One can only design the injection brine in such a way that adsorption is avoided, and get as close as possible to lower IFT. Comparison of {1-1, 1-3}[no Ca^{2+}], {1-2, 1-4}[medium Ca^{2+}] and {2-2, 2-3, 2-4}[too much Ca^{2+}], shows that it led to low, higher, and low recovery, respectively. The higher recovery of LSS flood in {1-2, 1-4}[medium Ca^{2+}] can be attributed to being close to optimal ratio.

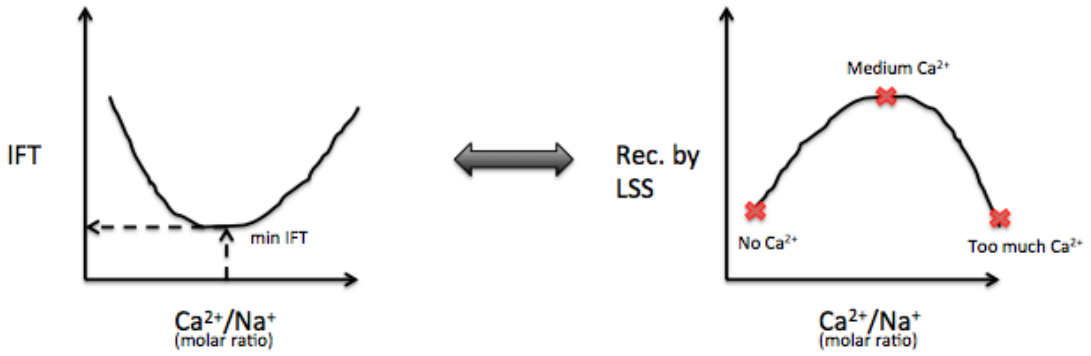

Figure 8.8: IFT and recovery versus molar ratio of Ca^{2+} to Na^{+}

8.7 Further discussion

Since sandstones are sedimentary rocks, it is very common to find small amounts of clay particles among the mineral grains. The cores that were used for rounds 1 and 2 in this experiment were taken from block 6. Small samples from the rock was sent for XRD analysis, and the results indicated that the samples did not contain any clay particles. It should be noted that bulk clay content, which is measured by XRD, does not necessarily correlate with surface clay coverage. Suijkerbuijk et al. (2013) used X-ray Photoelectron Spectroscopy (XPS) and Scanning Auger electron Microscopy (SAM) to measure the average elemental composition of the rock surface where it comes in contact with the fluids. Aluminosilicate coverage on the surface showed much higher clay content than previously measured XRD. They concluded that low salinity injection effect should not be correlated to bulk clay content. Therefore, clay content and its impact in low salinity injection, should be investigated via advanced surface studies rather than relying only on XRD results. This means that one can not conclude that the cores from block 6 were void of clay content. The results indicate that injection of low salinity brine was indeed able to change the wettability of some cores toward a more water-wet state. This belief was also reinforced by observations made from a test flooding performed to test the quality of the flooding apparatus. A core from block 6 was flooded with a brine diluted to $1/100^{th}$ ionic strength, which resulted in a substantial production of fines, as was also see by Tang and Morrow (1999a). The conclusion drawn from this is that the cores from block 6 did indeed contain clay in the form of surface coverage.

An observation that was done during the experiment was that the effective permeability calculated based on stabilized pressure during injection was, for some cores, higher than the permeability measured by the air permeability apparatus. It is not uncommon to have discrepancies between these values, but it is usually the other way around, where the air permeability overestimates the value. The pressure during flooding was measured using high accuracy manometers that are

believed to yield the correct value. It is therefore assumed that the permeability of the cores is, in reality, slightly higher than what is sown by the air permeability apparatus.

No measurements were done to investigate the IFT between the oil and the different surfactant solutions. This was due to time constraints and high demand for the spinning drop apparatus. No tests were performed to investigate the microemulsion phase behavior either. The tailoring of the surfactant solutions were done solely based on surfactant concentration and associated precipitation. It is therefore no way of knowing the values for IFT. Still, the tertiary LSS flooding recovered incremental oil for all the cores after the secondary LS flooding could not. The reduction in IFT is also evident when looking at the pressure behavior during flooding. The pressure drop across the core decreased consistently for all the cores during LSS flooding, corresponding to an increase in permeability, indicating lower IFTs. Still, the LSS recoveries were nowhere near that obtained by Riisøen (2012), so it is believed that the surfactant solution could be optimized even further by doing proper testing before selecting the type of surfactant and appropriate concentration. It should, however, be noted that the Bentheimer cores used in that study had very large permeability, and a narrow pore size distribution, which indicates an excellent quality reservoir rock.

There were large pressure fluctuations during low salinity water injection and low salinity surfactant injection in many of the core floodings. These were often associated with additional oil recovery, but that was not always the case. When the pressure drop behaves like this, it means that the fluids are redistributed inside the core. In most cases, this was indeed associated with oil recovery. In other cases, there were still redistribution of fluids, but not enough to produce oil. Discontinuous oil can move around inside the core without reaching the outlet, and that is what caused those large spikes in pressure drop.

Chapter 9

Conclusion

- Oil recovery was highest in the cores with the greatest contrast between divalent cation content in in-situ brine and injection brine. Flooding with a pure NaCl brine in cores saturated with 10% divalent cations allowed for the divalents to be stripped from the rock surface, and promoted a change towards a more water-wet system.
- Low salinity waterflooding in secondary mode recovered between 42.3 and 57.7% OOIP, while tertiary low salinity surfactant flooding recovered an additional 2.1-8.5%.
- Bulk clay content was not found to be crucial for the low salinity performance in these experiments. The lower permeability, and the the heterogeneity of the cores from round 3, had a greater impact on recovery than the bulk clay content. Overall, cores from round 1 and 2 performed better than the cores from round 3 during low salinity waterflooding. Wettability alteration was observed for several of the cores containing no bulk clay.
- The oil recovery by low salinity surfactant flooding in round 3 was high for all the cores, ranging from 5.2 to 7.3%. This was attributed to the higher capillarity, which has a greater potential for improvement by IFT reduction.
- Evidence of a reduction in IFTs between oil and water were observed from the pressure drop across the cores during low salinity waterflooding. The pressure decreased consistently for all the corefloods, which was an indication of a reduction in capillarity resulting from the lower IFT.
- At 60 °C, Mg^{2+} appeared to behave almost like Na^{+} in wettability alteration during aging, and during injection. The Ca^{2+} content played a more crucial role in promoting oil-wetness during aging, and was the most important factor in low salinity surfactant flooding.

Chapter 10

Recommendations for future work

COBR interactions are extremely complex, and therefore requires further research. This is necessary in order to obtain a better understanding of the parameters that affect the performance of low salinity waterflooding and low salinity surfactant flooding. Here are some suggestions on how to expand the research started in this Thesis:

- Based on the observations of this Thesis, further focus should be on the use of pure NaCl as injection brine. The bottle tests, carried out during this experiment, indicate that the surfactant concentration can be increased from 500 to at least 3000 ppm without experiencing precipitation. This should be coupled with IFT measurements and an adsorption study in order to optimize the surfactant slug.
- It could also be interesting to investigate different Ca^{2+}/Na^{+} ratios of surfactant solution salinity and their impact on performance. This should be coupled with IFT measurements, and done in such a way that Ca^{2+} does not adsorb the surfactant onto the rock surface, nor precipitates out of the aqueous solution. This idea can also be tested for low salinity flooding.
- The micro-CT scanning apparatus can be utilized to obtain a better understanding of the saturation distribution in the core sample. This is important in order to locate the residual oil saturation, and the source of the produced oil during flooding.
- A more extensive phase behavior, and temperature dependence study of the surfactant, should be conducted prior to waterflooding, in order to optimize the low salinity surfactant recovery.
- Extensive effluent analysis, such as ions, pH, and fines analysis, should be carried out in order to obtain a better understanding of the mechanisms behind the low salinity waterflooding and low salinity surfactant process.
- In addition, based on the results from the bottle tests, a further study of the apparent synergy of Ca^{2+} and Mg^{2+} should be carried out in order to identify the reasons why Mg^{2+} seems to counteract the effect of Ca^{2+} in surfactant precipitation.

References

Abdallah, W., J.S. Buckley, A. Carnegie, J. Edwards, B. Herold, E. Fordham, A. Graue, T. Habashy, C. Signer, H. Hussein, B. Montaron, and M. Ziauddin (2007). "Fundamentals of Wettability". In: *Oilfield Review* 19.2, pp. 44–61.

Abdulla, F., H.S. Hashem, B. Abdulraheem, M. Al-Naqi, A. Al-Qattan, and H. John (2013). *First EOR Trial using Low Salinity Water Injection in the Greater Burgan Field, Kuwait*. Paper SPE 164341 presented at the SPE Middle East Oil and Gas Show and Conference held in Manama, Bahrain, 10-13 March 2013.

Alagic, E. (2010). "Combination of low salinity water flooding with surfactant injection - A new hybrid process". PhD thesis. University of Bergen.

Alagic, E. and A. Skauge (2010). "Combined Low Salinity Brine Injection and Surfactant Flooding in Mixed-Wet Sandstone Cores". In: *Energy & Fuels* 24, pp. 3551–3559.

Alagic, E., K. Spildo, A. Skauge, and J. Solbakken (2011). "Effect of crude oil aging on low salinity and low salinity surfactant flooding". In: *Journal of Petroleum Science and Engineering* 78, pp. 220–227.

Ashraf, A., N.J. Hadia, O. Torsæter, and M.T.Tweheyo (2010). *Laboratory Investigation of Low Salinity Waterflooding as Secondary Recovery Process*. Paper SPE 129012 presented at the SPE Oil and Gas India Conference and Exhibition held in Mumbai, India, 20-22 January 2010.

Atkinson, H. (1927). *Recovery of Petroleum from Oil Bearing Sands*. US Patent 1,651,311. URL: `http://www.google.com/patents/US1651311`.

Austad, T., A. RezaeiDoust, and T. Puntervold (2010). *Chemical Mechanism of Low Salinity Water Flooding in Sandstone Reservoirs*. Paper SPE 129767 presented at the SPE Improved Oil Recovery Symposium held in Tulsa, Oklahoma, USA, 24-28 April 2010.

Berea Sandstone^{TM} Cores (2013). *Berea Sandstone^{TM} Petroleum Cores*. Accessed 14.11.13. URL: `http://www.bereasandstonecores.com/`.

Bernard, G.G. (1967). *Effect of Floodwater Salinity on Recovery of Oil from Cores Containing Clays*. Paper SPE 1725 presented at the 38th Annual California Regional Meeting of the Society of Petroleum Engineers of Aime held in Los Angeles, California, USA, 26-27 October 1967.

Boussour, S., M. Cissokho, P. Cordier, H. Bertin, and G. Hamon (2009). *Oil Recovery by Low Salinity Brine Injection: Laboratory Results on Outcrop and Reservoir Cores*. Paper SPE 124277 presented at the 2009 SPE Annual Technical Conference and Exhibition held in New Orleans, Louisiana, USA, 4-7 October 2009.

Buckley, J.S., Y. Liu, and S.G. Monsterleet (1998). "Mechanisms of Wetting Alteration by Crude Oils". In: *SPE Journal* 3.1, pp. 54–61.

Cayias, J.L., R.S. Schechter, and W.H. Wade (1977). "The Utilization of Petroleum Sulfonates for Producing Low Interfacial Tensions Between Hydrocarbons and Water". In: *Journal of Colloid and Interface Science* 59.01, pp. 31–38.

Cissokho, M., S. Boussor, P. Cordier, H. Bertin, and G. Hamon (2009). *Low Salinity Oil Recovery on Clayey Sandstone: Experimental Study*. Society of Core Analysts, SCA2009-05.

Cuong, T.Q.D., C. Zhangxin, N.T.B. Nguyen, W. Bae, and T.H. Phung (2011). *Development of Isotherm Polymer/Sufactant Adsorption Models in Chemical Flooding*. Paper SPE 147872 presented at SPE Asia Pacific Oil and Gas Conference and Exhibition, Jakarta, Indonesia.

Dispensetips (2013). *A Guide for Electronic Assembly Materials*. Accessed 20.09.13. URL: `http://www.dispensetips.com/pages/rheology.html`.

Emadi, A. and M. Sohrabi (2013). *Visual Investigation of Oil Recovery by Low Salinity Water Injection: Formation of Water Micro-Dispersions and Wettability Alteration*. Paper SPE 166435 presented at the SPE Annual Technology Conference and Exhibition held in New Orleans, Louisiana, USA, 30 September - 2 October 2013.

Evans, D.F. and H. Wennerström (1999). *The Colloidal Domain: where physics, chemistry, biology and technology meet*. 2nd ed. Wiley - VCH.

Foster, W.R. (1973). "A Low-Tension Waterflooding Process". In: *Journal of Petroleum Technology* 25.02, pp. 205–210.

Gamage, P. and G. Thyne (2011). *Comparison of Oil Recovery by Low Salinity Waterflooding in Secondary and Tertiary Recovery Modes*. Paper SPE 147375 presented at the SPE Annual Technical Conference and Exhibition held in Denver, Colorado, USA, 30 October-2 November 2011.

Hadia, N.J., A. Ashraf, M.T. Tweheyo, and O. Torsæter (2013). "Laboratory Investigation on Effects of Initial Wettabilities on Performance of Low Salinity Waterflooding". In: *Journal of Petroleum Science and Engineering* 105, pp. 18–25.

Hadia, N.J., T. Hansen, M.T. Tweheyo, and O. Torsæter (2012). "Influence of Crude Oil Components on Recovery by High and Low Salinity Waterflooding". In: *Energy & Fuels* 26, pp. 4328–4335.

Healy, R.N., R.L. Reed, and D.K. Stenmark (1976). "Multiphase Microemulsion Systems". In: *SPE Journal* 16.03, pp. 147–160.

Hill, H.J., J. Reisberg, and G.L. Stegmeier (1973). "Aqueous Surfactant Systems for Oil Recovery". In: *Journal of Petroleum Technology* 25.02, pp. 186–194.

Hirasaki, G., C.A. Miller, and M. Puerto (2011). "Recent Advances in Surfactant EOR". In: *SPE Journal*, pp. 889–907.

Jadhunandan, P.P. and N.R. Morrow (1995). "Effect of Wettability on Waterflood Recovery for Crude-Oil/Brine/Rock Systems". In: *SPE Reservoir Engineering* 10.01, pp. 40–46.

Jansson, M. (2007). *DLVO(E) Theory and Limitations, Rrefined Models*. Accessed 22.01.14. URL: `http://www.kemi.kth.se/nuchem/colloid/mj_070420.pdf`.

Kleppe, J. (2013). *Handout note 3: Review of relative permeabilities and capillary pressures*. TPG4150 Reservoir Recovery Techniques. Accessed 18.11.13. URL: `%7Bhttp://www.ipt.ntnu.no/~kleppe/TPG4150/krpc.pdf%7D`.

Lager, A., K.J. Webb, C.J.J Black, M. Singleton, and K.S. Sorbie (2006). *Low Salinity Recovery - An Experimental Investigation*. Paper SCA2006-36 presented at the International Symposium of the Society of Core Analysts held in Trondheim, Norway, 12-16 September 2006.

Lager, A., K.J. Webb, I.R. Collins, and D.M. Richmond (2008). *LoSal^{TM} Enhanced Oil Recovery: Evidence of Enhanced Oil Recovery at the Reservoir Scale*. Paper SPE 113976 presented at the 2008 SPE/DOE Improved Oil Recovery Symposium held in Tulsa, Oklahoma, USA, 19-23 April 2008.

Lake, L.W. (1989). *Enhanced Oil Recovery*. Englewood Cliffs, New Jersey 07632: Prentice Hall.

Lee, S.Y., K.J. Webb, I.R. Collins, A. Lager, S.M. Clarke, M. O'Sullivan, A.F. Routh, and X. Wang (2010). *Low Salinity Oil Recovery - Increasing Understanding of the Underlying Mechanisms*. Paper SPE 129722 presented at the 2010 SPE Improved Oil Recovery Symposium held in Tulsa, Oklahoma, USA, 24-28 April 2010.

Lemon, P., A. Zeinijahromi, P. Bedrikovetsky, and I. Shahin (2011). "Effects of Injected-Water Salinity on Waterflood Sweep Efficiency Through Induced Fines Migration". In: *Journal of Canadian Petroleum Technology* 50.9-10, pp. 82–94.

Ligthelm, D.J., J. Gronsveld, J.P. Hofman, N.J Brussee, F. Marcelis, and H.A. van der Linde (2009). *Novel Waterflooding Strategy by Manipulation of Injection Brine Composition*. Paper SPE 119835 presented at the 2009 SPE EUROPEC/EAGE Annual Conference and Exhibition held in Amsterdam, The Netherlands, 8-11 June 2009.

McGuire, P.L., J.R. Chatham, F.K Paskvan, D.M. Sommer, and F.H. Carini (2005). *Low Salinity Oil Recovery: An Exciting New EOR Opportunity for Alaska's North Slope*. Paper SPE 93903 presented at the 2005 SPE Western Regional Meeting held in Irvine, CA, USA, 30 March - 1 April 2005.

Melrose, J.C. and C.F. Brandner (1974). "Role of Capillary Forces In Detennining Microscopic Displacement Efficiency For Oil Recovery By Waterflooding". In: *Journal of Canadian Petroleum Technology* 13.04, pp. 54–62.

Morrow, N.R. and J.S. Buckley (1999). "Improved Oil Recovery by Low-Salinity Waterflooding". In: *Journal of Petroleum Technology*, pp. 106–112.

Morrow, N.R., G.Q. Tang, M. Valat, and X. Xie (1998). "Prospects of Improved Oil Recovery Related to Wettability and Brine Composition". In: *Journal of Petroleum Science and Technology* 20.3-4, pp. 267–276.

Mwangi, P. (2010). "An Experimental Study of Surfactant Enhanced Waterflooding". Masters thesis. Louisiana State University, Agricultural, and Mechanical College.

Nasralla, R.A., M.B. Alotiabi, and H.A. Nasr-El-Din (2011). *Efficiency of Oil Recovery by Low Salinity Water Flooding in Sandstone Reservoirs*. Paper SPE 144602 presented at the SPE Western North American Regional Meeting held in Anchorage, Alaska, USA, 7-11 May 2011.

Paria, S. and K.C. Khilar (2004). "A review on experimental studies of surfactant adsorption at the hydrophilic solid–water interface". In: *Advances in Colloid and Interface Science* 110.3, pp. 75–95.

Pu, H., X. Xie, P. Yin, and N.R. Morrow (2008). *Application of Coalbed Methane Water to Oil Recovery by Low Salinity Waterflooding*. Paper SPE 113410 presented at the 2008 SPE/DOE Improved Oil Recovery Symposium held in Tulsa,Oklahoma, USA, 19-23 April 2008.

Pumps and Systems (2013). *Pumps and Systems*. Accessed 20.09.13. URL: `http://www.pump-zone.com/topics/pumps/centrifugal-pumps/newtonian-and-non-newtonian-fluids-0`.

ReservoirBlog (2014). *Chapter 1- Enhanced Oil Recovery (EOR)- Classification*. Accessed 29.04.14. URL: http://randomwave.wordpress.com/2010/03/18/chapter-1-enhanced-oil-recovery-eor-classification/.

RigZone (2013). *RigZone*. Accessed 19.09.13. URL: http://www.rigzone.com/training/insight.asp?insight_id=313&c_id=4.

Riisøen, S. (2012). "Effect of Combined Low Salinity and Surfactant Injection on Oil Recovery in Aged Bentheimer Sandstones at Different Temperatures". Master Thesis. University of Bergen.

Rivet, S.M., L.W. Lake, and G.A. Pope (2010). *A Coreflood Investigation of Low-Salinity Enhanced Oil Recovery*. Paper SPE 134297 presented at the SPE Annual Technical Conference and Exhibition held in Florence, Italy, 19-22 September 2010.

Robertson, E.P. (2007). *Low-Salinity Waterflooding to Improve Oil Recovery - Historical Field Evidence*. Paper SPE 109965 presented at the 2007 SPE Annual Technical Conference and Exhibition held in Anaheim, California, USA, 11-14 November 2007.

Roshanfekr, M. and R. T. Johns (2011). "Prediction of Optimum Salinity and Solubilization Ratio for Microemulsion Phase Behavior with Live Crude at Reservoir Pressure". In: *Fluid Phase Equilibria* 304.1-2, pp. 52–60.

Royal Society of Chemistry (2014). *ChemSpider - Search and Share Chemistry*. Accessed 02.04.14. URL: http://www.chemspider.com/Chemical-Structure.30411.html.

Schlumberger (2013). *Schlumberger Oilfield Glossary*. Last accessed 05.11.13. URL: http://www.glossary.oilfield.slb.com/.

Seccombe, J., A. Lager, G. Jerauld, B. Jhaveri, T. Buikema, S. Bassler, J. Denis, K. Webb, A. Cockin, E. Fueg, and F. Paskvan (2010). *Demonstration of Low-Salinity EOR at Interwell Scale, Endicott Field, Alaska*. Paper SPE 129692 presented at the 2010 SPE Improved Oil Recovery Symposium held in Tulsa, Oklahoma, USA, 24-28 April 2010.

Sheng, J.J. (2011). *Modern Chemical Enhanced Oil Recovery: Theory and Practice*. Englewood Cliffs, New Jersey 07632: Elsevier.

— (2013). *A Comprehensive Review of Alkaline-Surfactant-Polymer (ASP) Flooding*. Paper SPE 165358 presented at the SPE Western Regional & AAPG Pacific Section Meeting 2013 Joint Technical Conference held in Monterey, California, USA, 19-25 April 2013.

Skjæveland, S.M. and J. Kleppe (1992). *Recent Advances in Improved Oil Recovery Methods for North Sea Sandstone Reservoirs*. Stavanger: Norwegian Petroleum Directorate.

Skrettingland, K., T. Holt, M.T. Tweheyo, and I. Skjevrak (2011). "Snorre Low-Salinity-Water Injection - Coreflooding Experiments and Single-Well Field Pilot". In: *SPE Reservoir Evaluation & Engineering* 14.02, pp. 182–192.

Sorbie, K.S. and I.R. Collins (2010). *A Proposed Pore-Scale Mechanism for How Low Salinity Waterflooding Works*. Paper SPE 129833 presented at the 2010 SPE Improved Oil Recovery Symposium held in Tulsa, Oklahoma, USA, 24-28 April 2010.

Sorop, T.G., B.M.J.M. Suijkerbuijk, S.K. Masalmeh, M.T. Looijer, A.R Parker, D.M. Dindoruk, S.G. Goodyear, and I.S.M. Al-Qarshubi (2013). *Integrated Approach in Deploying Low Salinity Waterflooding*. Paper SPE 165277 presented at the SPE Enhanced Oil Recovery Conference held in Kuala Lumpur, Malaysia, 2-4 July 2013.

Suijkerbuijk, B.M.J.M, J.P. Hofman, D.J. Ligthelm, J. Romanuka, N. Brussee, H.A. van der Linde, and A.H.M. Marcelis (2012). *Fundamental Investigations Into Wettability and Low Salinity Flooding by Parameter Isolation*. Paper SPE 154204 presented at the Eighteenth SPE Improved Oil Recovery Symposium held in Tulsa, Oklahoma, USA, 14-18 April 2012.

Suijkerbuijk, B.M.J.M, H. Kuipers, C. van Kruijsdijk, S. Berg, J. van Winden, D. Ligthelm, H. Mahani, M. Pingo Almada, E. Van den Pol, V. Joekar Niasar, J. Romanuka, E. Vermolen, and I. Al-Qarshubi (2013). *Development of a Workflow to Improve Predictive Capability of Low Salinity Response*. Paper IPTC 17157 presented at the International Petroleum Technology Conference in Beijing, China.

Taber, J.J. (1969). "Dynamic and Static Forces Required to Remove a Discontinuous Oil Phase from Porous Media Containing Both Oil and Water". In: *SPE Journal* 9.01, pp. 3–12.

Tang, G.Q. and N.R. Morrow (1997). "Salinity, Temperature, Oil Composition, and Oil Recovery by Waterflooding". In: *SPE Reservoir Engineering* 12.04, pp. 269–276.

— (1999a). "Influence of Brine Composition and Fines Migration on Crude Oil/Brine/Rock Interactions and Oil Recovery". In: *Journal of Petroleum Science and Engineering* 24, pp. 99–111.

— (1999b). *Oil Recovery by Waterflooding and Imbibition - Invading Brine Cation Valency and Salinity*. Society of Core Analysts, SCA-9911.

Thomas, S. (2007). "Enhanced Oil Recovery - An Overview". In: *Oil & Gas Science and Technology* 63.1, pp. 9–19.

Tichelkamp, T., Y. Vu, M. Nourani, and G. Øye (2014). *Interfacial Tension Between Low Salinity Soultions of Sulfonate Surfactants and Crude and Model Oils*. Just accepted manuscript for Energy & Fuels.

Torsæter, O. and M. Abtahi (2003). *Experimantal Laboratory Engineering: Laboratory Workbook*. Course Workbook, Reservoir Properties.

Uren, L.C. and E.H. Fahmy (1927). "Factors Influencing the Recovery of Petroleum from Unconsolidated Sands by Waterflooding". In: *Transactions of the AIME* 77.01, pp. 318–335.

Vledder, P., J.C. Fonseca, T. Wells, I. Gonzales, and D. Ligthelm (2010). *Low Salinity Water Flooding: Proof of Wettability Alteration on a Field Wide Scale*. Paper SPE presented at the 2010 SPE Improved Oil Recovery Symposium held in Tulsa, Oklahoma, USA, 24-28 April 2010.

Webb, K.J., C.J.J Black, and H. Al-Ajeel (2004). *Low Salinity Oil Recovery - Log-Inject-Log*. Paper SPE 89379 presented at the 2004 SPE/DOE Fourteenth Symposium on Improved Oil Recovery held in Tulsa, Oklahoma, USA, 17-21 April 2004.

Yousef, A.A., S. Al-Saleh, and M. Al-Jawfi (2012). *The Impact of the Injection Water Chemistry on Oil Recovery from Carbonate Reservoirs*. Paper SPE 154077 presented at the SPE EOR Conference at Oil and Gas West Asia held in Muscat, Oman, 16-18 April 2012.

Zhang, Y. and N.R. Morrow (2006). *Comparison of Secondary and Tertiary Recovery with Change in Injection Brine Composition for Crude Oil/Sandstone Combinations*. Paper SPE 99757 presented at the 2006 SPE/DOE Symposium on Improved Oil Recovery held in Tulsa, Oklahoma, USA, 22-26 April 2006.

Zhu, B.Y. and T. Gu (1991). "Surfactant Adsorption at Solid-Liquid Interfaces". In: *Advances in Colloid and Interface Science*.

Zolotukhin, A.B. and J-R. Ursin (2000). *Introduction to Petroleum Reservoir Engineering*. Kristiansand: Høyskoleforlaget.

Appendix A

Production and Pressure curves

All production curves together with differential pressures can be found in this appendix. The blue lines represent the LS production, while the red lines represent the LSS production in all the plots. The differential pressures are the green lines, and the red dot represents the water breakthrough.

A.1 Round 1

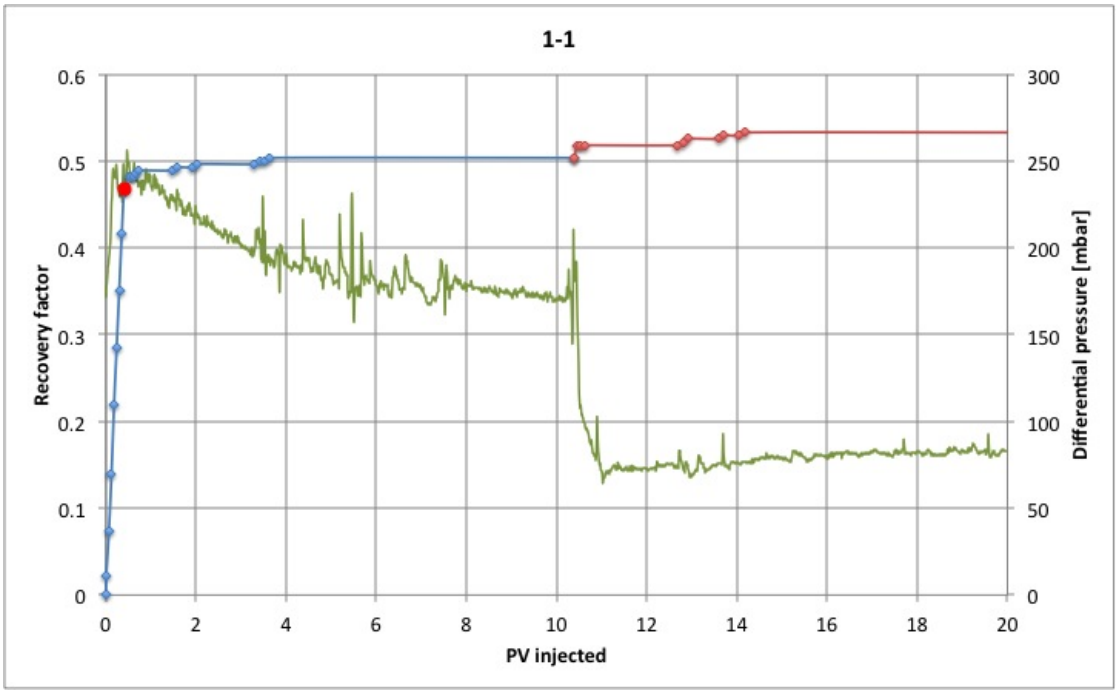

Figure A.1: Production and differential pressure for core 1-1

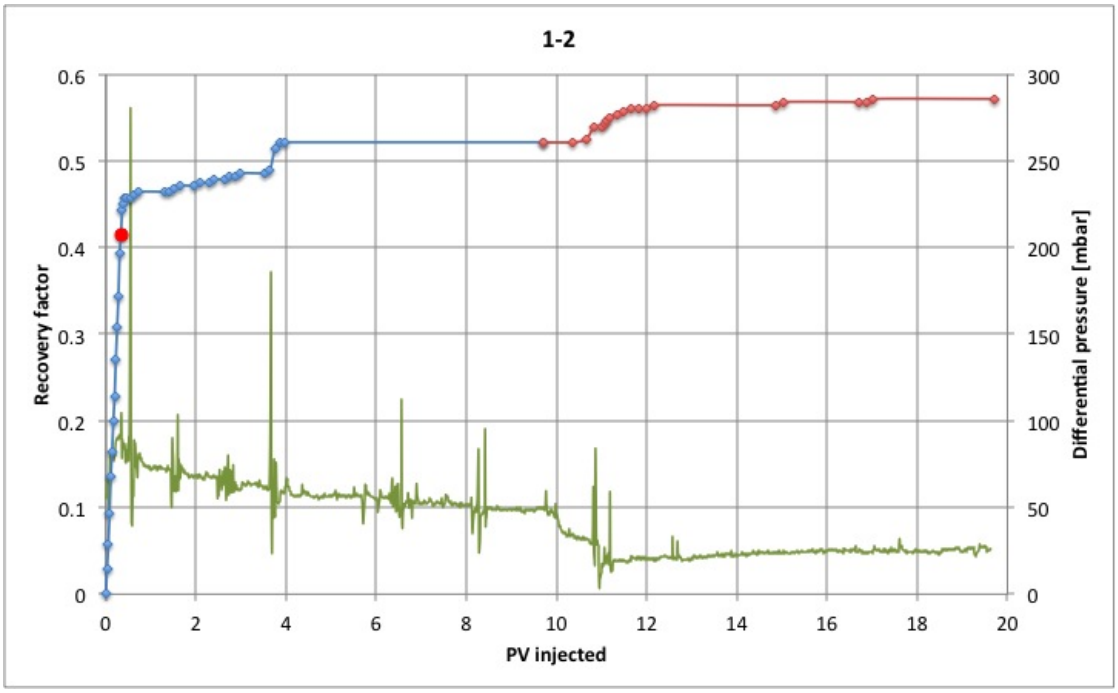

Figure A.2: Production and differential pressure for core 1-2

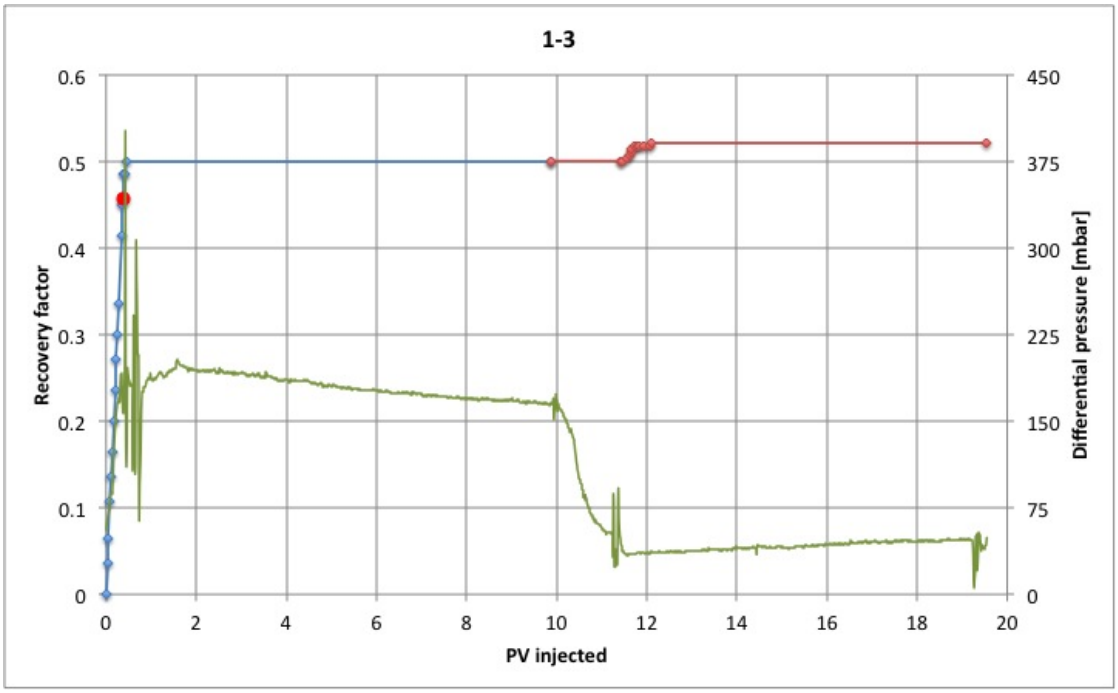

Figure A.3: Production and differential pressure for core 1-3

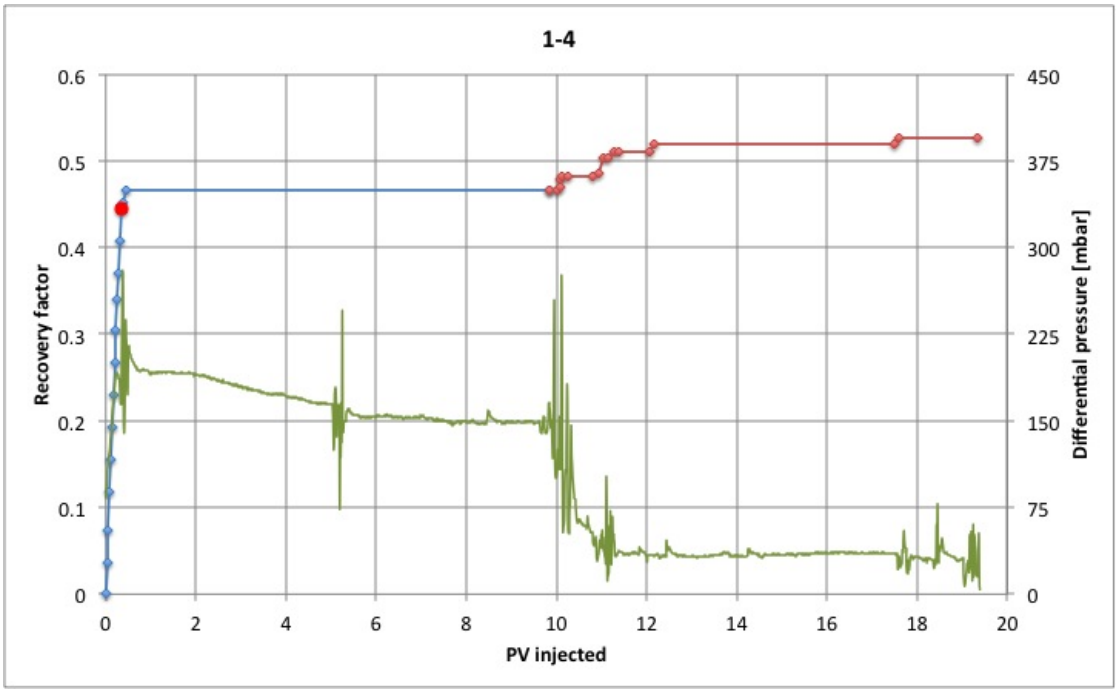

Figure A.4: Production and differential pressure for core 1-4

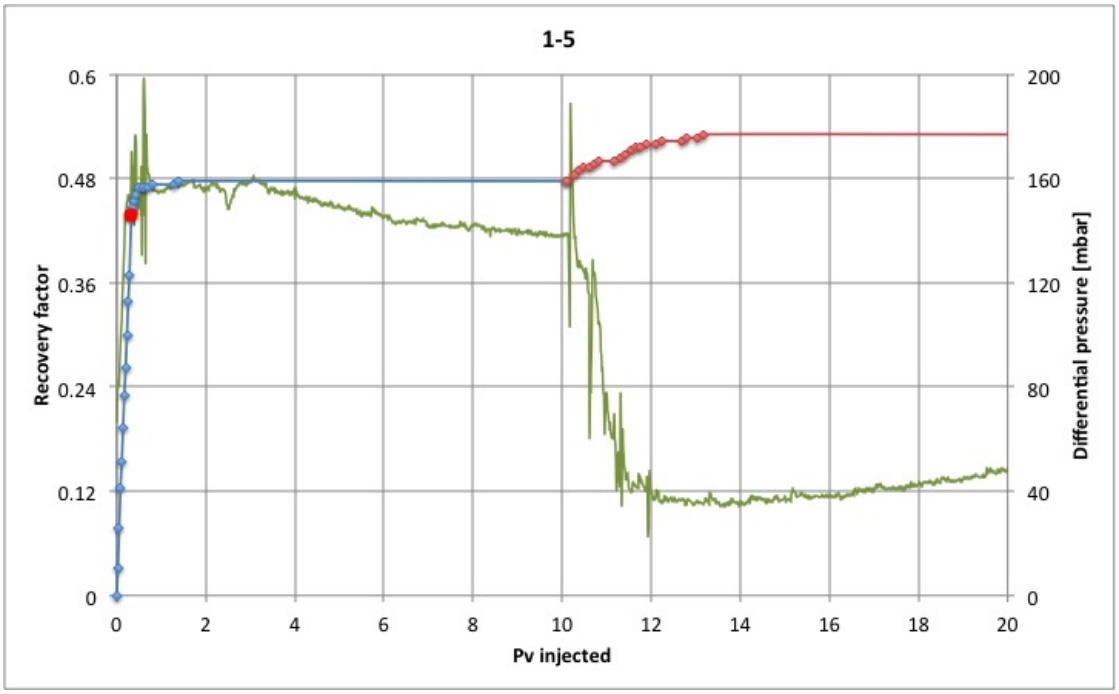

Figure A.5: Production and differential pressure for core 1-5

A.2 Round 2

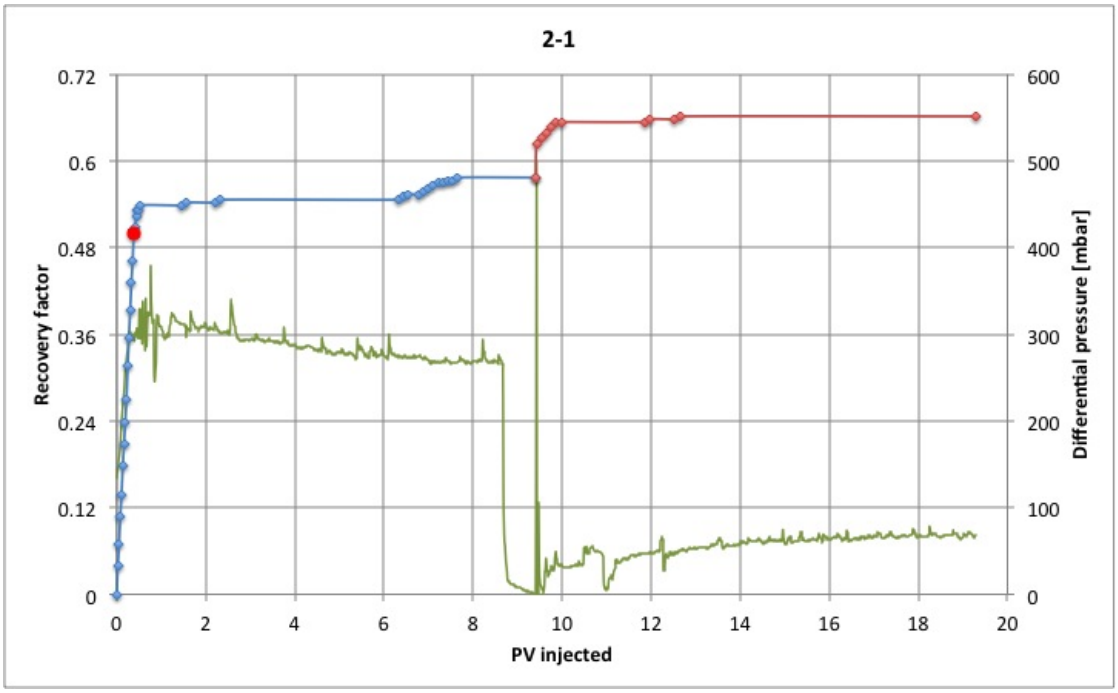

Figure A.6: Production and differential pressure for core 2-1

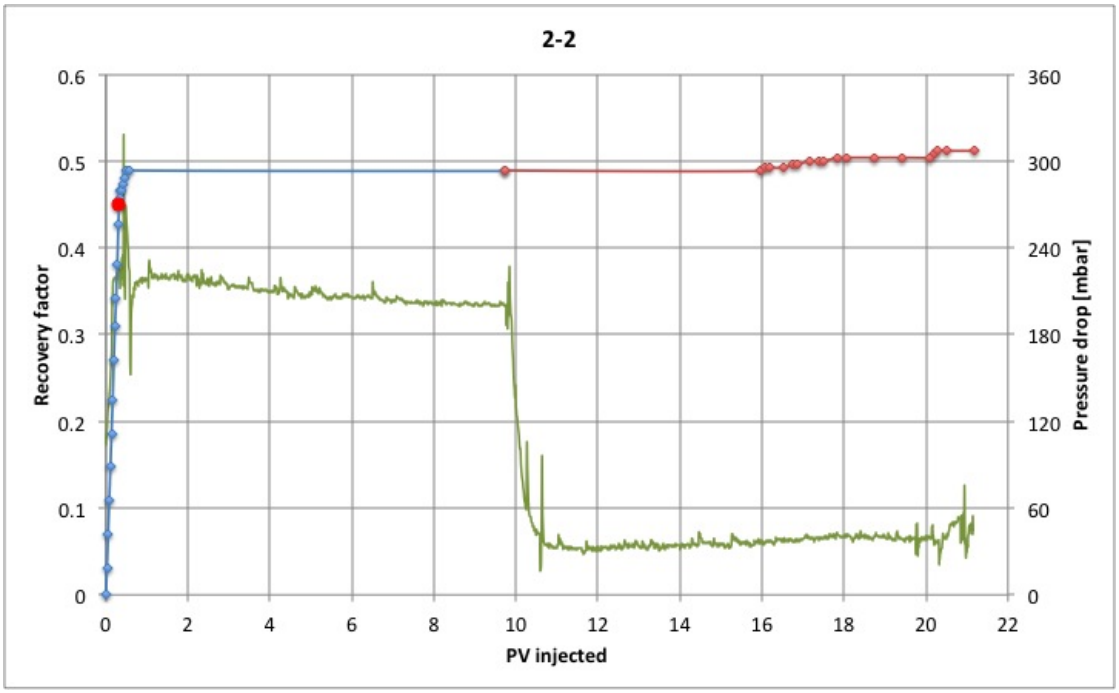

Figure A.7: Production and differential pressure for core 2-2

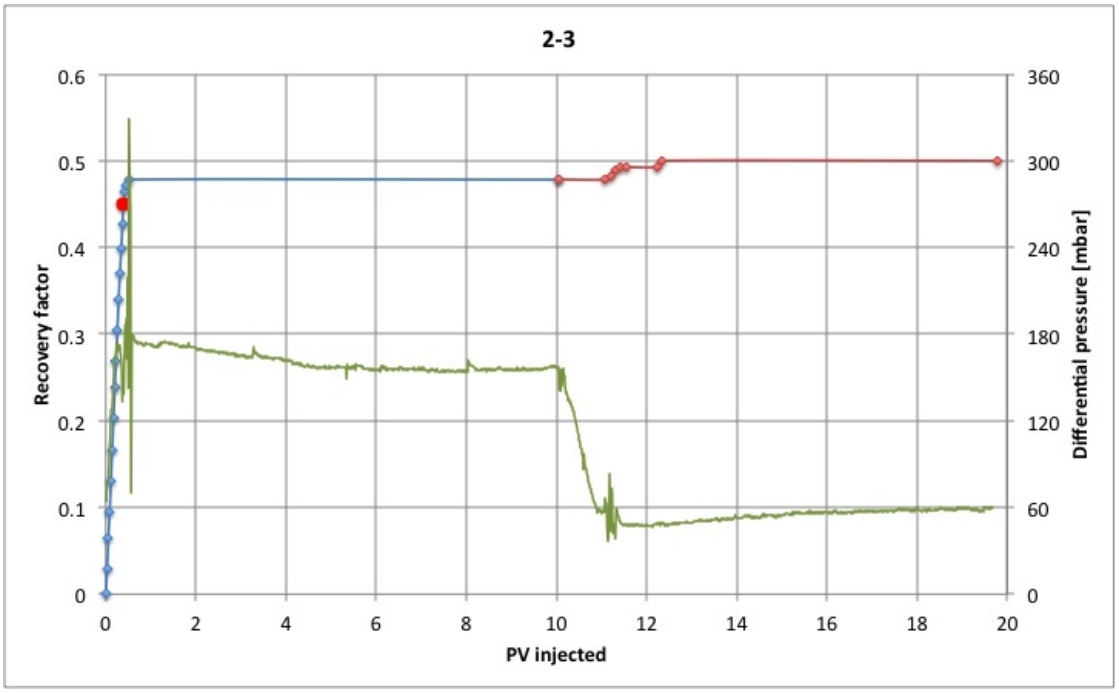

Figure A.8: Production and differential pressure for core 2-3

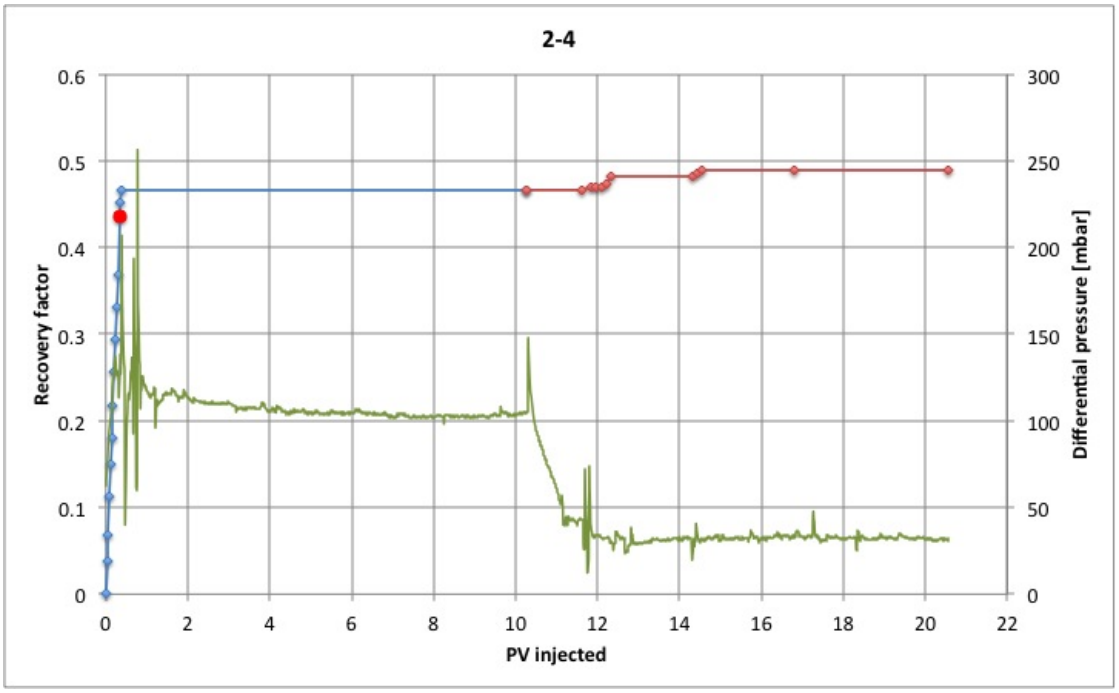

Figure A.9: Production and differential pressure for core 2-4

A.3 Round 3

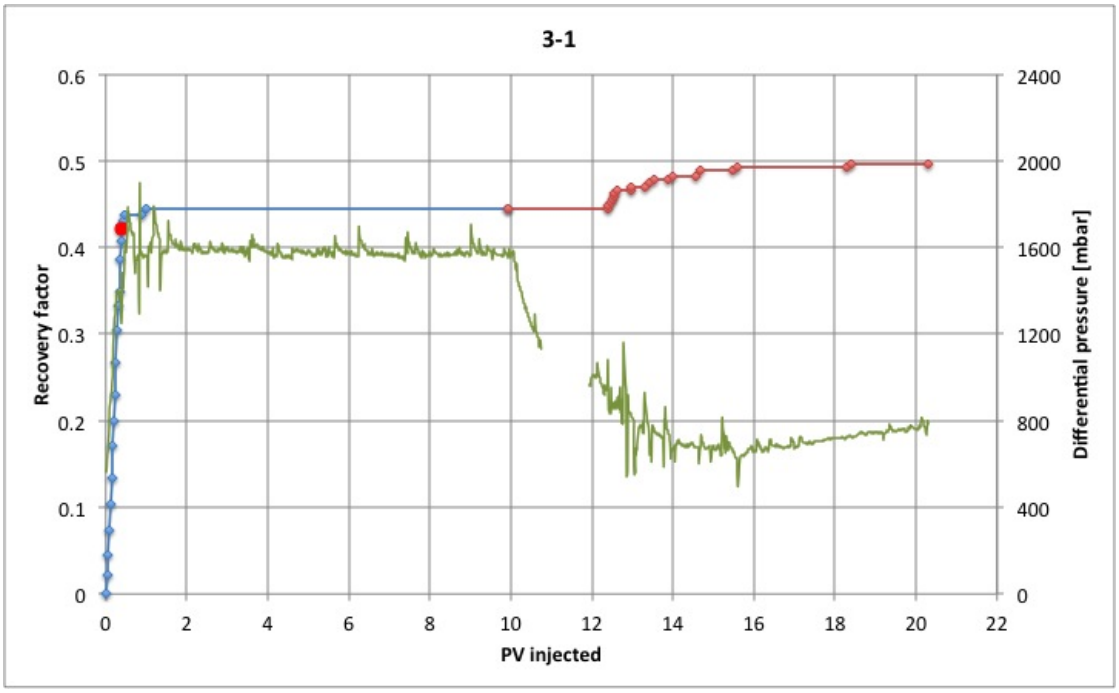

Figure A.10: Production and differential pressure for core 3-1

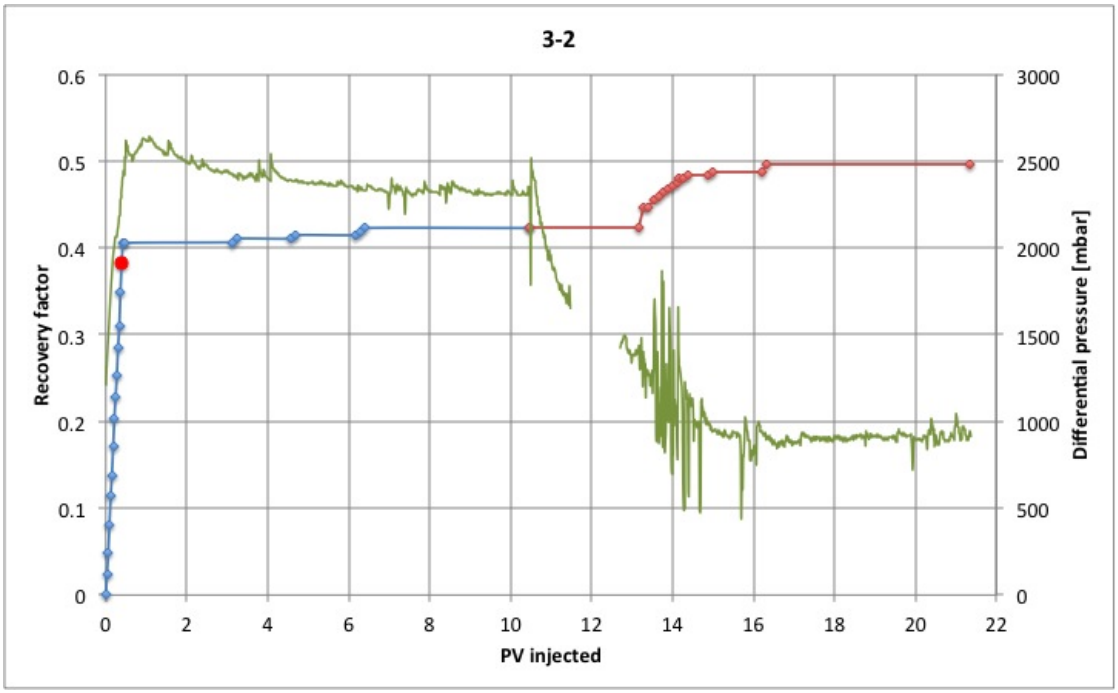

Figure A.11: Production and differential pressure for core 3-2

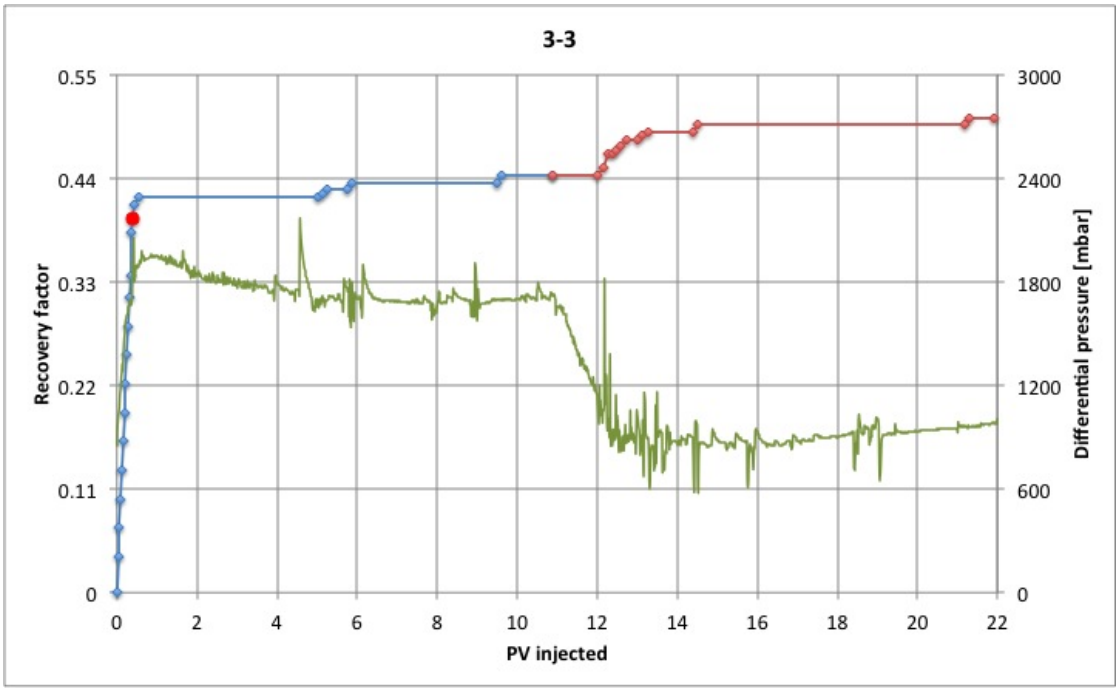

Figure A.12: Production and differential pressure for core 3-3

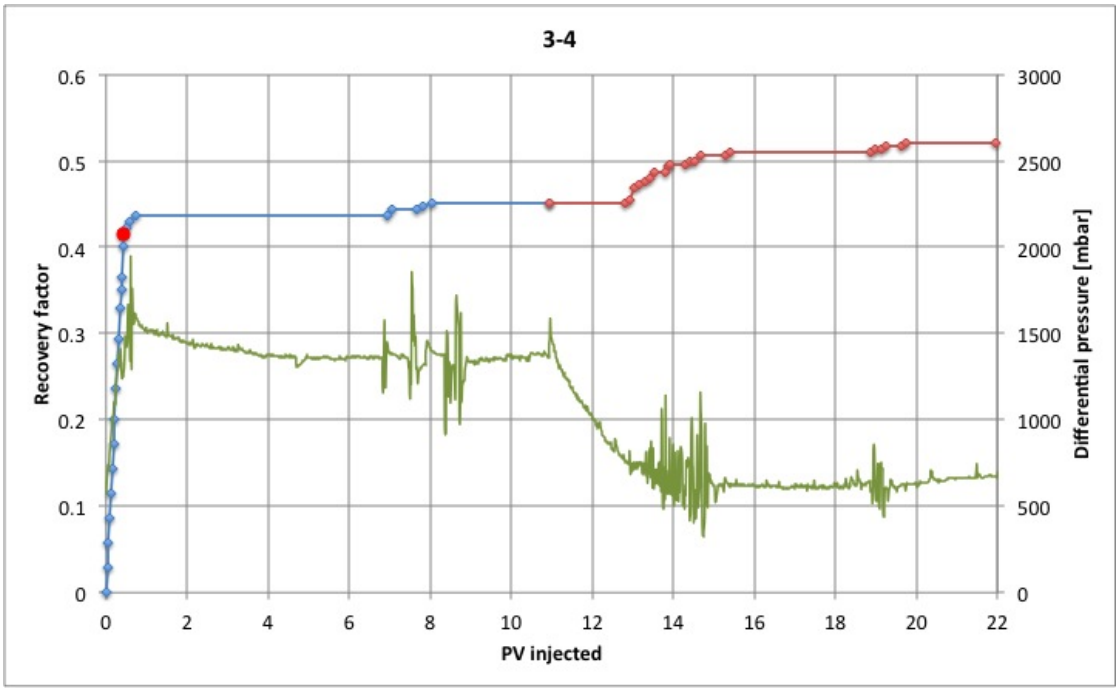

Figure A.13: Production and differential pressure for core 3-4

Appendix B

Differential pressure during initial oil flooding

This appendix presents the differential pressure across the core during the initial oil-flooding. The stabilized pressure was used to calculate effective permeability of oil at irreducible water saturation by using Darcy's law.

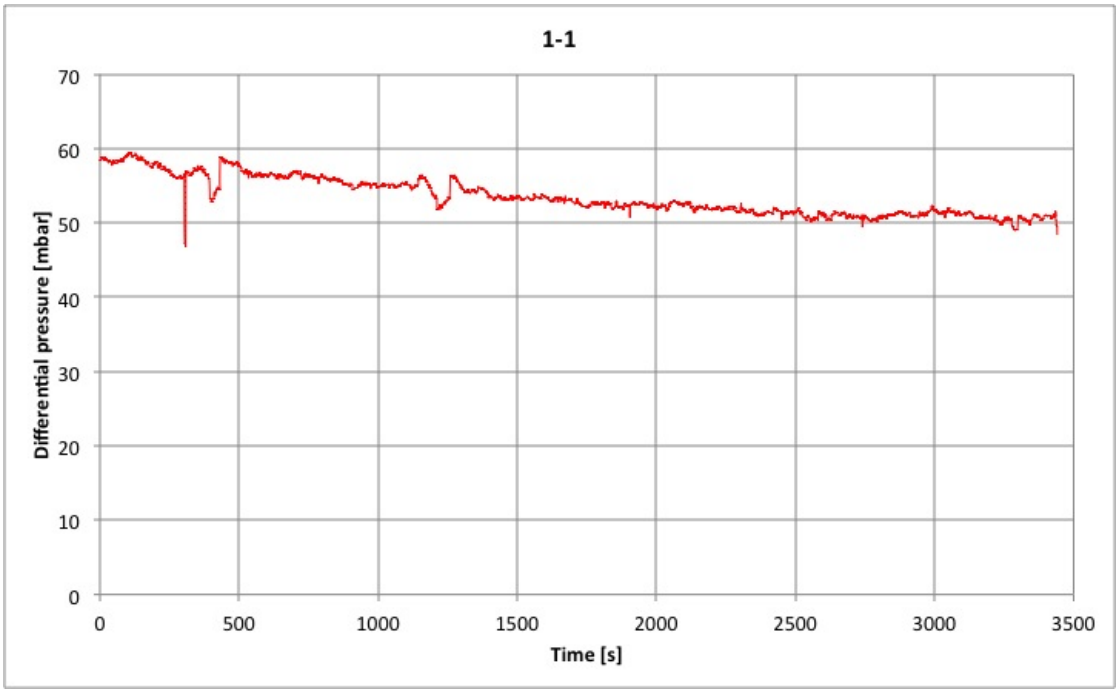

Figure B.1: Differential pressure during initial oilflooding for k_o-calculation for core 1-1

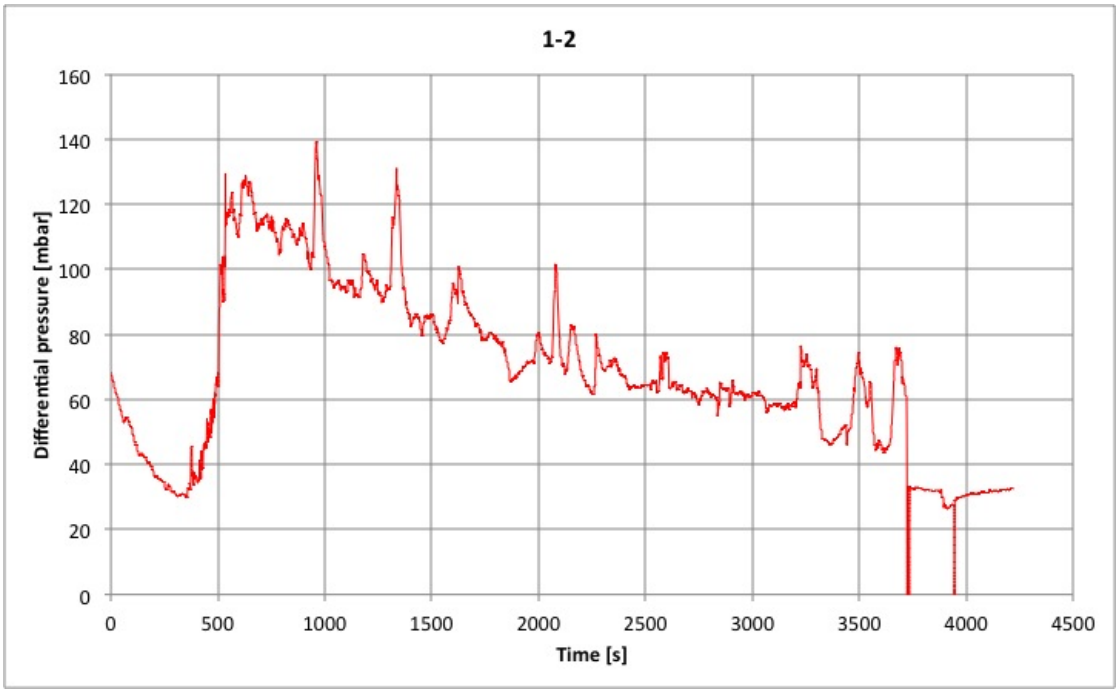

Figure B.2: Differential pressure during initial oilflooding for k_o-calculation for core 1-2

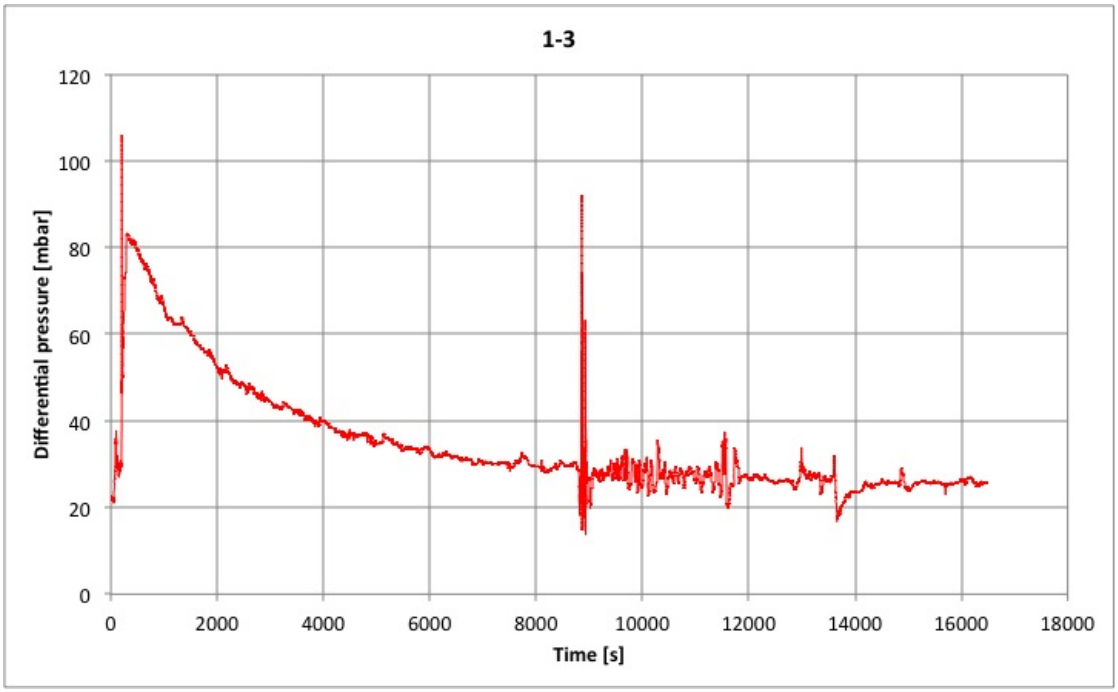

Figure B.3: Differential pressure during initial oilflooding for k_o-calculation for core 1-3

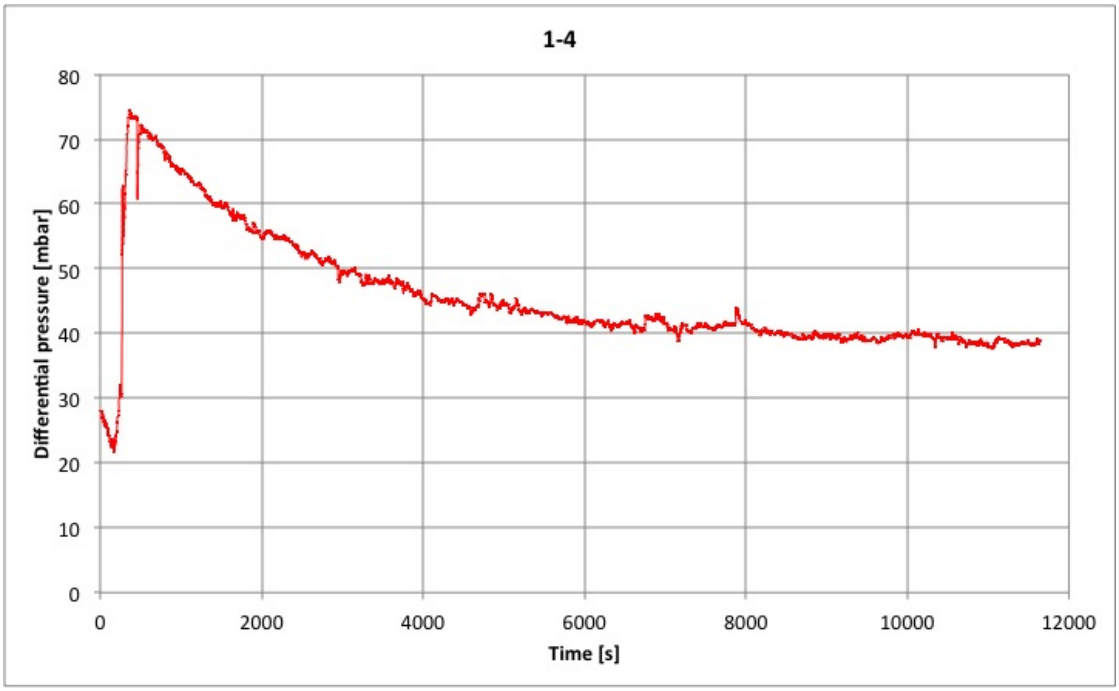

Figure B.4: Differential pressure during initial oilflooding for k_o-calculation for core 1-4

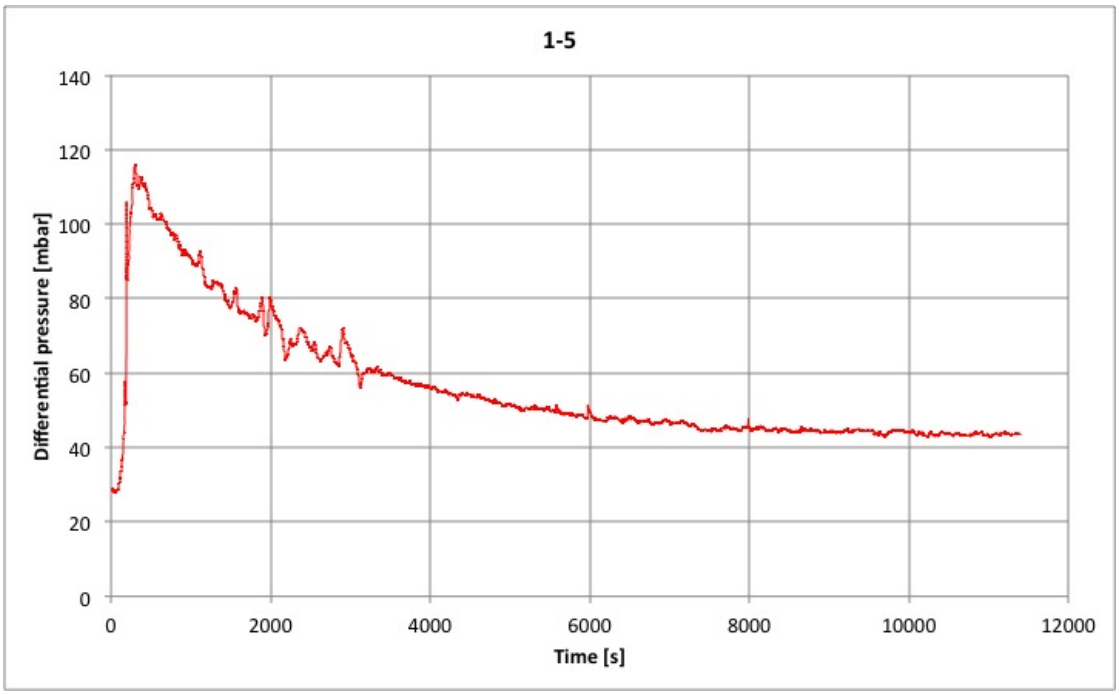

Figure B.5: Differential pressure during initial oilflooding for k_o-calculation for core 1-5

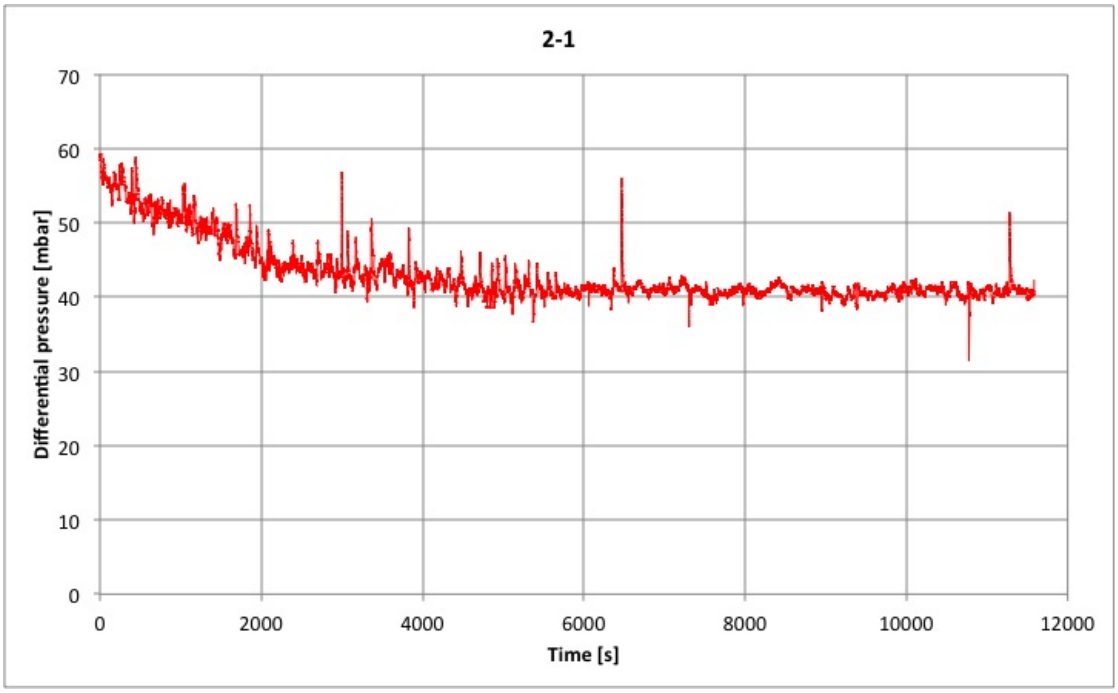

Figure B.6: Differential pressure during initial oilflooding for k_o-calculation for core 2-1

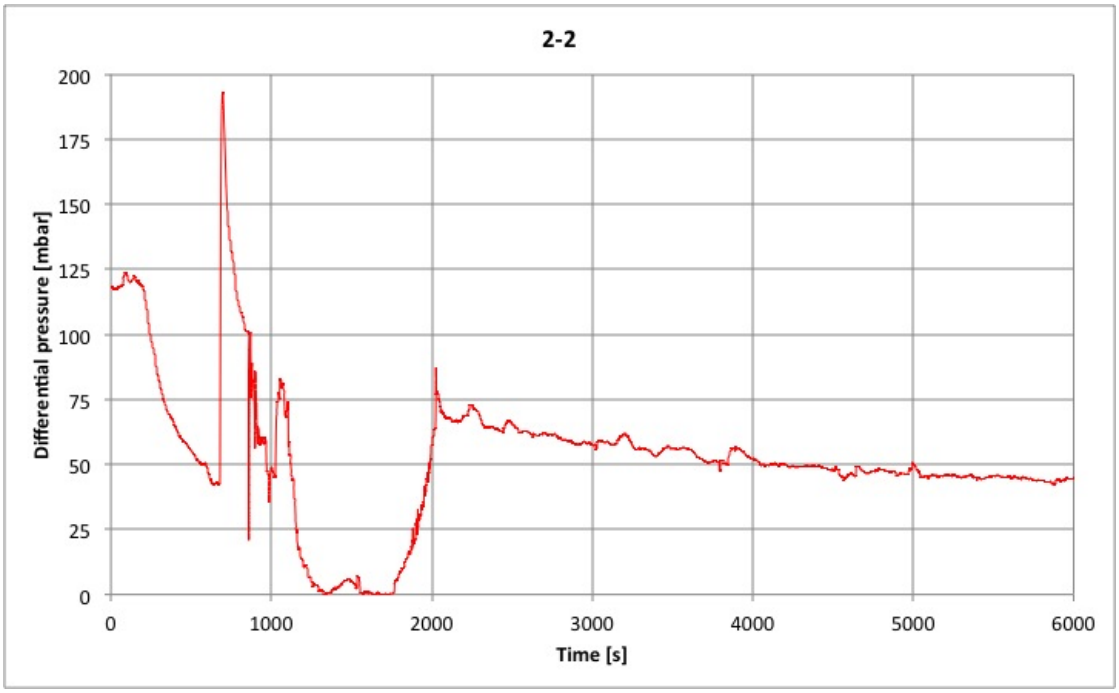

Figure B.7: Differential pressure during initial oilflooding for k_o-calculation for core 2-2

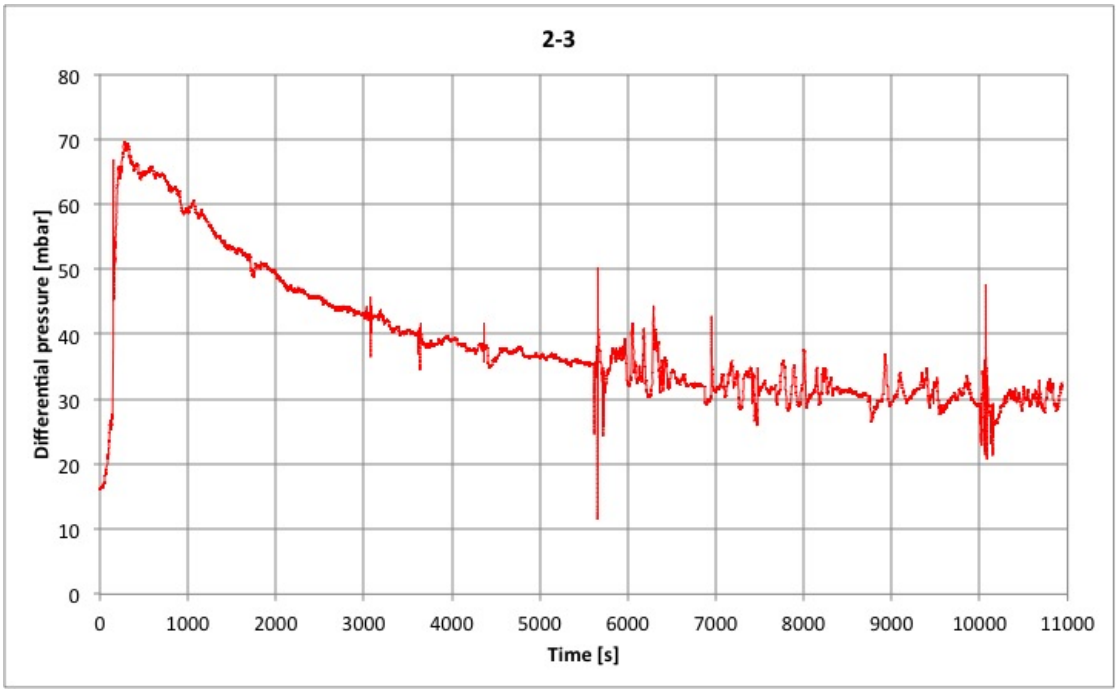

Figure B.8: Differential pressure during initial oilflooding for k_o-calculation for core 2-3

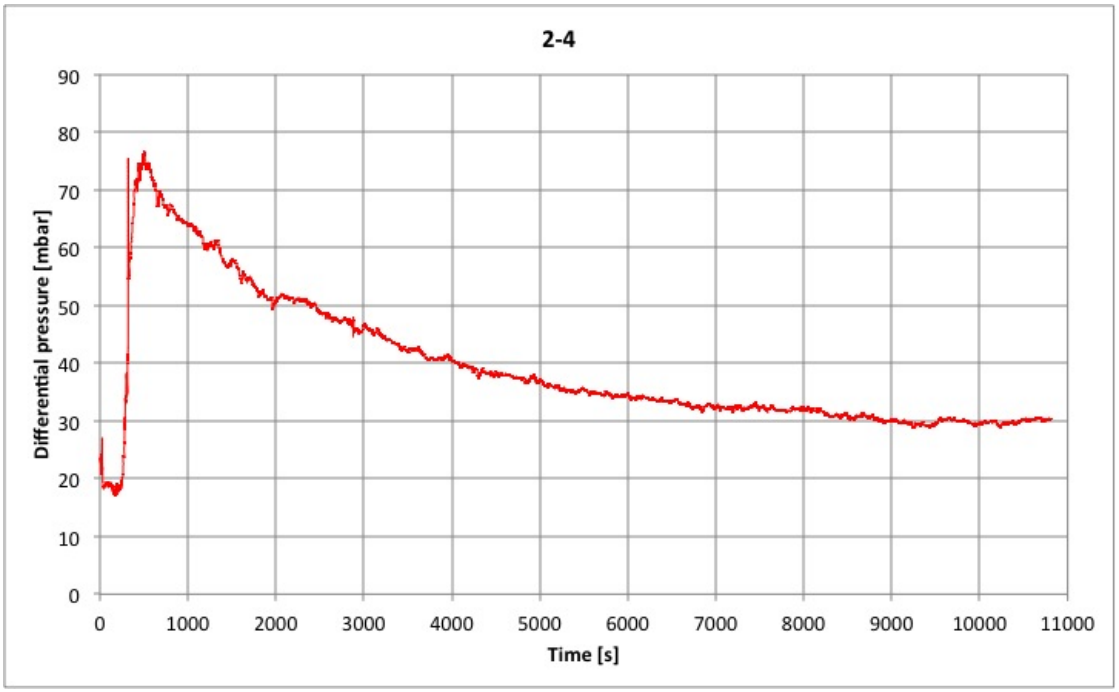

Figure B.9: Differential pressure during initial oilflooding for k_o-calculation for core 2-4

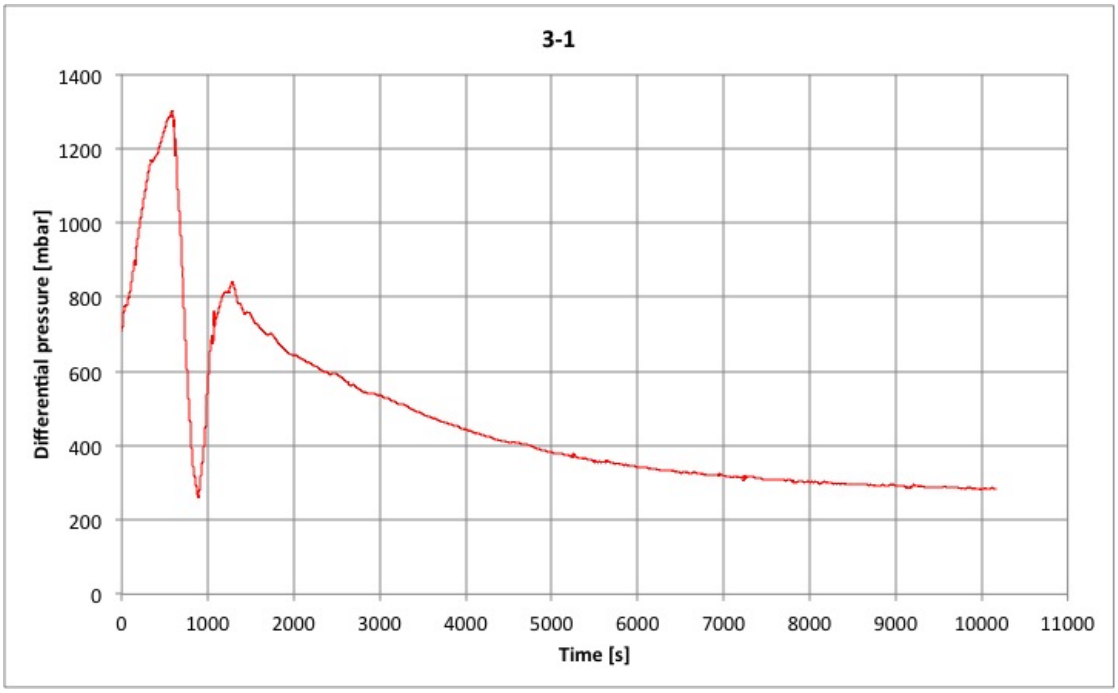

Figure B.10: Differential pressure during initial oilflooding for k_o-calculation for core 3-1

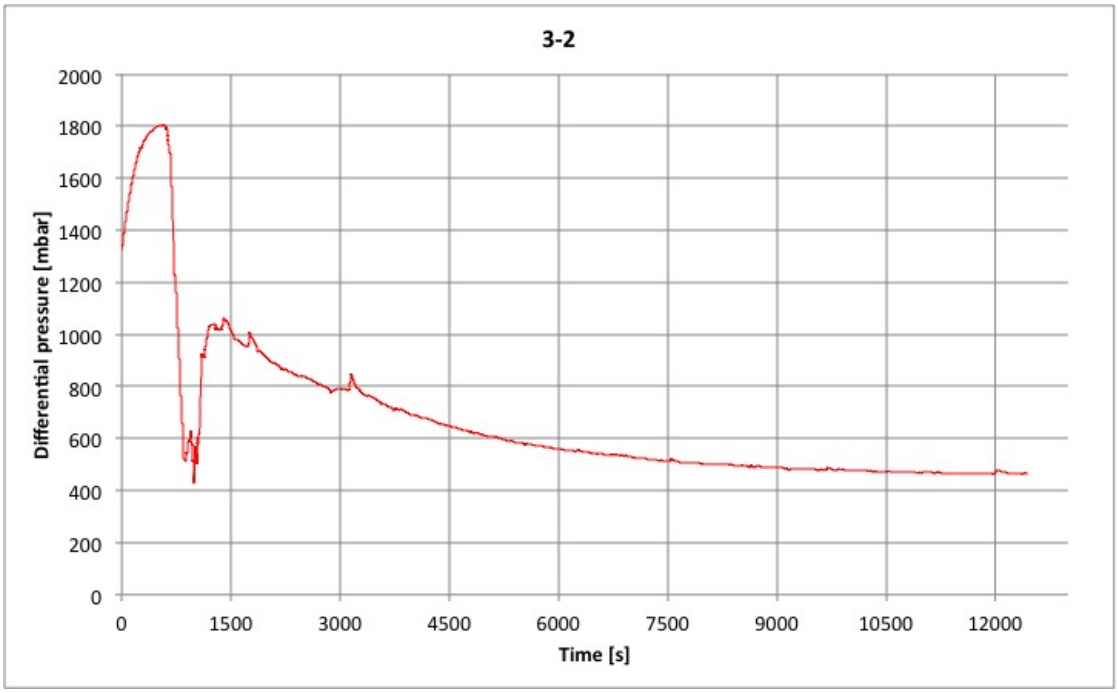

Figure B.11: Differential pressure during initial oilflooding for k_o-calculation for core 3-2

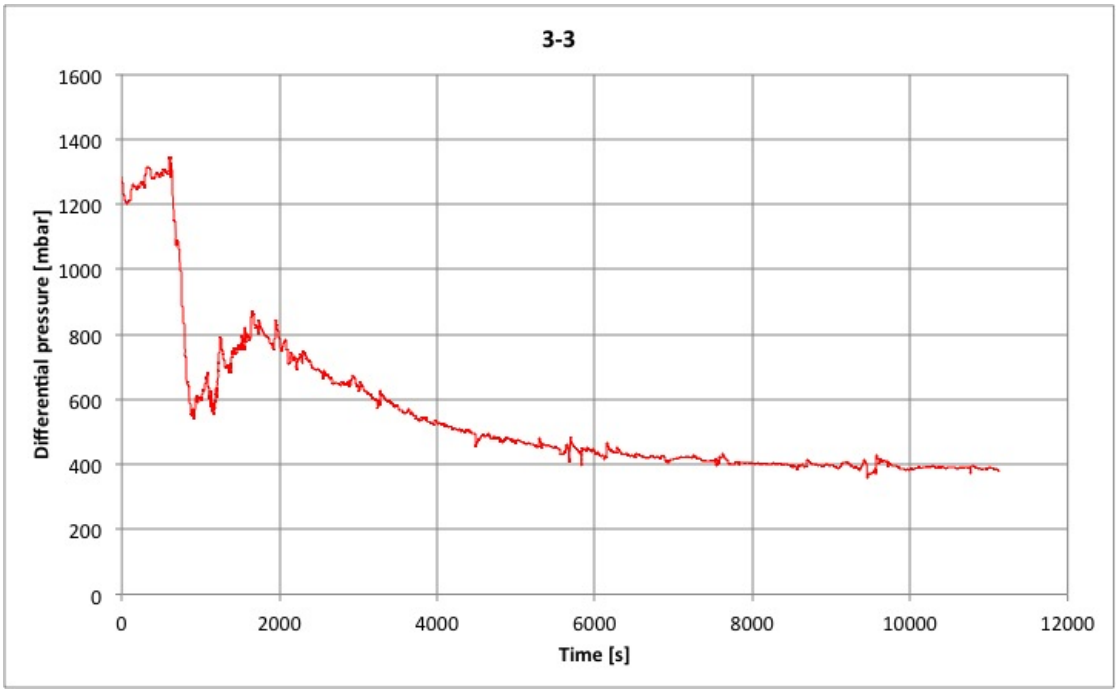

Figure B.12: Differential pressure during initial oilflooding for k_o-calculation for core 3-3

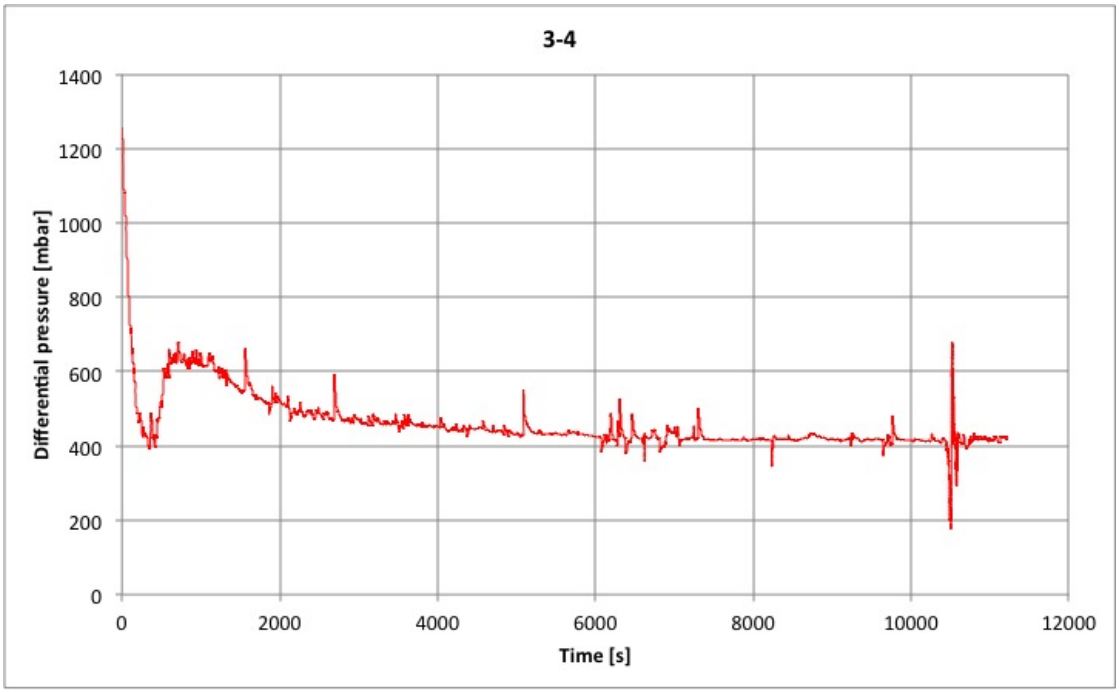

Figure B.13: Differential pressure during initial oilflooding for k_o-calculation for core 3-4